AD-A125 320 PROCEDURES FOR PREDICTION OF CONSOLIDATION IN SOFT FINE-GRAINED DREDGED MATERIAL(U) ARMY ENGINEER WATERWAYS EXPERIMENT STATION VICKSBURG MS K W CARGILL 1/2

UNCLASSIFIED JAN 83 WES-TR-D-83-1 F/G 13/2 NL

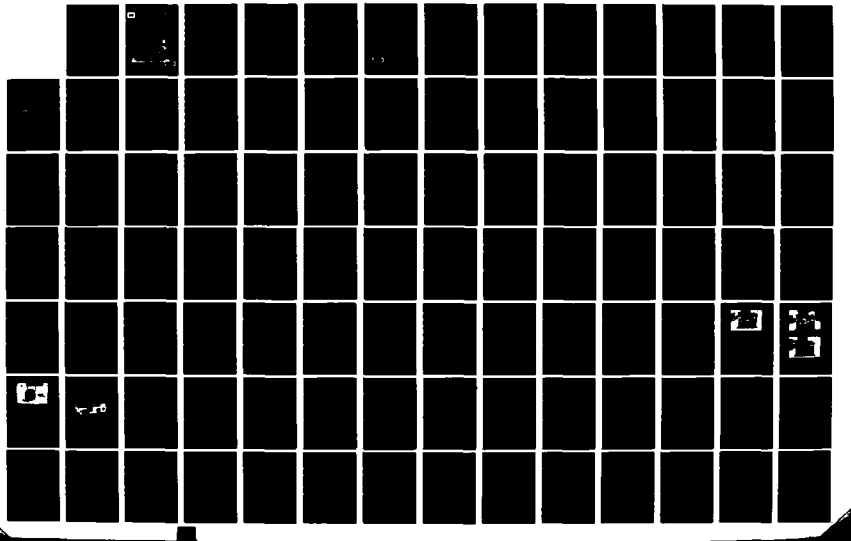

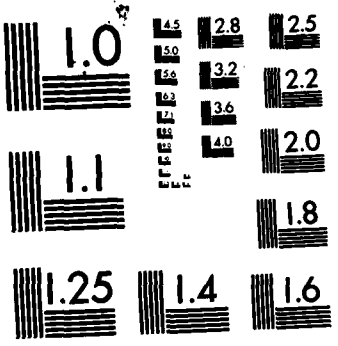

DREDGING OPERATIONS TECHNICAL SUPPORT

TECHNICAL REPORT D-83-1

PROCEDURES FOR PREDICTION OF CONSOLIDATION IN SOFT FINE-GRAINED DREDGED MATERIAL

by

Kenneth W. Cargill

Geotechnical Laboratory
U. S. Army Engineer Waterways Experiment Station
P. O. Box 631, Vicksburg, Miss. 39180

January 1983

Final Report

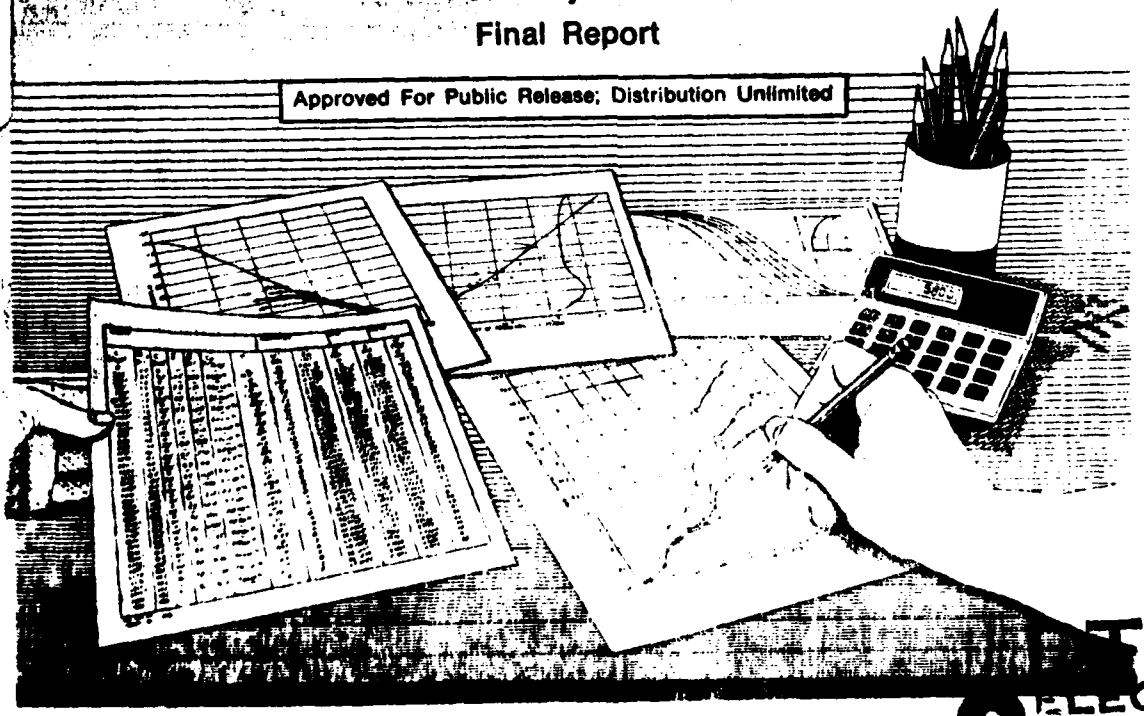

Prepared for Water Resources Support Center
Fort Belvoir, Va 22060

and Office, Chief of Engineers, U. S. Army
Washington, D. C. 20314

Monitored by Environmental Laboratory
U. S. Army Engineer Waterways Experiment Station
P. O. Box 631, Vicksburg, Miss. 39180

Destroy this report when no longer needed. Do not return it to the originator.

The findings in this report are not to be construed as an official Department of the Army position unless so designated by other authorized documents.

The contents of this report are not to be used for advertising, publication, or promotional purposes. *Citation of trade names does not constitute an* official endorsement or approval of the use of such commercial products.

This report series includes publications of the following programs:

Dredging Operations Technical Support (DOTS)

Long-Term Effects of Dredging Operations (LEDO)

Interagency Field Verification of Methodologies for Evaluating Dredged Material Disposal Alternatives (FVP)

Unclassified

SECURITY CLASSIFICATION OF THIS PAGE (When Data Entered)

REPORT DOCUMENTATION PAGE		READ INSTRUCTIONS BEFORE COMPLETING FORM
1. REPORT NUMBER Technical Report D-83-1	2. GOVT ACCESSION NO.	3. RECIPIENT'S CATALOG NUMBER
4. TITLE (and Subtitle) PROCEDURES FOR PREDICTION OF CONSOLIDATION IN SOFT, FINE-GRAINED DREDGED MATERIAL		5. TYPE OF REPORT & PERIOD COVERED Final report 6. PERFORMING ORG. REPORT NUMBER
7. AUTHOR(s) Kenneth W. Cargill		8. CONTRACT OR GRANT NUMBER(s)
9. PERFORMING ORGANIZATION NAME AND ADDRESS U. S. Army Engineer Waterways Experiment Station Geotechnical Laboratory P. O. Box 631, Vicksburg, Miss. 39180		10. PROGRAM ELEMENT, PROJECT, TASK AREA & WORK UNIT NUMBERS Dredging Operations Technical Support Program
11. CONTROLLING OFFICE NAME AND ADDRESS Water Resources Support Center, Fort Belvoir, Va. 22060 and Office, Chief of Engineers, U. S. Army, Washington, D. C. 20314		12. REPORT DATE January 1983 13. NUMBER OF PAGES 152
14. MONITORING AGENCY NAME & ADDRESS(if different from Controlling Office) U. S. Army Engineer Waterways Experiment Station Environmental Laboratory P. O. Box 631, Vicksburg, Miss. 39180		15. SECURITY CLASS. (of this report) Unclassified 15a. DECLASSIFICATION/DOWNGRADING SCHEDULE

16. DISTRIBUTION STATEMENT (of this Report)

Approved for public release; distribution unlimited.

17. DISTRIBUTION STATEMENT (of the abstract entered in Block 20, if different from Report)

18. SUPPLEMENTARY NOTES

Available from National Technical Information Service, 5285 Port Royal Road, Springfield, Va. 22151.

19. KEY WORDS (Continue on reverse side if necessary and identify by block number)

Computer programs
Consolidation (Soils)
Dredged material
Fine grained soils
Soft soils

20. ABSTRACT (Continue on reverse side if necessary and identify by block number)

The report documents studies refining the procedures for calculation of one-dimensional consolidation behavior of very soft fine-grained dredged material. Both the conventional small strain theory of consolidation, which requires linear or constant soil properties, and the more general finite strain theory, which provides for nonlinear soil properties, are presented. Implications of the simplifying assumptions necessary in practical application of the theories are discussed and the general finite strain theory is

(Continued)

DD FORM 1 JAN 73 1473 EDITION OF 1 NOV 65 IS OBSOLETE

Unclassified

SECURITY CLASSIFICATION OF THIS PAGE (When Data Entered)

20. ABSTRACT (Continued).

shown to be superior for the treatment of dredged material.

The governing equations for both theories are written in nondimensional terms and appropriate boundary and initial conditions are specified. Solutions in terms of figures relating the percent consolidation to the nondimensional time factor for small strain theory have been previously published. However, similar solutions based on the finite strain theory were not available and thus had to be developed. Using a computer program, a linearized nondimensional form of the general finite strain governing equation was solved for the cases of singly/doubly drained normally consolidated clays, and singly/doubly drained dredged fill. The figures given represent a significant advancement in the ability to accurately predict the consolidation behavior of thick deposits of very soft fine-grained materials having nonlinear soil properties. A method of obtaining soil parameters necessary for use of the new solution charts is proposed.

A procedure for calculating consolidation of multiple lifts of material placed on prior lifts of underconsolidated material is also proposed and validated by using the procedure to predict settlements of actual field sites where settlements have been measured. For two of three field sites, good agreement was obtained between predictions and measurements when the finite strain theory and the proposed solution technique were used. Behavior at the third site was not well predicted due to the geometry of the site and its particular filling history. In all cases, the finite strain theory solutions were far more accurate than small strain theory solutions. The calculation procedure is also applicable to a single lift subjected to multiple surcharge loadings as would be the case in a phased construction.

This report concludes that the nondimensional finite strain solutions offer more realistic estimates of soft fine-grained material consolidation than similar small strain solutions and that the procedure proposed for multiple lifts is applicable to field problems. The report recommends the use of given finite strain solutions and procedures for prediction of consolidation behavior of fine-grained dredged material deposited in confined disposal areas.

PREFACE

This report was prepared by the Geotechnical Laboratory (GL), U. S. Army Engineer Waterways Experiment Station (WES), as part of the Dredging Operation Technical Support Program (DOTS) work unit for verification and refinement of engineering methodologies for dredging and dredged material disposal sponsored by the Dredging Division of the Water Resources Support Center, Fort Belvoir, Va., and managed by the WES Environmental Laboratory (EL).

Mr. Charles C. Calhoun, Jr., was DOTS Program Manager and Mr. Michael R. Palermo, Chief, Water Resources Engineering Group, was work unit Principal Investigator. The report was written by CPT Kenneth W. Cargill during the period May 1981 to April 1982 under the general supervision of Mr. C. L. McAnear, Chief, Soil Mechanics Division, GL, and Dr. William F. Marcuson III, Chief, GL. Acknowledgement is made to Mr. Palermo who established general goals for the report and contributed significantly to its organization and development. Dr. John Harrison was Chief, EL, during this period.

Commander and Director of the WES during the preparation and publication of this report was COL Tilford C. Creel, CE. Technical Director was Mr. F. R. Brown.

This report should be cited as follows:

Cargill, K. W. 1983. "Procedures for Prediction of Consolidation in Soft, Fine-Grained Dredged Material," Technical Report D-83-1, U. S. Army Engineer Waterways Experiment Station, CE, Vicksburg, Miss.

CONTENTS

LIST OF FIGURES

CONVERSION FACTORS, U. S. CUSTOMARY TO METRIC (SI) UNITS OF MEASUREMENT

U. S. customary units of measurement used in this report can be converted to metric (SI) units as follows:

Multiply	By	To Obtain
acres	4046.873	square metres
cubic yards	0.7645549	cubic metres
feet	0.3048	metres
feet per day	0.3048	metres per day
feet per minute	0.3048	metres per minute
inches	0.0254	metres
pounds (force) per square foot	0.04788026	kilopascals
pounds (mass) per cubic foot	16.01846	kilograms per cubic metre
square feet	0.09290304	square metres
square feet per day	0.09290304	square metres per day
square inches	645.16	square millimetres
tons (force) per square foot	95.76052	kilopascals

PROCEDURES FOR PREDICTION OF CONSOLIDATION IN SOFT FINE-GRAINED DREDGED MATERIAL

PART I: INTRODUCTION

Background

1. Diked containment areas are used to retain dredged material solids while allowing the carrier water to be released from the containment area. The two objectives inherent in the design and operation of a containment area are to provide adequate storage capacity to meet dredging requirements and to attain the highest possible efficiency in retaining solids during the dredging operation in order to meet effluent suspended solids requirements. These considerations are basically interrelated and depend upon effective design, operation, and management of the containment area.

2. The major components of a dredged material containment area are shown schematically in Figure 1. A tract of land is surrounded by dikes to form a confined surface area, and the dredged channel sediments are then pumped into this area hydraulically. Storage capacity of a containment area is defined as the total volume available to hold dredged material and is equal to the total unoccupied volume minus the volume associated with ponding and freeboard requirements.

3. After fine-grained dredged material undergoes sedimentation within a containment area, self-weight consolidation occurs resulting in gains in storage capacity. The placement of dredged material also imposes a loading on the containment area foundation; therefore, additional settlement may result due to consolidation of compressible foundation soils. Settlement due to consolidation is therefore a major factor in the estimation of long-term storage capacity. Since the consolidation process is slow, especially in the case of fine-grained materials, it is likely that total settlement will not have taken place before the containment area is required for additional placement of dredged material.

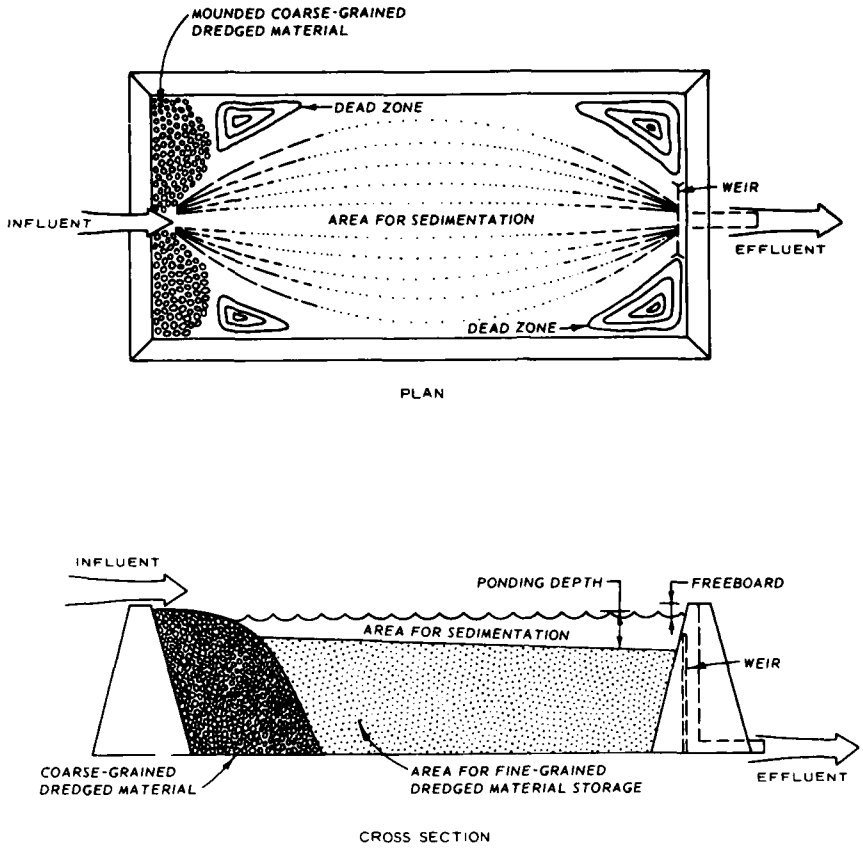

Figure 1. Elements of a confined disposal area (after Montgomery 1978)

For this reason, the time-consolidation relationship is also an important consideration in estimating long-term containment area storage capacity.

4. The estimation of long-term storage capacity is an important consideration for long-term planning and design of new containment areas or evaluation of the remaining service life of existing sites. Guidelines for estimating gains in long-term storage capacity due to consolidation were initially developed as part of the Corps of Engineers' Dredged Material Research Program (DMRP) (Palermo, Montgomery, and Poindexter 1978). The guidelines were later published as Engineer Manual (EM) 1110-2-5006 (Headquarters, Department of the Army 1980). The guidelines are based on the principles of small strain consolidation theory and consider the self-weight consolidation behavior of newly

placed dredged material. Procedures for application of the finite strain theory of consolidation to soft dredged fill layers were not available when initial guidelines were developed. Inclusion of the finite strain technique and procedures for handling multiple lifts in this report represent a refinement of existing procedures.

Purpose and Scope

5. The purpose of this report is to document studies refining the procedures for calculating the consolidation behavior of confined dredged material and verifying their applicability to field problems. Conventional oedometer consolidation testing and constant rate of strain testing were used to define the consolidation parameters of highly compressible fine-grained dredged material from three field sites. Results of the laboratory tests were used to predict consolidation behavior at these sites. These results were then compared to actual field data obtained from instrumentation and surveys.

6. Specific objectives of the verification studies documented in this report include the following:

a. Evaluate the adequacy of hand calculation procedures in estimating ultimate magnitude of potential dredged material consolidation.

b. Evaluate the adequacy of small strain consolidation theory in estimating rate of dredged material settlement.

c. Evaluate the adequacy of the finite strain theory of consolidation in estimating rate of dredged material settlement.

d. Develop refined hand calculation procedures for estimating dredged material settlements for any number of lifts deposited over a period of time.

e. Evaluate the adequacy of standard oedometer consolidation tests in defining a material's consolidation parameters for fine-grained dredged material.

Related Studies

7. This report is one of a series to be published documenting

results of verification studies concerning all aspects of containment area design, operation, and management. Related topics in other reports include: design for effective sedimentation, hydraulic efficiency, design for initial storage capacity, techniques for chemical clarification of effluent, and dredged material dewatering. A closely related study concerns the evaluation of computer-based mathematical models for calculation of consolidation behavior due to repetitive dredging operations occurring over long time periods.

PART II: CONSOLIDATION THEORY AND PROCEDURES

8. The design of confined disposal areas for fine-grained dredged material during and immediately after a single disposal operation is a relatively simple and straightforward exercise utilizing the results of column sedimentation tests as described in previous reports (Montgomery 1978; Palermo, Montgomery, and Poindexter 1978). However, the efficient design of such areas subject to numerous disposal operations occurring intermittently over a period of years requires consideration of the consolidation behavior of the fine-grained materials. Successful prediction of the consolidation behavior of fine-grained materials requires an understanding of the theoretical basis governing the process and the procedures whereby the theory can be applied to real dredged material in the actual containment area. The purpose of this part of the report is to provide the theoretical background and procedures necessary for a rational evaluation of dredged fill consolidation as a function of the material's consolidation properties and as a function of time.

General Problem Description

9. The ideal dredged material disposal operation involves the discharge of a uniform slurry into a confined area where the slurry undergoes an initial sedimentation and later self-weight consolidation. For maximum efficiency, the area should be relatively large in surface area and the lifts relatively thin (3-5 ft).* The slurry distribution should be uniform over the area. A pond of water is maintained over the area during disposal to facilitate sedimentation. This ponded water also promotes a more uniform slurry distribution.

10. Once the slurry is exposed to the more quiescent conditions of the containment area, several things happen. The coarser grains (sands and larger particles) immediately fall out and form a mound at

* A table of factors for converting U. S. customary units of measurements to metric (SI) is presented on page 7.

the point of inflow. Since this material assumes its final configuration essentially as soon as it is deposited, there is a direct relationship between its volume before and after dredging, and it will not be further considered. The remaining fine-grained material is carried rather quickly to all other parts of the area where it initially settles by mechanisms described either as zone settling or flocculent settling. In zone settling, particles consist of individual grains, while in flocculent settling, particles consist of aggregations of grains (flocs). At some point in this initial sedimentation, soil particles and/or flocs begin touching each other and form a continuous matrix. Further settling becomes controlled by the rate at which water can be expelled from the soil matrix rather than how fast the particles and/or flocs can descend through the water. When this continuous matrix is formed, further settlement is governed by the process called "primary consolidation."

11. While the above may be an oversimplification of the dredged material disposal operation, it basically describes the mechanisms considered in containment area design and enables some simplifying assumptions in the theoretical development of the problem. The first of these assumptions is that the consolidation process is one-dimensional. A one-dimensional formulation is possible because the depth of the consolidating layer is usually very small in comparison to its areal extent. The next assumption is that the material is completely saturated because it is deposited as a slurry and will normally be subjected to ponded water. Lastly, it may be assumed that the initial void ratio in the layer at the start of consolidation can be determined from a column sedimentation test as described by Montgomery (1978). This last assumption is valid if the fine-grained material is spread quickly and evenly over the entire containment area.

12. Any deviation from the ideal simplified disposal operation will have a bearing on the accuracy and even relevance of theoretical solutions. Since there is no way to account for the many possible variations in the operation of a particular area in a practical analysis, the results must be tempered with good engineering judgment, and allowances must be made for a less than ideal operation. However, a theoretical

approach still provides a rational basis for an estimate of the disposal area settlements.

One-Dimensional Primary Consolidation

13. There are many variations of the theory of one-dimensional primary consolidation. These variations come about because of the difference in simplifying assumptions made at particular points in the derivation of the governing equation. The original and most simple governing equation was derived by Terzaghi (1924). Because of its simplicity, it has received widespread use among geotechnical engineers and continues to be the first choice when a quick approximation of settlements is required. Since it is used so often, the Terzaghi or "small strain theory" (as it will subsequently be called) will also be presented so that an appreciation for the limiting qualifications it implies may be gained.

14. In contrast to the small strain theory, a governing equation first advanced by Gibson, England, and Hussey (1967) will also be developed. This theory is the most general thus far presented for one-dimensional consolidation and is particularly suited for describing the large settlements common to the primary consolidation of fine-grained dredged material. Because large strains are accounted for in this theory, it has been and will here be referred to as the "finite strain theory."

Small strain theory

15. The governing equation for small strain consolidation theory is based on the continuity of fluid flow in a differential soil element, Darcy's law, a linear stress-strain relationship for the soil matrix, and the effective stress equation.

16. The equation of fluid continuity may be established by considering the differential soil element fixed in space and flow conditions as shown in Figure 2 where the coordinate x is an independent variable not related to time. The quantity of water flowing into the element, which is assumed to be completely saturated, per unit area can be

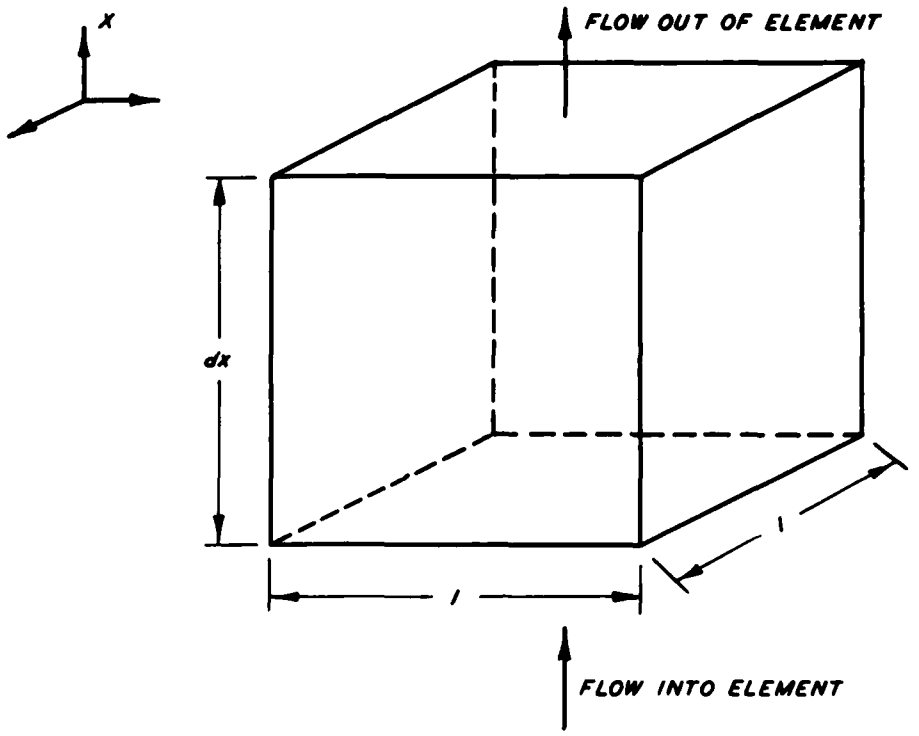

Figure 2. Fluid flow through a differential soil element

calculated by the expression

$$n \cdot v \cdot \gamma_w \tag{1}$$

where n is the volume porosity and assumed to be the proportion of the cross-sectional area conducting fluid, v is the actual velocity of the water, and γ_w is the unit weight of water. The quantity of water flowing out of the element per unit area is

$$n \cdot v \cdot \gamma_w + \frac{\partial}{\partial x} (n \cdot v \cdot \gamma_w)\, dx \tag{2}$$

17. The difference in the quantity of water flowing in and the quantity flowing out of the element is equal to the time rate of change of the quantity of water in the element. The quantity of water in a saturated element per unit area can be written

$$n \cdot dx \cdot \gamma_w \tag{3}$$

or

$$\frac{e}{1 + e} \cdot dx \cdot \gamma_w \tag{4}$$

since

$$n = \frac{e}{1 + e} \tag{5}$$

where e is the void ratio in the element. Thus, its time rate of change is

$$\frac{\partial}{\partial t} \left(\frac{\gamma_w dx}{1 + e} e \right) \tag{6}$$

18. Now $dx/(1 + e_o)$ defines the volume of solids in the differential element at the initial time if e_o is the initial void ratio. At some later time the volume of solids in the element has increased since water has been expelled and it remains saturated. However, if small strains are assumed, the volume of solids in the element remains essentially constant and

$$\frac{dx}{1 + e_o} = \frac{dx}{1 + e} = \text{constant} \tag{7}$$

Therefore, Equation 6 can be written

$$\gamma_w \frac{dx}{1 + e_o} \frac{\partial e}{\partial t} \tag{8}$$

if γ_w is constant with respect to time also.

19. Equating this time rate of change to inflow minus outflow results in

$$\frac{\partial}{\partial x} \left(n \cdot v \cdot \gamma_w \right) dx + \frac{\gamma_w dx}{1 + e_o} \frac{\partial e}{\partial t} = 0 \tag{9}$$

which reduces to

$$\frac{\partial (n \cdot v)}{\partial x} + \frac{1}{1 + e_o} \frac{\partial e}{\partial t} = 0 \tag{10}$$

if γ_w is also constant with respect to the vertical coordinate.

20. Equation 10 is the equation of fluid continuity expressed in

terms of seepage velocity and void ratio. This equation can be put in a more familiar form by application of Darcy's law. Again applying the restriction that strains are small and, additionally, that seepage velocities remain in the laminar range, Darcy's law can be used to relate seepage velocity to excess pressure head in the soil element. The usual form of the equation is

$$n \cdot v = -k \frac{\partial h}{\partial x} \tag{11}$$

where k is soil permeability and h is excess pressure head. The equation of fluid continuity can now be written

$$\frac{\partial k}{\partial x} \frac{\partial h}{\partial x} + k \frac{\partial^2 h}{\partial x^2} - \frac{1}{1 + e_o} \frac{\partial e}{\partial t} = 0 \tag{12}$$

and if soil permeability is considered a constant quantity, Equation 12 reduces to

$$k \frac{\partial^2 h}{\partial x^2} - \frac{1}{1 + e_o} \frac{\partial e}{\partial t} = 0 \tag{13}$$

21. By equating the excess head to its equivalent excess pressure term by

$$h = \frac{u}{\gamma_w} \tag{14}$$

Equation 13 becomes

$$\frac{k}{\gamma_w} \frac{\partial^2 u}{\partial x^2} - \frac{1}{1 + e_o} \frac{\partial e}{\partial t} = 0 \tag{15}$$

where u is the excess pore pressure.

22. At this point a stress-strain or effective stress-void ratio relationship must be introduced. The simplest and the one originally proposed by Terzaghi is

$$\frac{de}{d\sigma'} = -a_v \tag{16}$$

where σ' is effective vertical stress and a_v is called the coefficient of compressibility. Substituting this relationship into Equation 15 results in

$$\frac{k}{\gamma_w} \frac{\partial^2 u}{\partial x^2} + \frac{a_v}{1 + e_o} \frac{\partial \sigma'}{\partial t} = 0 \tag{17}$$

23. By application of the effective stress principle, the effective stress can be expressed in terms of total stress and pore water pressures:

$$\frac{\partial \sigma'}{\partial t} = \frac{\partial \sigma}{\partial t} - \frac{\partial u_w}{\partial t} \tag{18}$$

where σ is the total stress and u_w is the total pore water pressure which is composed of a static or steady-state water pressure and an excess pressure. By definition, the time rate of change of the static pressure is zero, $\partial u_o / \partial t = 0$. Therefore,

$$\frac{\partial \sigma'}{\partial t} = \frac{\partial \sigma}{\partial t} - \frac{\partial u}{\partial t} \tag{19}$$

and Equation 17 can be written

$$\frac{k(1 + e_o)}{\gamma_w a_v} \frac{\partial^2 u}{\partial x^2} = \frac{\partial u}{\partial t} - \frac{\partial \sigma}{\partial t} \tag{20}$$

which is the Terzaghi consolidation equation.

24. The more usual form for the governing equation for small strain consolidation theory is obtained by setting

$$c_v = \frac{k(1 + e_o)}{\gamma_w a_v} \tag{21}$$

where c_v is called the coefficient of consolidation and by setting the time rate of change of total stress to zero, $\partial \sigma / \partial t = 0$, since many situations can be portrayed through a one time quick application of a constant consolidating load. Thus, the governing equation is

$$c_v \frac{\partial^2 u}{\partial x^2} = \frac{\partial u}{\partial t} \tag{22}$$

for small strain consolidation theory with constant boundary loads.

Finite strain theory

25. The governing equation for finite strain consolidation theory is based on the continuity of fluid flow in a differential soil element, Darcy's law, and the effective stress principle similar to the small strain theory. However, finite strain theory additionally considers vertical equilibrium of the soil mass and places no restriction on the form of the stress-strain relationship. Other differences will become apparent during the governing equation development in this section.

26. Figure 3 defines a differential soil element of constant unit plan area whose vertical coordinate ξ is free to change with time (unlike the previous coordinate, x , of Figure 2) such that the element continuously encloses the same solid soil particles. Thus, there is no

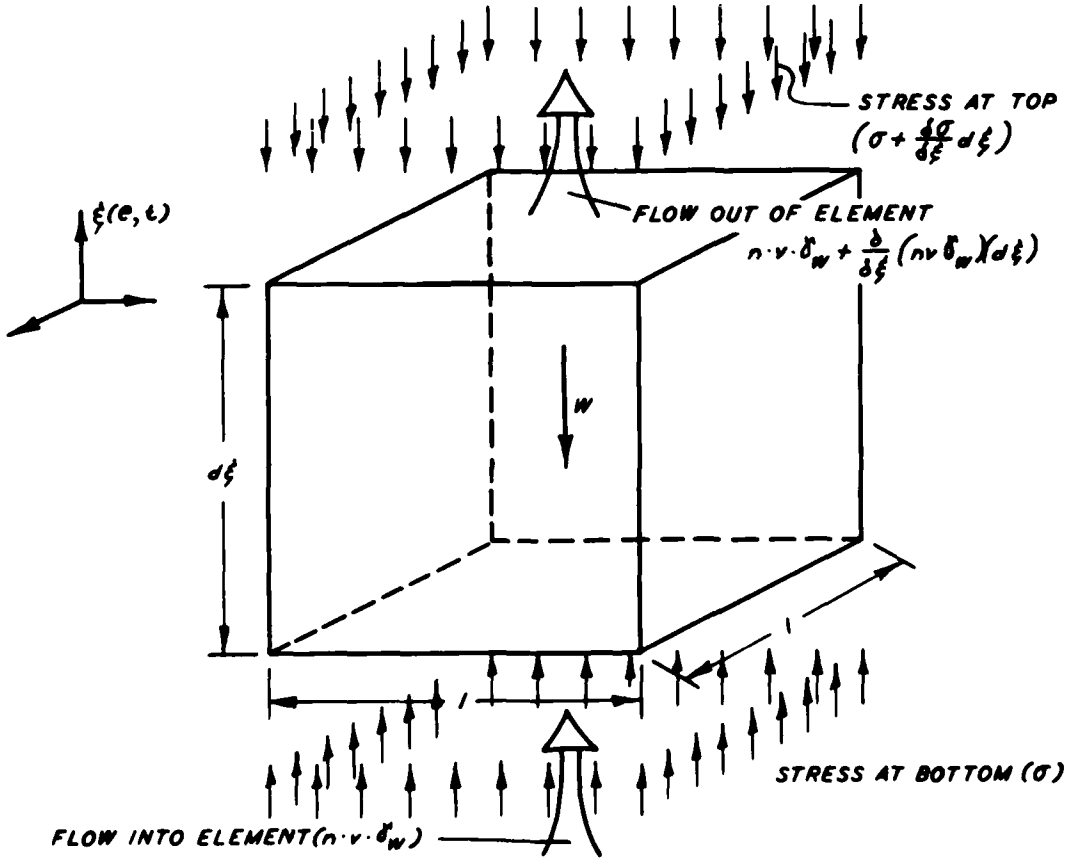

Figure 3. Equilibrium and flow conditions in a differential soil element

limit to the strain which the element may undergo. Also shown in the figure are total stress and flow conditions at the top and bottom of the element.

27. The weight W of the element is the sum of the weights of the pore fluid and solid particles:

$$W = (e\gamma_w + \gamma_s) \frac{d\xi}{1 + e} \tag{23}$$

where γ_s is the unit weight of the soil solid particles. Therefore, equilibrium of the soil mixture is given by

$$\sigma + \frac{\partial \sigma}{\partial \xi} d\xi + (e\gamma_w + \gamma_s) \frac{d\xi}{1 + e} - \sigma = 0 \tag{24}$$

which means

$$\frac{\partial \sigma}{\partial \xi} + \frac{e\gamma_w + \gamma_s}{1 + e} = 0 \tag{25}$$

28. It is also necessary to establish an expression for equilibrium of the pore fluid. If the total water pressure u_w is decomposed into its static and excess parts,

$$\frac{\partial u_w}{\partial \xi} - \frac{\partial u_o}{\partial \xi} - \frac{\partial u}{\partial \xi} = 0 \tag{26}$$

but

$$\frac{\partial u_o}{\partial \xi} = -\gamma_w \tag{27}$$

and, therefore,

$$\frac{\partial u_w}{\partial \xi} + \gamma_w - \frac{\partial u}{\partial \xi} = 0 \tag{28}$$

29. The equation of fluid continuity is derived similarly to that for small strain theory except that now the fluid velocity must be defined as a relative velocity equal to the difference in the velocities of the fluid and solids in the soil matrix:

$$v = v_f - v_s \tag{29}$$

Therefore, the fluid continuity equation is

$$\frac{\partial}{\partial \xi}\left[\frac{e}{1+e}\,(v_f - v_s)\right] d\xi + \frac{\partial}{\partial t}\left(\frac{d\xi}{1+e}\,e\right) = 0 \qquad (30)$$

30. Now $d\xi/(1 + e)$ defines the volume of solids in the differential element; and since a time-dependent element enclosing the same solid volume throughout the consolidation process has been chosen, the quantity $d\xi/(1 + e)$ defines the volume of solids for all time. Equation 30 can therefore be reduced to

$$\frac{\partial}{\partial \xi}\left[\frac{e}{1+e}\,(v_f - v_s)\right] + \frac{1}{1+e}\,\frac{\partial e}{\partial t} = 0 \qquad (31)$$

31. The velocity terms in the above equation may be eliminated by application of Darcy's law which can be written in terms of ξ coordinates as

$$n(v_f - v_s) = -\frac{k}{\gamma_w}\,\frac{\partial u}{\partial \xi} \qquad (32)$$

32. Equation 32 substituted into Equation 31 results in

$$\frac{1}{\gamma_w}\,\frac{\partial}{\partial \xi}\left(k\,\frac{\partial u}{\partial \xi}\right) - \frac{1}{1+e}\,\frac{\partial e}{\partial t} = 0 \qquad (33)$$

where k will <u>not</u> be assumed constant but a function of the void ratio which varies with depth in the layer.

33. By using Equation 28 to replace the excess pressure term and the effective stress principle to replace the resulting total pore pressure term, Equation 33 can be written

$$\frac{1}{\gamma_w}\,\frac{\partial}{\partial \xi}\left[k\left(\gamma_w + \frac{\partial \sigma}{\partial \xi} - \frac{\partial \sigma'}{\partial \xi}\right)\right] - \frac{1}{1+e}\,\frac{\partial e}{\partial t} = 0 \qquad (34)$$

34. The term for total stress may be eliminated from the above by substitution of the relation in Equation 25 such that

$$\frac{1}{\gamma_w}\,\frac{\partial}{\partial \xi}\left[k\left(\gamma_w - \frac{e\gamma_w + \gamma_s}{1+e} - \frac{\partial \sigma'}{\partial \xi}\right)\right] - \frac{1}{1+e}\,\frac{\partial e}{\partial t} = 0 \qquad (35)$$

Equation 35 is the governing equation for finite strain consolidation, but this form is very difficult to solve because of the time dependency of the coordinate system.

35. Ortenblad (1930) proposed a coordinate system uniquely suited

for calculating consolidation in soft materials such as fine-grained dredged fill. These reduced coordinates are based on the volume of solids in the consolidating layer and are therefore time-independent. Transformation between the time-dependent ξ coordinate and the time-independent z coordinate is accomplished by the equation

$$dz = \frac{d\xi}{1 + e} \tag{36}$$

36. Additionally, by utilizing the chain rule for differentiation, the relationship

$$\frac{\partial F}{\partial z} = \frac{\partial F}{\partial \xi} \frac{d\xi}{dz} \tag{37}$$

can be written where F is any function. (See Gibson, Schiffman, and Cargill (1981) for a more mathematically correct treatment of this functional relationship.)

37. Applying Equations 36 and 37 enables Equation 35 to be written

$$\frac{\partial}{\partial z}\left[\frac{k}{1 + e}\left(1 - \frac{\gamma_s}{\gamma_w} - \frac{1}{\gamma_w}\frac{\partial \sigma'}{\partial z}\right)\right] - \frac{\partial e}{\partial t} = 0 \tag{38}$$

or

$$(\gamma_s - \gamma_w)\frac{\partial}{\partial z}\left[\frac{k}{1 + e}\right] + \frac{\partial}{\partial z}\left[\frac{k}{\gamma_w(1 + e)}\frac{\partial \sigma'}{\partial z}\right] + \frac{\partial e}{\partial t} = 0 \tag{39}$$

Again, by the chain rule of differentiation, the relationship

$$\frac{\partial F}{\partial z} = \frac{dF}{de}\frac{\partial e}{\partial z} \tag{40}$$

can be written and Equation 39 thus becomes

$$(\gamma_s - \gamma_w)\frac{d}{de}\left[\frac{k}{1 + e}\right]\frac{\partial e}{\partial z} + \frac{\partial}{\partial z}\left[\frac{k}{\gamma_w(1 + e)}\frac{d\sigma'}{de}\frac{\partial e}{\partial z}\right] + \frac{\partial e}{\partial t} = 0 \tag{41}$$

which constitutes the governing equation of one-dimensional finite strain consolidation in terms of the void ratio e and the functions $k(e)$ and $\sigma'(e)$

38. An analytical solution to Equation 41 is not practical, but once appropriate initial and boundary conditions are specified, its

solution by numerical techniques is feasible with the aid of a computer (see Cargill 1982). Of course, the relationships between permeability and void ratio and effective stress and void ratio must also be specified.

39. In its present form, the governing equation for finite strain consolidation is highly nonlinear. Gibson, Schiffman, and Cargill (1981) have shown how it may be linearized and its solution simplified through the use of nondimensional variables. As shown in their paper, there are two basic assumptions necessary for the linearization of Equation 41. The first is that there is a function

$$g(e) = - \frac{k}{\gamma_w (1 + e)} \frac{d\sigma'}{de} \tag{42}$$

which is constant over the range of void ratios expected in the problem for which a solution is sought. The similarity between g and c_v of small strain theory should be noted. If g can be assumed constant, the governing equation becomes

$$\frac{\partial^2 e}{\partial z^2} + (\gamma_s - \gamma_w) \frac{d}{de} \left(\frac{de}{d\sigma'} \right) \frac{\partial e}{\partial z} = \frac{1}{g} \frac{\partial e}{\partial t} \tag{43}$$

which is still nonlinear due to the variable coefficient

$$\lambda(e) = - \frac{d}{de} \left(\frac{de}{d\sigma'} \right) \tag{44}$$

If λ may also be assumed constant, void ratio would then obey the linear equation

$$\frac{\partial^2 e}{\partial z^2} - \lambda(\gamma_s - \gamma_w) \frac{\partial e}{\partial z} = \frac{1}{g} \frac{\partial e}{\partial t} \tag{45}$$

Implications of assumptions

40. It is appropriate here to examine the implications of the assumptions previously made in formulating the small strain and finite strain theories of consolidation as they apply to the fine-grained materials common to most dredged fill operations. The assumptions of saturation and one dimensionality are not examined since they are basic to the development of both theories and, in general, are valid assumptions.

41. The validity of assuming small strains for dredged material as was necessary in obtaining the Terzaghi equation may be judged from the strain measured by Hammer (1981) in prototype tests. After only 1 year of consolidation, strains of over 50 percent were measured in some of the test areas which contained dredged material from Mobile Bay. This suggests that if a small strain formulation is to be used, some method of constantly updating the computation to account for these large strains must be included.

42. Figure 4 shows an effective stress-void ratio curve developed from oedometer tests conducted by the U. S. Army Engineer Waterways Experiment Station (WES) on a typical fine-grained dredged material. The applicability of a constant relationship for soil compressibility (an assumption of the small strain theory) should be evaluated in light of these test data.

43. In linearizing the finite strain formulation, Equation 44 was used. This equation implies an exponential relationship between void ratio and effective stress of the form

$$e = (e_{oo} - e_{\infty}) \exp(-\lambda\sigma') + e_{\infty} \tag{46}$$

where e_{oo} is void ratio at zero effective stress and e_{∞} is the void ratio at infinite effective stress. Such a curve is also shown in Figure 4 where λ, e_{oo}, and e_{∞} were chosen to give the best apparent fit to the oedometer test data. As can be seen, there is a close similarity between the curves. The fact that Equation 46 is good only for limited ranges is shown by Figure 5 where the oedometer test data are extended into the higher stress ranges. As can also be seen, totally different values of λ, e_{oo}, and e_{∞} must be used to get an acceptable fit with test data.

44. Using small strain theory to analyze the oedometer data of the dredged fill for each increment of applied load (where small strain theory is most applicable), an estimate of the variation of permeability with void ratio can be obtained. Then using the specific value of permeability with the corresponding value of void ratio and the specific value of coefficient of compressibility at the same void ratio, the

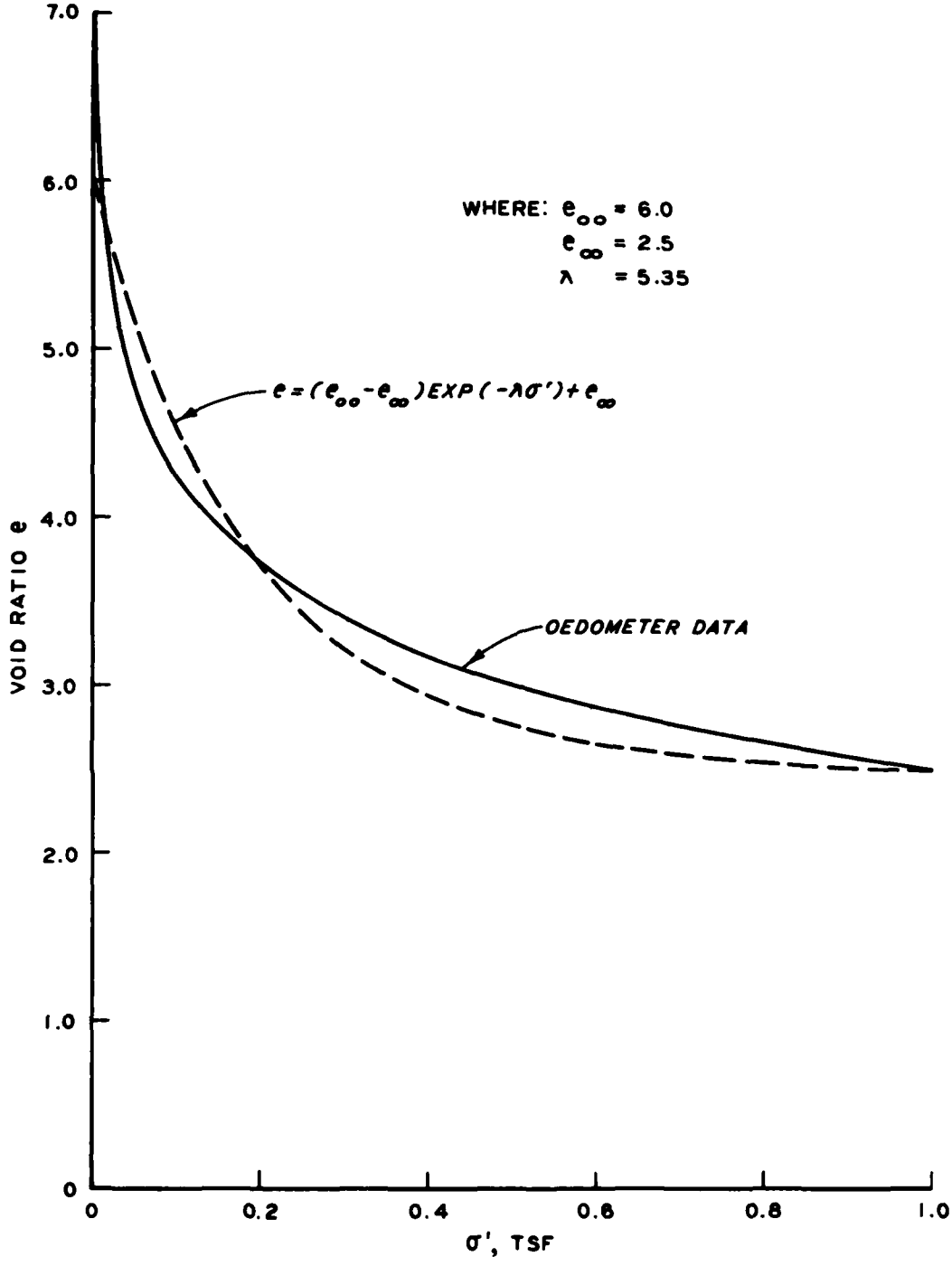

Figure 4. Exponential void ratio-effective stress relationship compared to oedometer data, 0-1.0 tsf

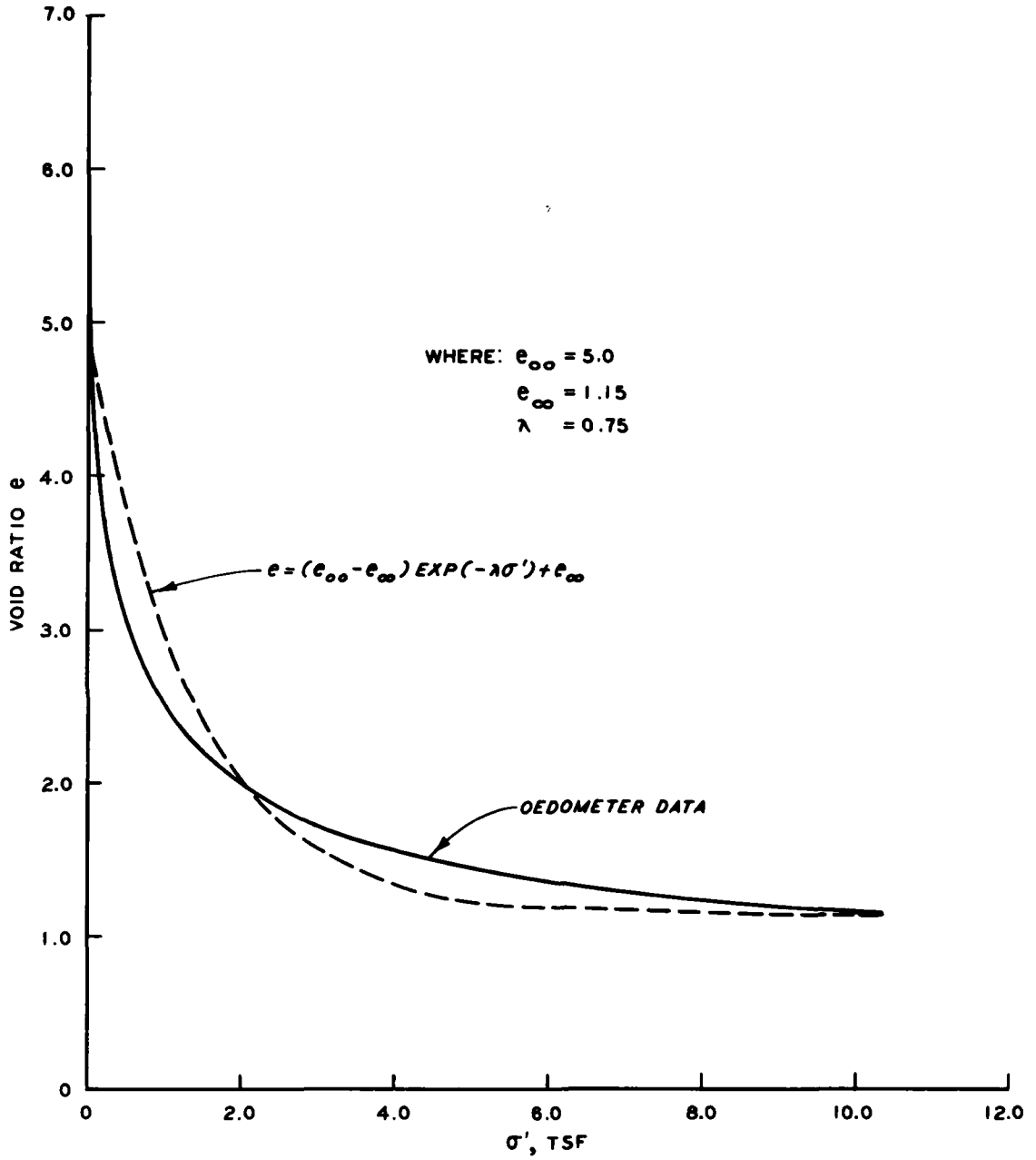

Figure 5. Exponential void ratio-effective stress relationship compared to oedometer data, 0-12.0 tsf

variation of the coefficient of consolidation with void ratio can be obtained. Figure 6 shows the resulting curves. The accuracy of these curves could be improved by using smaller increments of load, but are considered adequate to illustrate the implications of assuming a constant permeability or constant coefficient of consolidation.

45. As can be seen, for the material tested, the assumption of a constant coefficient of consolidation is very good for void ratios between 3 and 7. The assumption is fair for void ratios less than 3 because, at the lower void ratios, the coefficient of compressibility varies less and there is less change in void ratio for typical changes in effective stress. This constancy, no doubt, is one of the primary reasons for the popularity of the small strain theories.

46. Also shown in Figure 6 is the variation of the finite strain coefficient of consolidation g with void ratio. This quantity appears to be more constant at the lower void ratios.

47. When considering the importance of these various assumptions, it is important to remember that rarely can the validity of one assumption be used to justify a particular analysis procedure. For instance, the engineer unfamiliar with the basics of small strain theory might look at the fact that c_v in reality is essentially a constant and conclude that small strain theory is the best method of analyzing a consolidation problem. However, when he is told or remembers that before such a quantity as c_v existed it was necessary to assume that the coefficient of compressibility a_v is constant, it may become apparent that a finite strain formulation is better.

Secondary Consolidation

48. The process of secondary consolidation or creep in fine-grained soils has not received nearly as much attention or study as primary consolidation; therefore, its prediction is not generally possible. Terzaghi and Peck (1967) have stated that the secondary settlement of buildings on "normally loaded clay" can be between 1/8 and 1/2 in. per year based on experience. If these experiences hold true for typical

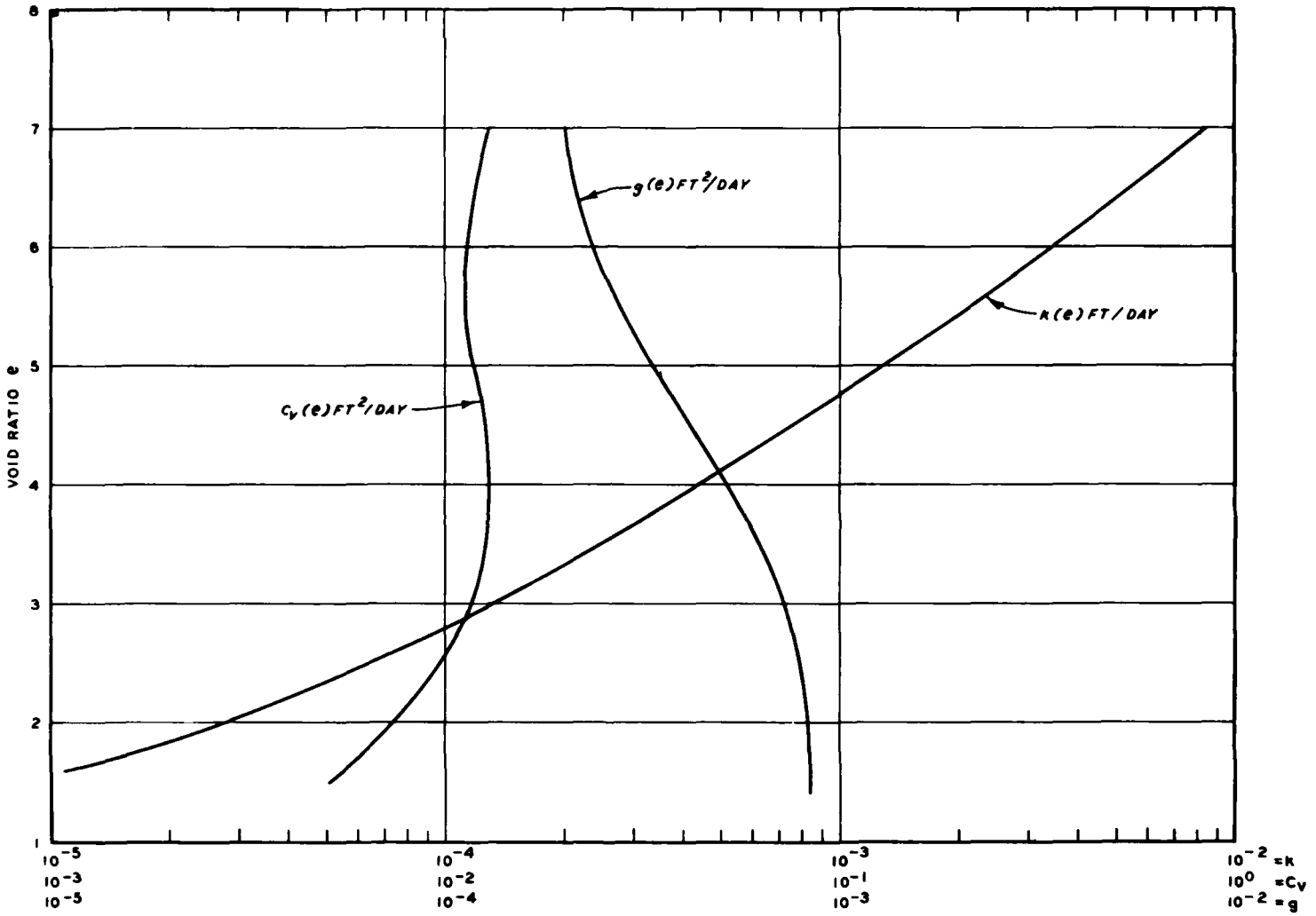

Figure 6. Typical permeability and coefficients of consolidation as a function of void ratio

dredged material deposits, it could be that secondary consolidation is insignificant and can therefore be ignored.

49. Clearly there is a requirement for research geared specifically to the secondary consolidation behavior of fine-grained dredged material before it is completely discounted as negligible since it is generally known that organic soils found in some dredged material exhibit a high degree of secondary consolidation. However, it is possible to gain some insight into the order of magnitude of secondary settlements in nonorganic dredged material by looking at the time curves from oedometer testing.

50. Figure 7 shows a typical time curve plotted from the results of an oedometer test on dredged material from Craney Island. It is commonly accepted that the portion of the settlement beyond the point of 100 percent primary consolidation as identified in the figure is due to secondary consolidation. The average rate of secondary settlement indicated by this curve between 100 and 3000 min is 0.9 in. per year. Though this amount is somewhat higher than the 1/8 to 1/2 in. per year from Terzaghi and Peck, it is still a relatively insignificant amount in comparison to the settlements due to primary consolidation.

51. Three consolidation tests on fine-grained nonorganic sediments and dredged material conducted by the WES indicated secondary settlement rates varying between 0.2 and 1.9 in. per year with an average value of 0.7 in. per year. Based on these tests, it was concluded that secondary consolidation is negligible in comparison to primary consolidation for nonorganic dredged material and will therefore be disregarded. This conclusion is, of course, based on limited data and future research may indicate differently.

Desiccation Consolidation

52. The last type of consolidation to be considered here is that due to the physical drying of fine-grained materials by the environment. There are basically two phenomena which control the amount of consolidation caused by desiccation.

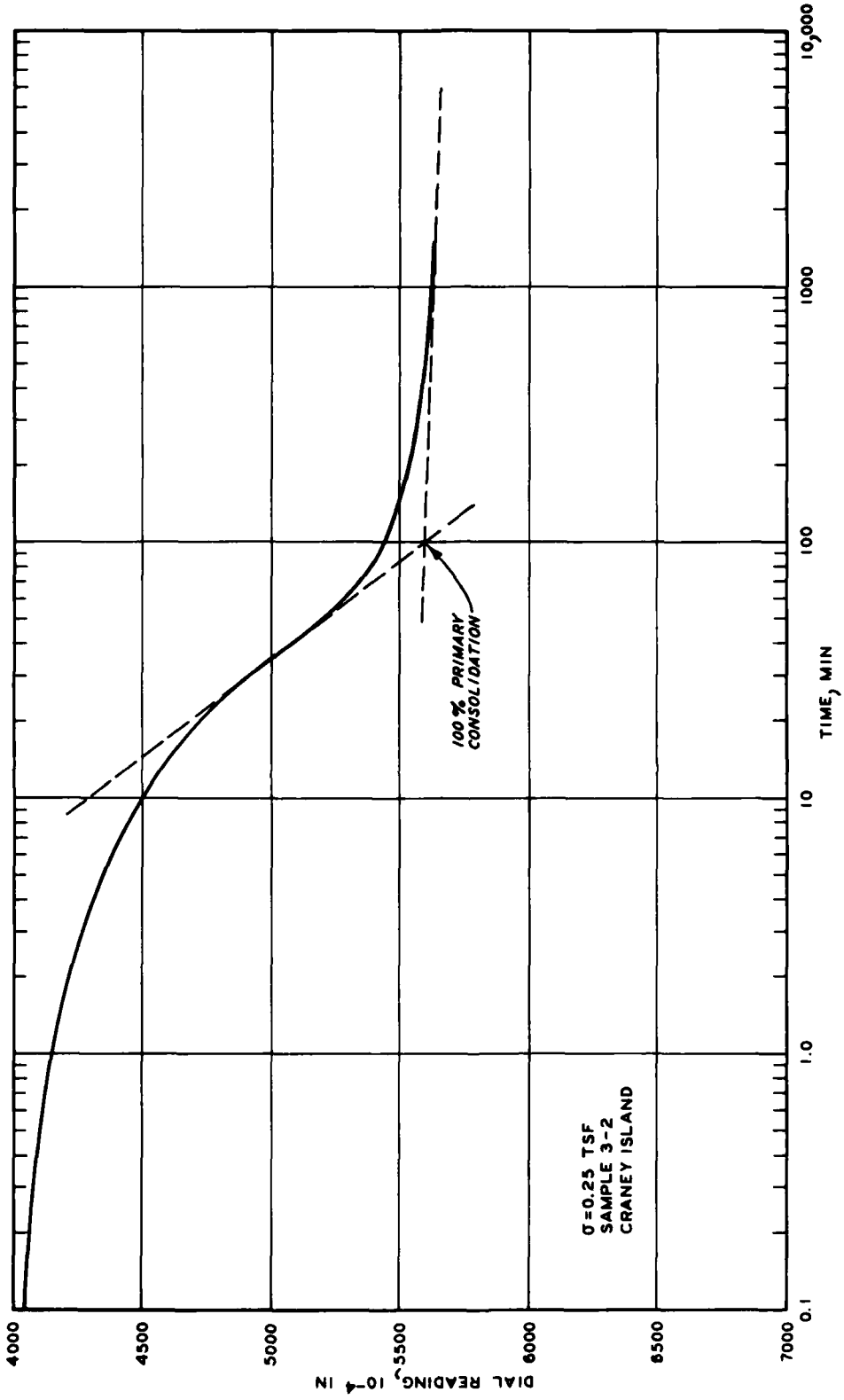

Figure 7. Typical time curve from oedometer test on dredged material (CH)

53. The first process involves the evaporation of water from the upper sections of the dredged material and thereby a reduction in its moisture content which causes a reduction in void ratio or volume occupied due to the negative pore water pressure induced by the drying. Haliburton (1978) has presented some empirical relationships based on class A pan evaporation estimates which provide rough estimates of the amount of consolidation due to desiccation of the upper material. These equations require the assumption that the material remains saturated throughout the desiccation process and therefore an inch of water loss is equated to an inch of material settlement and that desiccation is a linear function of evaporation potential independent of material depth. The method is the only one presently available and can be used where very rough estimates are required and where field experience indicates the assumptions are justified.

54. The other process involves the additional primary consolidation in lower material caused by the lowering of the water table due to desiccation of the upper material. When the free water surface is lowered, buoyant forces above the new level are canceled, and the material below the new level is therefore subjected to an additional surcharge. This additional surcharge induces an additional excess pore pressure which is dissipated during the primary consolidation process. The ultimate settlement of the dredged material will be greater in this case than if the water table had remained at or above the surface because of the increase in effective stresses through the layer. From a theoretical standpoint, there is also a possibility that this effect will be offset to some degree due to the lowered permeability in the desiccated layer. If fact, where dredged material deposition is occurring almost continuously, it may be counterproductive to the long-term capacity of the site if intermediate layers are only allowed to dry to the point of thin surface crust formation just before a new layer is placed. However, if the drying is taken to the point of crack formation, experience indicates that the effects are beneficial to long-term storage capacity.

Governing Equation Solutions

55. Now that the equations governing the one-dimensional primary consolidation of fine-grained dredged material have been theoretically derived, it remains to solve the equations so that they may be used to compute time-dependent settlements in practical problems. In the solution procedures to follow, it is assumed that the final or ultimate settlement has been previously calculated by assuming complete dissipation of excess pore pressures and some relationship between void ratio and effective stress. Particular methods of calculating this final settlement will be given in the next section.

56. Even though solutions of the governing equation of small strain theory have been published numerous times, a brief recapitulation will be given here for completeness. Solutions of the governing equation of finite strain theory are limited to those published by Gibson, Schiffman, and Cargill (1981) and do not cover the cases of double drainage nor the initial conditions found in a dredged fill. Therefore, the solutions will be more fully developed here.

Small strain solutions

57. The general solution of Equation 22 is greatly simplified by introducing the nondimensional variables

$$X = \frac{x}{H} \tag{47}$$

and

$$T_{ss} = \frac{c_v t}{H^2} \tag{48}$$

where X is the nondimensional layer height, H is the length of the longest drainage path in the consolidating layer, and T_{ss} is the nondimensional small strain time factor. That is, if h is the thickness of the layer then $H = h$ for drainage from one surface and $H = h/2$ for drainage from both surfaces. In nondimensional terms, the governing equation is then

$$\frac{\partial^2 u}{\partial X^2} = \frac{\partial u}{\partial T_{ss}} \tag{49}$$

which can be solved analytically for u for many different initial and boundary conditions (Carslaw and Jaeger 1959).

58. Once an expression for u throughout the consolidating layer has been determined, the percent consolidation U can be calculated as

$$U(T_{ss}) = 1 - \frac{\int_0^H u(X)\, dX}{\int_0^H u_{oo}(X)\, dX} \tag{50}$$

where $u(X)$ is the excess pore pressure distribution at time factor T_{ss} and $u_{oo}(X)$ is excess pore pressure distribution at time factor $T_{ss} = 0$. Thus, the percent consolidation is actually a measure of the excess pore pressure dissipated, although in small strain theory it can also be interpreted as a measure of the ultimate settlement currently achieved.

59. Figure 8 shows the solutions of Equations 49 and 50 for a layer drained from one surface and three commonly encountered initial conditions. Curve I represents a uniform initial excess pore pressure distribution as would be found in a foundation layer which was suddenly subjected to a surcharge of large areal extent. Curve II represents an initial excess pore pressure varying linearly from a maximum at the top of the consolidating layer to zero at the bottom. This is approximately the case when a surcharge whose areal extent is small in comparison to the depth of the consolidating layer is applied. Curve III approximates the case of a dredged fill where the initial excess pore pressure varies linearly from zero at the top of the layer to a maximum at the bottom. In all cases where there is drainage from both surfaces of the layer, curve I should be used and H set to $h/2$.

60. When initial conditions are between those for which the exact solutions have been derived, Terzaghi and Peck (1967) suggest that

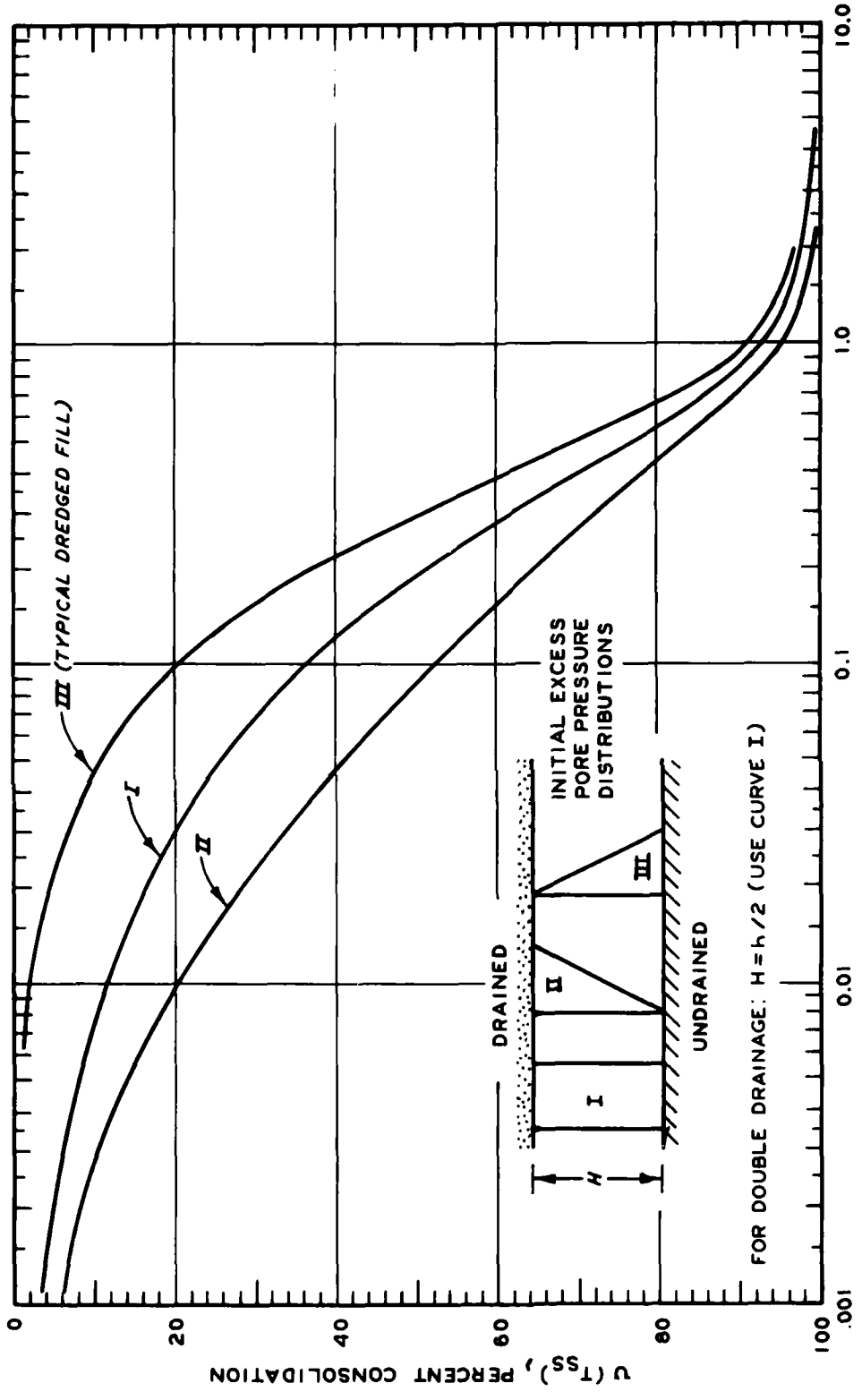

Figure 8. Degree of consolidation as a function of the time factor for various initial conditions by small strain theory

sufficiently accurate results can be obtained by interpolating between the given curves. Considering the approximating assumptions upon which these solutions are based, interpolation should not lead to any less accurate results.

Finite strain solutions

61. Solutions to the linear governing Equation 45 are also possible in terms of nondimensional variables which enable the computation of settlements as a function of time similar to the small strain procedure. Partial solutions for the case of a normally consolidated layer are given by Gibson, Schiffman, and Cargill (1981). These solutions will be supplemented here by the cases of normally consolidated layers with drainage from both surfaces and of underconsolidated dredged fill type deposits both singly and doubly drained.

62. For consistency with the sign convention used by the above cited authors, it is necessary to measure the z-coordinate from the top of the consolidating layer positive downwards or against gravity. This has the effect of changing the minus sign in Equation 45 to a positive sign. Defining the nondimensional variables as

$$E(z,t) = \frac{e(z,t)}{e(0,0)} \tag{51}$$

$$Z = \frac{z}{\ell} \tag{52}$$

$$T_{fs} = \frac{gt}{\ell^2} \tag{53}$$

$$N = \lambda\ell(\gamma_s - \gamma_w) \tag{54}$$

$$B = \frac{e_\infty}{e(0,0)} \tag{55}$$

$$R = \frac{e(0,t)}{e(0,0)} \tag{56}$$

where ℓ is the total layer thickness in reduced coordinates, T_{fs} is

the dimensionless finite strain time factor, and other variables are as previously defined, the governing equation becomes

$$\frac{\partial^2 E}{\partial Z^2} + N \frac{\partial E}{\partial Z} = \frac{\partial E}{\partial T_{fs}} \tag{57}$$

63. The initial condition for a normally consolidated layer subjected to a sudden surcharge is

$$E(Z,0) = (1 - B) \exp(-NZ) + B \; ; \; 0 \leq Z \leq 1 \tag{58}$$

and boundary conditions for the case where both boundaries are free draining are

$$E(0,T_{fs}) = R \; ; \; T_{fs} > 0 \tag{59}$$

and

$$E(1,T_{fs}) = (R - B) \exp(-N) + B \; ; \; T_{fs} > 0 \tag{60}$$

If the lower boundary is impervious, Equation 60 is replaced by the condition

$$\frac{\partial E}{\partial Z} + N[E(1,T_{fs}) - B] = 0 \; ; \; T_{fs} > 0 \tag{61}$$

64. The initial condition for a dredged fill layer deposited at a uniform initial void ratio and subject to self-weight consolidation only is

$$E(Z,0) = 1 \; ; \; 0 \leq Z \leq 1 \tag{62}$$

and boundary conditions for the case of two pervious boundaries are

$$E(0,T_{fs}) = 1 \; ; \; T_{fs} > 0 \tag{63}$$

and

$$E(1,T_{fs}) = (1 - B) \exp(-N) + B \; ; \; T_{fs} > 0 \tag{64}$$

For an impervious lower boundary, Equation 64 is replaced by Equation 61.

65. If a nondimensional settlement is defined as

$$S(T_{fs}) = \frac{\delta(T_{fs})}{\ell e(0,0)} = \int_0^1 \left[E(Z,0) - E(Z,T_{fs})\right] dZ \tag{65}$$

where δ is the actual settlement, then a percent consolidation U can be calculated by

$$U(T_{fs}) = \frac{S(T_{fs})}{S(\infty)} \tag{66}$$

where $S(\infty)$ is the ultimate nondimensional settlement. This percent consolidation is therefore directly related to real settlements unlike small strain theory which depends on a linear coefficient of compressibility.

66. While the analytical solution of Equation 57 with appropriate initial and boundary conditions and Equations 65 and 66 would be a formidable if not impossible task, their solution by the techniques of finite differences and numerical integration is practical with the aid of a computer. With the aid of a version of the computer program FSCON1 (Cargill and Schiffman 1980) modified to accept the dredged fill boundary and initial conditions, the figures on the following pages were constructed. Figure 9 shows the degree of consolidation as a function of the time factor, T_{fs}, for various values of N and initial and boundary conditions corresponding to a normally consolidated clay layer whose bottom boundary is impervious, and Figure 10 depicts degree of consolidation for values of N where both boundaries are pervious. The case of a dredged fill deposit is shown in Figure 11 for drainage from the top only and Figure 12 for drainage from both surfaces.

67. Comparison of the $N = 0.0$ curve in Figure 9 with the type I curve in Figure 7 shows an almost exact correspondence until about 92 percent consolidation. This verifies the numerical technique used in FSCON1 since analytically the curves should be the same. The different pattern of the curves in Figure 12 is totally unpredicted by any small strain theory and probably due to the fact that the permeability decrease at the bottom-drained boundary causes this boundary to behave as if it were undrained for thick layers.

68. These figures can be used exactly the same way Figure 8 would be used in a small strain formulation once a final or ultimate settlement has been derived. The only difference is the requirement to

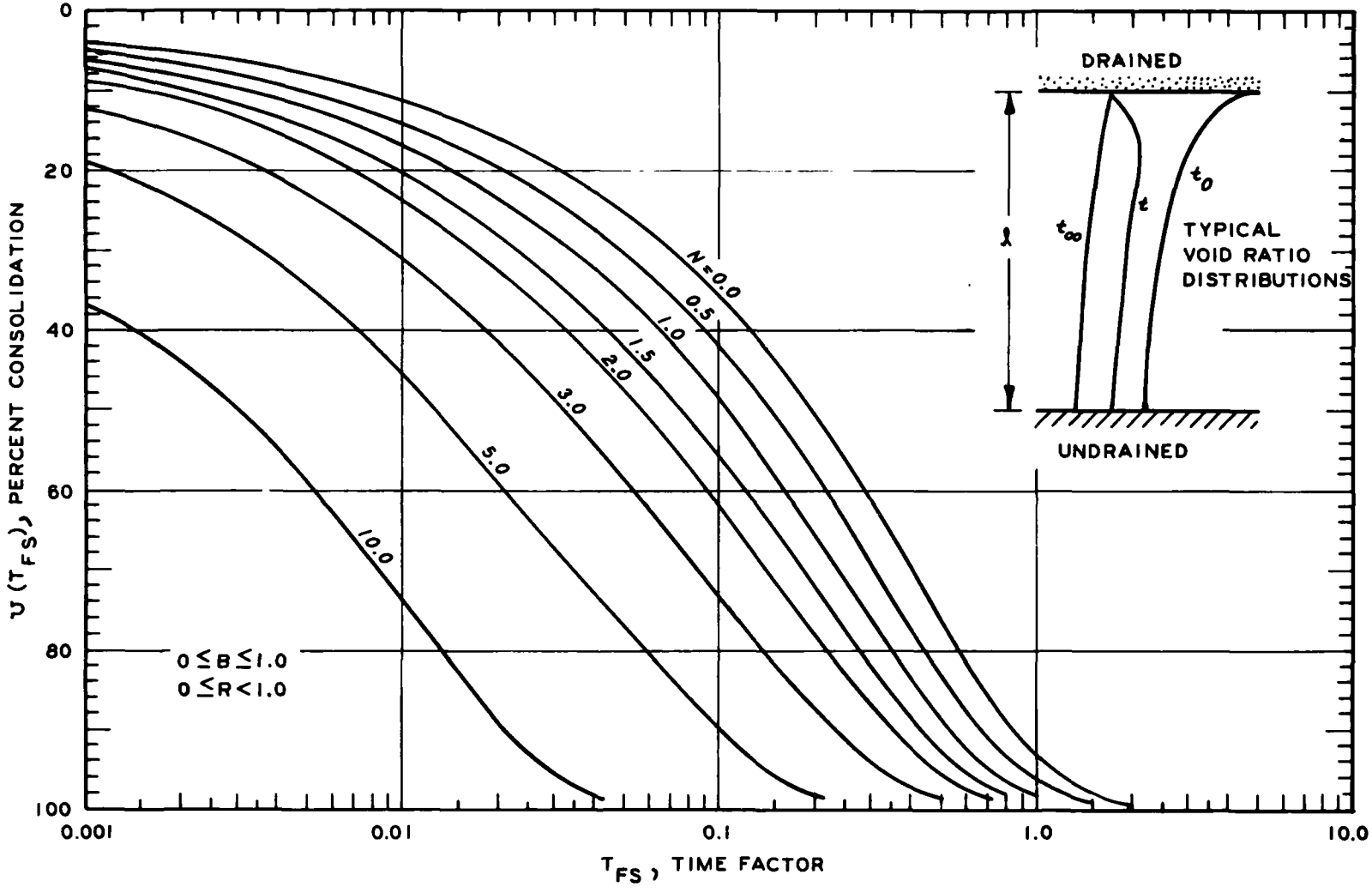

Figure 9. Degree of consolidation as a function of the time factor for normally consolidated, singly drained layers by linear finite strain theory

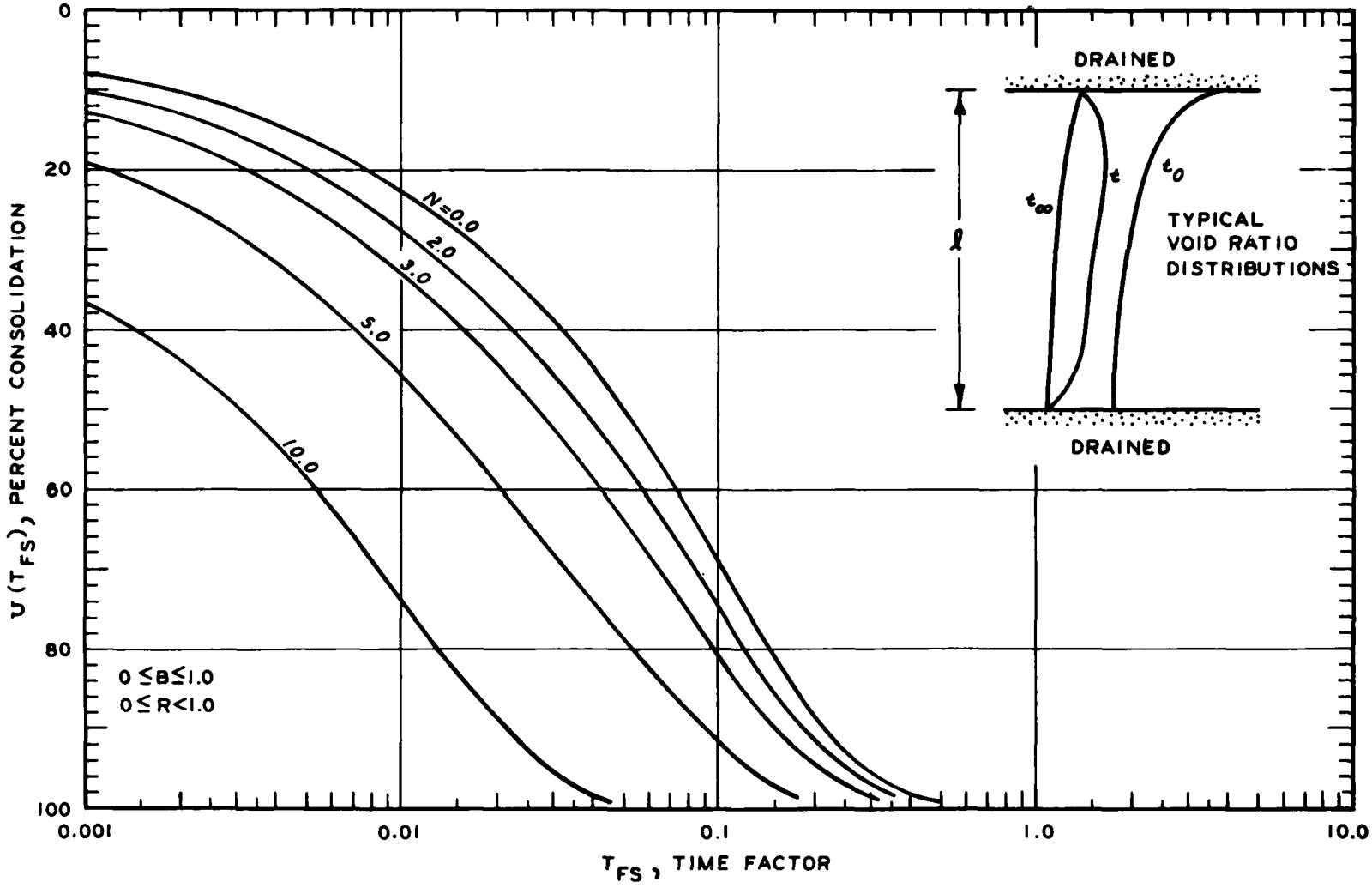

Figure 10. Degree of consolidation as a function of the time factor for normally consolidated, doubly drained layers by linear finite strain theory

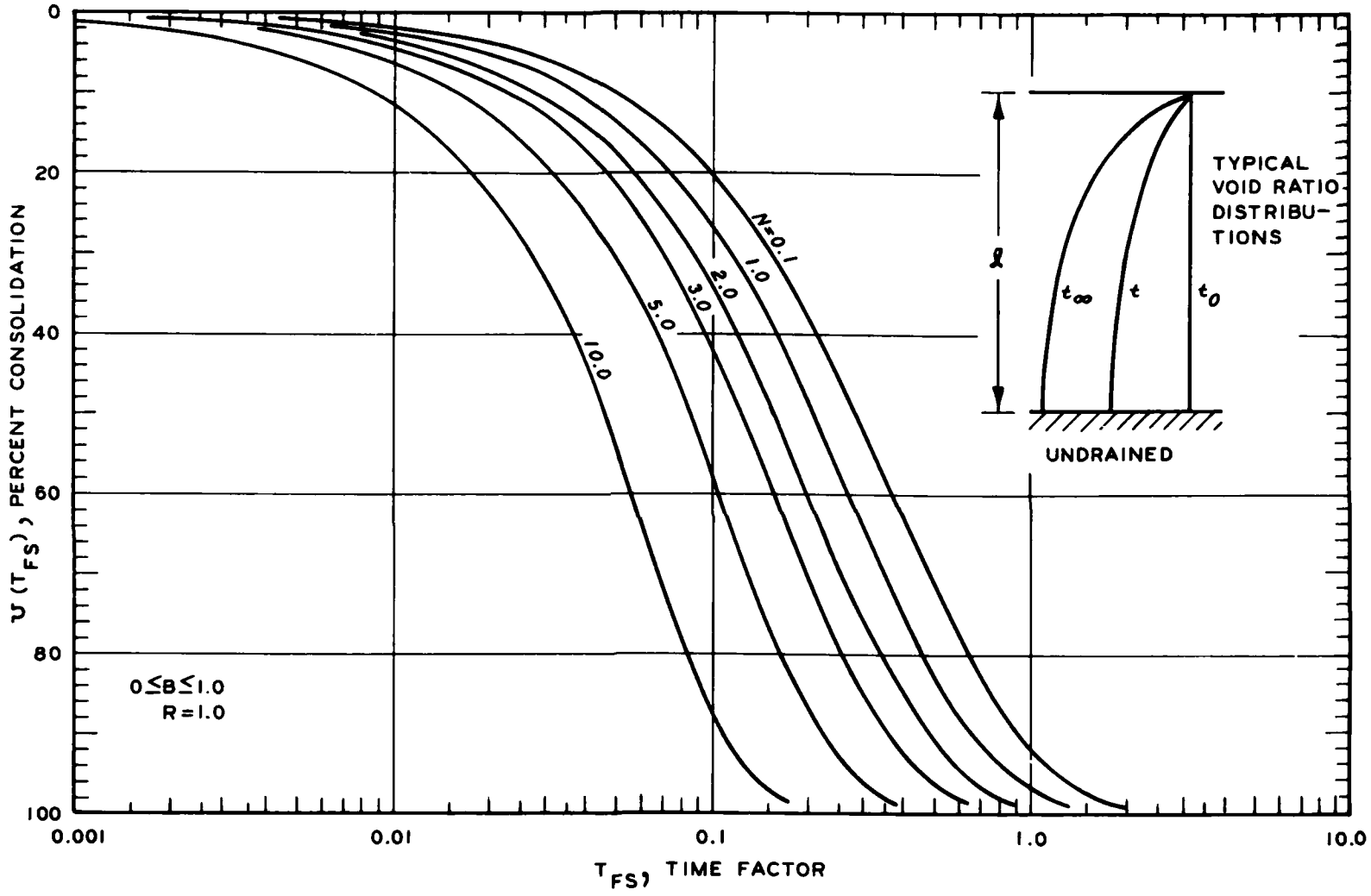

Figure 11. Degree of consolidation as a function of the time factor for dredged fill, singly drained layers by linear finite strain theory

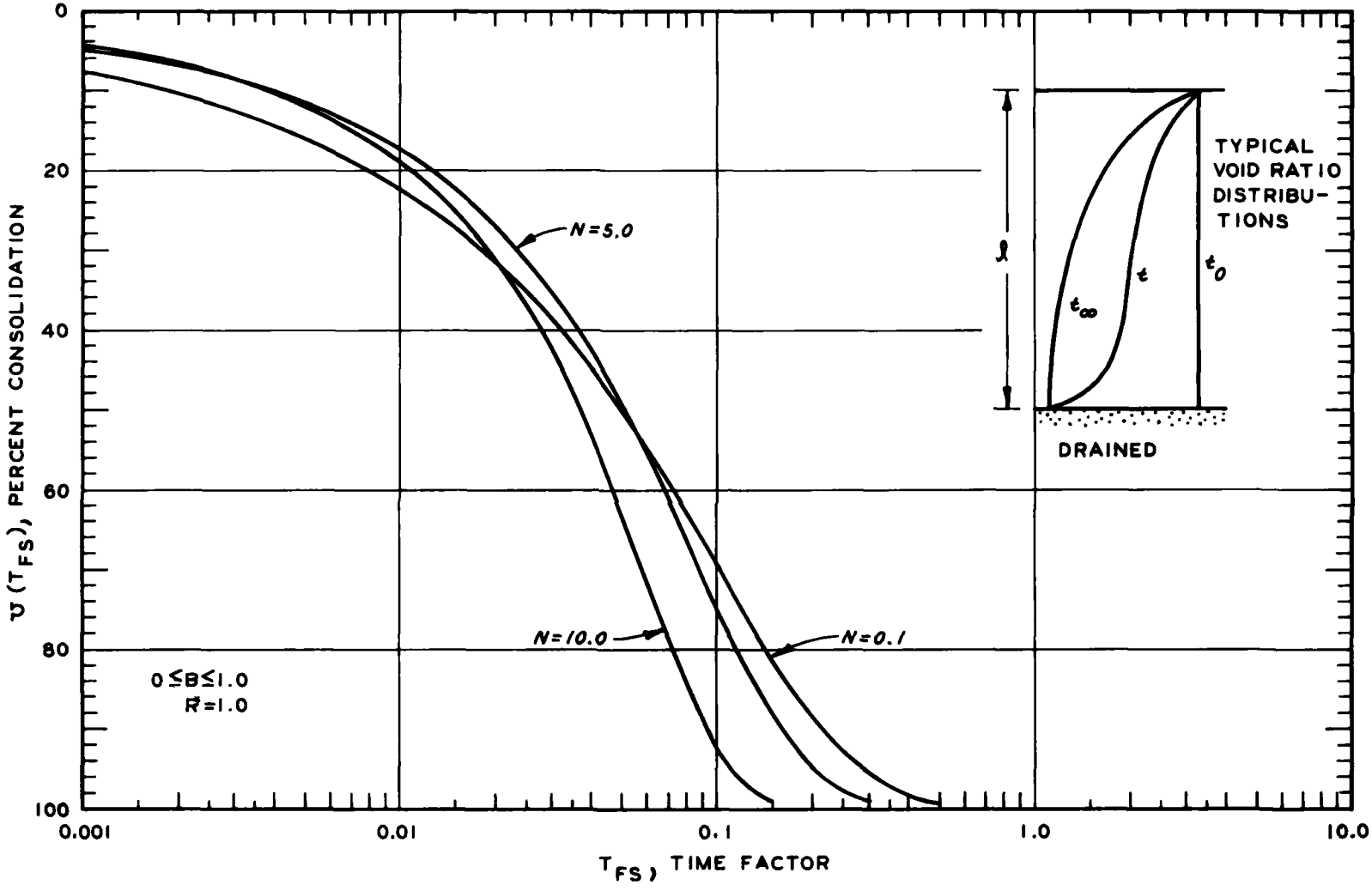

Figure 12. Degree of consolidation as a function of the time factor for dredged fill, doubly drained layers by linear finite strain theory

calculate ℓ , the layer thickness in reduced coordinates.

69. The calculation of ℓ is a very simple matter for dredged material deposited at a uniform initial void ratio. Here

$$\ell = \frac{h}{1 + e_{oo}} \tag{67}$$

where h is the layer thickness as deposited and e_{oo} is the initial void ratio since the effective stress is assumed initially zero throughout the layer. In a normally consolidated layer or layer having any other than uniform void ratio distribution, ℓ can be calculated to sufficient accuracy by dividing the layer into a number, m , of sublayers and using

$$\ell = \sum_{i=1}^{m} \ell_i = \sum_{i=1}^{m} \frac{h_i}{1 + e_i} \tag{68}$$

where h_i is the sublayer height and e_i is the average void ratio in the sublayer. The sublayer void ratio is obtained from the e - log σ' curve for the material by considering the effective weight of all material and surcharge above the center of the sublayer or by direct measurement of the saturated water content of the sublayer.

Calculation of Ultimate Settlement

70. The ultimate settlement of a consolidating fine-grained layer is defined as that which has occurred after all excess pore pressures have dissipated. Within the layer, the soil assumes a void ratio distribution due to the buoyant weight of material above plus any surcharge, and this void ratio is related to the effective stress by the material's e - log σ' curve which comes typically from an oedometer test. Therefore, initial and final void ratio distributions are known or can be calculated.

71. It can be shown (Cargill 1982) that ultimate settlement is given by

$$\delta(\infty) = \int_0^{\ell} [e(z,0) - e(z,\infty)]\, dz \qquad (69)$$

where $e(z,0)$ is the initial void ratio and $e(z,\infty)$ is the final void ratio. This equation can be solved with sufficient accuracy by dividing the total layer into a number, m, of sublayers such that

$$\delta(\infty) = \sum_{i=1}^{m} \delta_{i,\infty} = \sum_{i=1}^{m} (e_{i,o} - e_{i,\infty})\, \ell_i \qquad (70)$$

where ℓ_i is defined in Equation 68, and $e_{i,o}$ and $e_{i,\infty}$ are the average initial and final void ratios, respectively.

72. While Equation 69 could have been reduced to an analytical expression by making typical small strain or linearizing finite strain assumptions, there is no particular advantage in doing this when the actual relationship between void ratio and effective stress is available from oedometer testing. The ultimate average effective stress is simply calculated for each sublayer by

$$\sigma_i' = \frac{1}{2}\, \ell_i\, (\gamma_s - \gamma_w) + \begin{pmatrix}\text{effective weight}\\ \text{of all sublayers}\\ \text{above it}\end{pmatrix} + (\text{surcharge}) \qquad (71)$$

where the effective weight of each sublayer is $\ell_i\, (\gamma_s - \gamma_w)$ Then, using this average effective stress an average void ratio is picked from the oedometer test data and substituted into Equation 70.

Time-Dependent Settlements

73. Time-dependent settlements for a single layer subjected to a single consolidating load is readily calculated from information furnished in the previous sections by either a small strain or finite strain theory. However, if additional layers are added before the previous layers have completely consolidated or additional consolidating loads are placed before the layer is completely consolidated under the previous loads, the procedure for calculating time-dependent settlements is not so straightforward. In this section, a proposed procedure for

analyzing the time-settlement relationship for multiple consolidating loads by hand calculation will be described. However, for completeness, the conventional procedure for a single consolidating load will be given first.

Single consolidating load

74. In this case, the coefficient of consolidation, c_v or g, depending on whether a small strain or linear finite strain formulation is chosen, should be determined from a plot such as shown in Figure 6 for the void ratio corresponding to an average effective stress during the consolidation process if the coefficient is relatively constant over the range of expected void ratios. If there is substantial variation in the coefficient of consolidation over the expected range of void ratios, the coefficient can be periodically updated during the calculation to conform to the average void ratio in the layer at the time consolidation is calculated. For small strain theory, the drainage path length H can also be periodically updated to improve the calculation. The procedure for updating will be described in the next subsection.

75. Then using either Equation 48 or 53 a nondimensional time factor for the real time in question is calculated. The percent consolidation is then read from Figure 8, 9, 10, 11, or 12, depending on the theory, initial conditions, and boundary conditions for the calculated time factor. Of course, if the linear finite strain theory is chosen, an appropriate value of N must be obtained by Equation 54 before entering Figure 9, 10, 11, or 12. With the percent consolidation known, settlement is then

$$\delta(T) = \delta_{\infty} \cdot U(T) \tag{72}$$

at the real time t chosen in calculating T.

76. An example of this procedure for a single dredged fill layer deposited on a compressible foundation is solved in Appendix A by both a small strain and linear finite strain formulation. In the example, an updated coefficient of consolidation and layer height are used in calculating the dimensionless time factor.

Multiple consolidating loads

77. The procedure for calculating time-dependent settlements when additional consolidating loads are placed before consolidation is complete under previously placed loads is essentially the same whether small strain or linear finite strain theory is assumed. The accuracy of the procedure depends on the user's ability to successfully estimate initial conditions and interpolate between the previous solutions given for standard initial conditions. Procedurally, there is also no difference if the consolidating loads are caused by added dredged fill layers or added surcharges, which means that the time-dependent settlements are computed by the same method for a compressible foundation as for the dredged fill.

78. Basically, the methodology is an incremental and iterative process whereby each consolidating load is considered individually between the time it was placed and the time the next load or layer is placed with due account taken of all which has occurred previously. That is, for any time t' measured from when the last consolidating load or layer was placed,

$$T' = T(t') \tag{73}$$

where $T(t')$ comes from Equation 48 or 53;

$$U' = U(T') \tag{74}$$

where $U(T')$ comes from Figure 8, 9, 10, 11, or 12, depending on the theory and best estimate of initial conditions (interpolated if necessary);

$$\delta' = U'(\delta'_{\infty} - \delta'') + \delta'' \tag{75}$$

where δ' is the total settlement to time t, δ'_{∞} is the total ultimate settlement and is reevaluated after every new consolidating load or layer, and δ'' is the total settlement accumulated to the time when the new consolidating load or layer was placed; and

$$U(t) = \frac{\delta'}{\delta'_{\infty}} \tag{76}$$

where $U(t)$ is the percent consolidation at real time t since the

first consolidating load or layer was placed. There will be a discontinuity in the $U(t)$ - t curve where a new consolidating load is placed because of the difference in δ'_∞ just before and just after the new load is placed.

79. As an aid to interpolating the figures when initial conditions are different from those used in theoretical solutions, some typical intermediate conditions for single layers subject to one load and typical conditions for when a second load or layer is placed are shown in Figure 13 for small strain and Figure 14 for finite strain theory. The cases of double drainage are shown in subfigures (a), (b), (e), and (f). Single drainage is in (c), (d), (g), and (h). The curve at time t'_∞ is the ultimate distribution if no second consolidating load is placed.

80. An example of this procedure for multiple dredged fill layers deposited on a compressible foundation is solved in Appendix B by both a small strain and linear finite strain formulation. Due to the possibility of substantial changes in the coefficient of consolidation and layer height during the course of consolidation, these factors are continuously updated to correspond to the average void ratio in the layer when consolidation is calculated.

81. The procedure for updating the coefficients of consolidation and layer height is also an iterative process. First, an average void ratio for the time under consideration is assumed and an average layer height $\bar{h}$ for this void ratio is calculated by the equation

$$\bar{h} = \ell(1 + \bar{e}) \tag{77}$$

Then a coefficient of consolidation, c_v or g, is read from a plot such as Figure 6 for the assumed average void ratio. Using the coefficient of consolidation thus chosen and $\bar{h}$ for determining the drainage path length if small strain theory is used, a dimensionless time factor is calculated and settlement determined as previously described. This settlement is then used to determine the layer height which should favorably compare to that calculated by Equation 77. If it does not favorably compare, a new average void ratio is assumed and the process

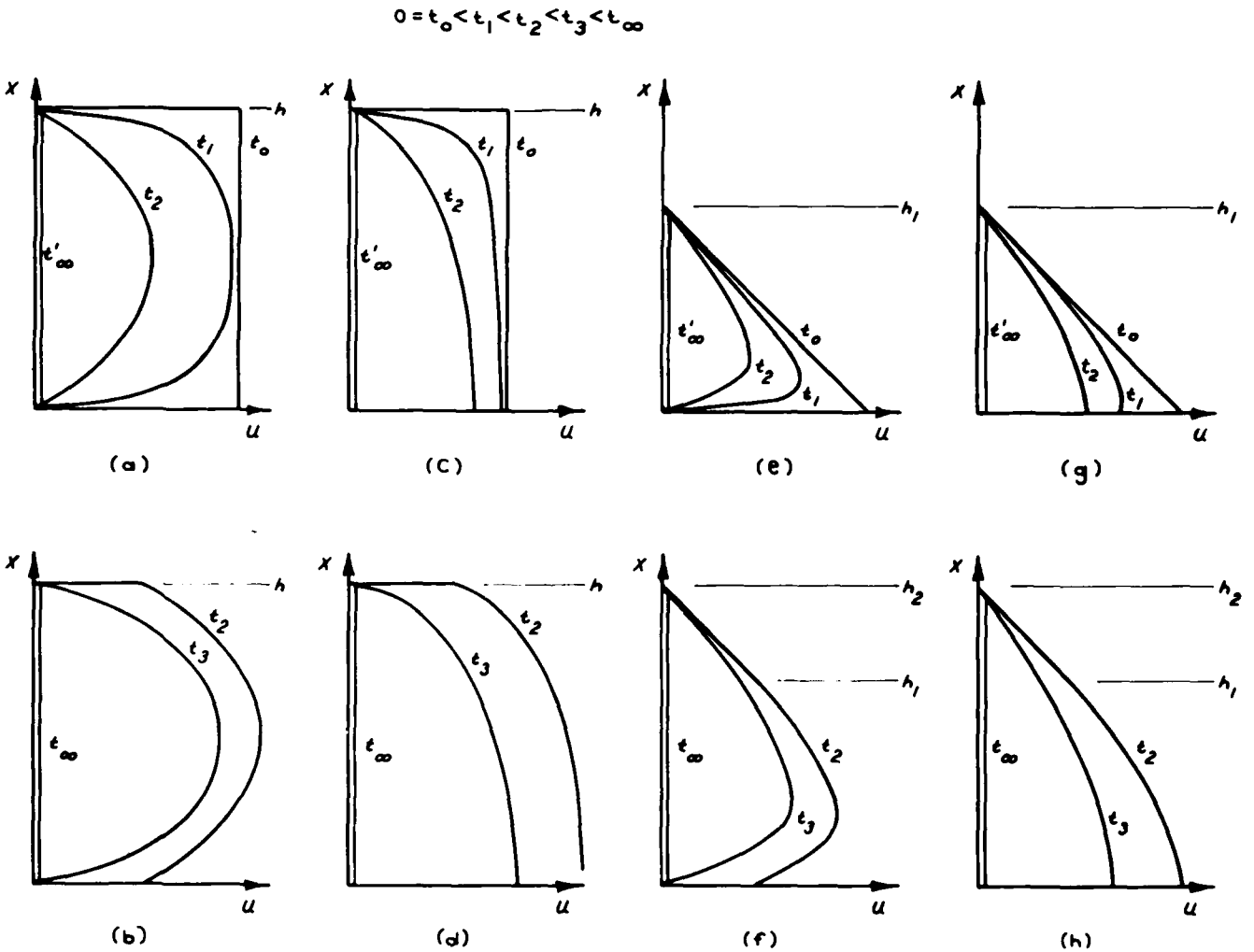

Figure 13. Typical excess pore pressure distributions for a single consolidating load (a, c, e, g) and a second consolidating load applied at t_2 (b, d, f, h)

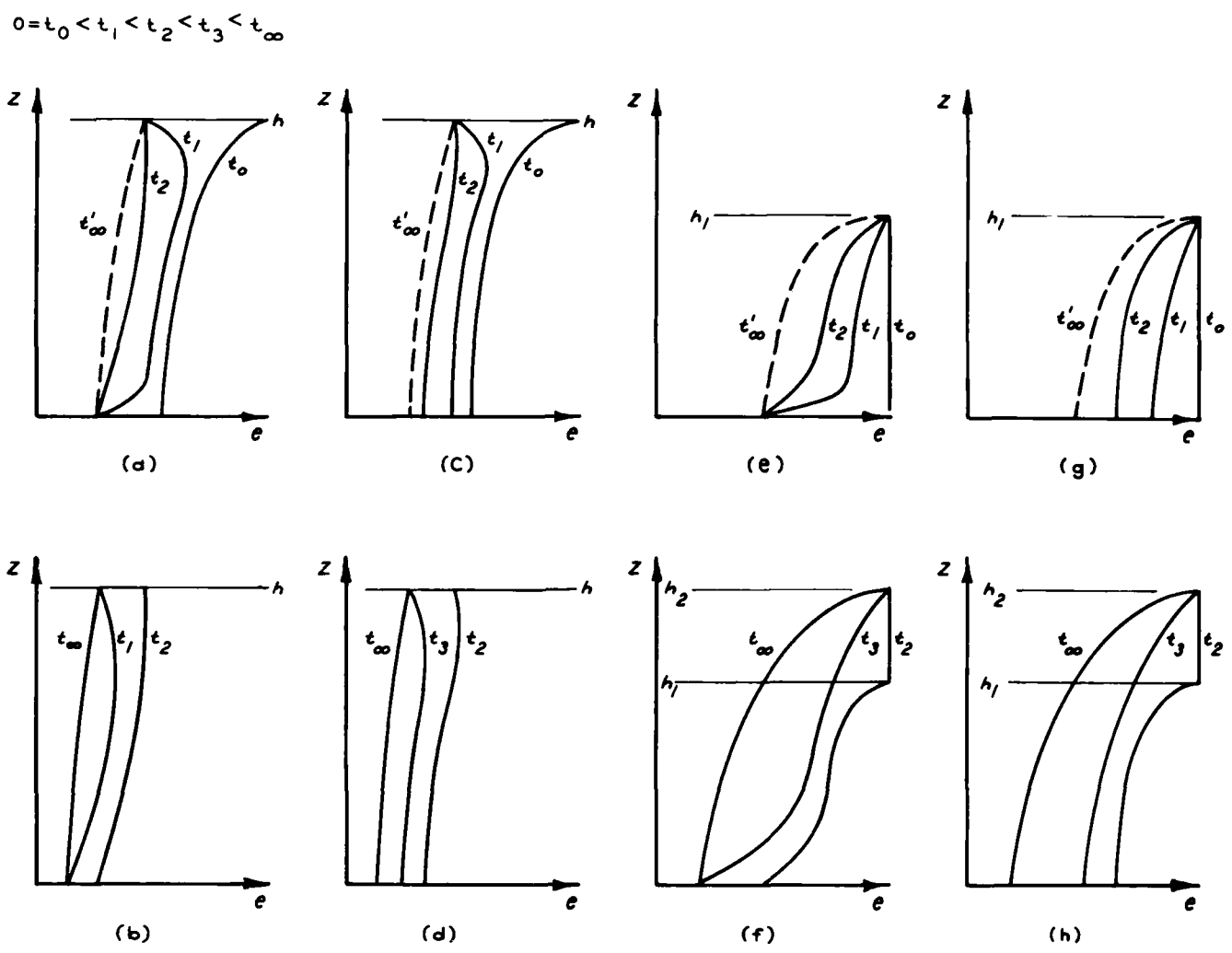

Figure 14. Typical void ratio distributions for a single consolidating load (a, c, e, g) and a second consolidating load applied at t_2 (b, d, f, h)

repeated until a favorable comparison is obtained.

Treating multiple consolidation loads as single consolidation loads

82. In actuality, all consolidating loads should be handled as in the multiple case because no load or layer can be placed instantaneously. Loads can be considered to be placed instantaneously only when the time required to place them is short in comparison to the length of time before the consolidation information is wanted. Therefore, consolidation behavior in many instances of periodic dredged fill disposal can be calculated by the simpler method given for the single consolidating load.

83. Figure 15 illustrates the above phenomenon. In the figure, percent consolidation is plotted against time for the two example problems worked in Appendices A and B which involve, respectively, one instantaneous deposition of 10 ft of dredged material and three incremental depositions which total 10 ft. As can be seen from the figure, after about 4000 days or twice the period of incremental deposition, there is very little difference in the predicted percent consolidation and therefore little difference in predicted settlements. Figure 16 provides the same type comparison using three different disposal schedules for a much softer material modeled in a computer program described by Cargill (1982). Again, after about twice the period of incremental deposition, there is very little difference in predicted percent consolidation.

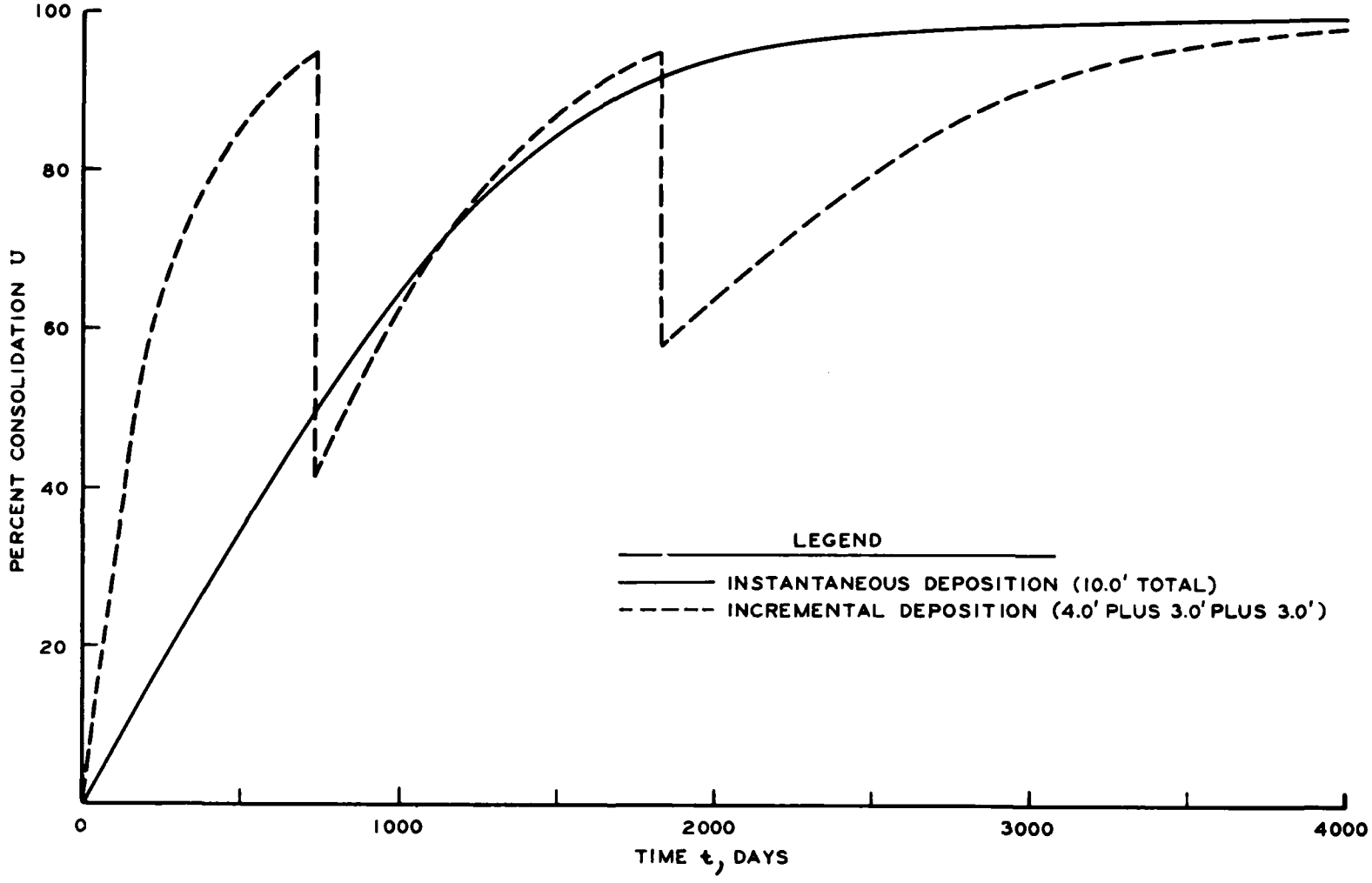

Figure 15. Percent consolidation as a function of time for two different disposal schemes for 10-ft thickness of soft dredged material

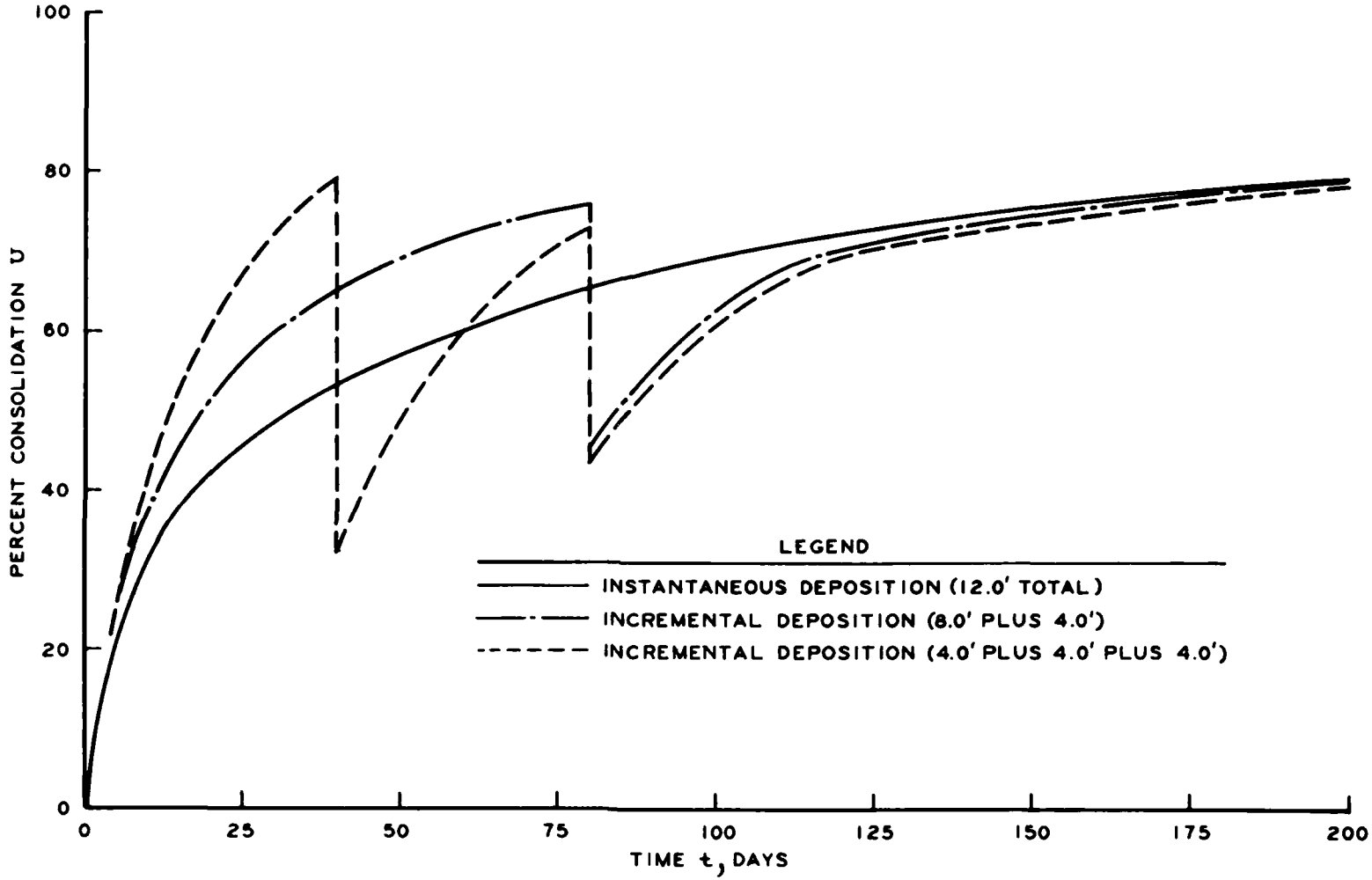

Figure 16. Percent consolidation as a function of time for three different disposal schemes for 12-ft thickness of very soft dredged material

PART III: FIELD VERIFICATION SITES

84. Before a theoretical analysis can be judged useful or appropriate for field design purposes, it should be tested against measured field performance. Therefore, the analysis procedures proposed in the previous part of this report will be used to predict consolidation behavior at two actual dredged material disposal sites and a test pit used in a prior research study. These comparisons are not ideal because, in addition to self-weight consolidation, the sites were also subjected to some surface desiccation and because of some uncertainties about the initial conditions in the dredged material after deposition. However, the sites chosen and information available are deemed the best available and suitable for validation of the proposed procedures.

85. The first site is the Craney Island disposal area near Hampton Roads, Va. Disposal history, field sampling, material testing, and results of area surveys are detailed by Palermo, Shields, and Hayes (1981). Pertinent disposal information will be repeated in this part for completeness. Results of laboratory oedometer testing are given in the next part of this report. The second site is a disposal area for Canaveral Harbor near Cape Canaveral, Fla. Results of field settlement surveys have not been previously reported. The test pit used as the third verification site was constructed in the Upper Polecat Bay disposal area near Mobile, Ala. Details of the test pit purpose and results are given by Hammer (1981). Pertinent information will also be repeated herein.

Craney Island

86. The Craney Island disposal site is a 2500-acre area confined by dikes about 28 ft high. Dike bottom elevation is about -10.0 ft mlw (mean low water), and top elevation averages about +18.0 ft mlw. Since dike construction started in August 1954, approximately 130 million cu yd of in situ channel sediments has been deposited in the area almost continuously by both direct pipeline discharge and hopper pumpout. Surface

desiccation at the site was not possible until about the end of 1965 when the average surface of the disposal area came above the surrounding mean low water elevation. Surface desiccation after 1965 was probably limited due to the almost continual input of large volumes of dredged material.

87. Field sampling and testing as reported by Palermo, Shields, and Hayes (1981) indicated that the average in situ void ratio of channel sediments was about 5.93, that the sediments averaged about 15 percent sand (particle size >0.075 mm), and that upon initial sedimentation the fine-grained portion of the dredged material assumed an average void ratio of about 12.0 in the disposal area. If it is assumed that the sand solids will settle separately immediately after disposition to a void ratio conservatively estimated at about 2.0 (the void ratio would usually be lower), then about 4 percent of the disposal area will be required for sand deposition. Thus, the fine-grained portion will then settle and consolidate in the remaining 2400 acres. The presence of sand mounds commonly found at the outfall of dredged material discharge pipes verifies the validity of this assumption. However, to assess the impact of accounting for the sand fraction in this manner, consolidation calculations will be performed both by assuming the fine-grained solids are 85 percent of the total deposited solids in a 2400-acre area and by assuming 100 percent of the deposited solids are fine grained and the area is 2500 acres.

88. Table 1 shows yearly totals of dredged material deposited at Craney Island and other information required in the consolidation calculations given later in this report. The "Height of Solids" column is the equivalent height of solids with no voids in the dredged fill layer calculated from the volume dredged, disposal area, and in situ void ratio by Equation 67. While volumes are shown rounded to the nearest 10,000 cu yd in the table, material height calculations are based on the more precise data reported by Palermo, Shields, and Hayes (1981).

Canaveral Harbor

89. This disposal site was constructed in 1980 and used for one dredging operation in Canaveral Harbor. The site covers an area of about 20 acres and was filled with dredged material during or about the last week of September 1980. Although detailed information on dredged volumes and disposal area foundation elevations is not available, a sampling program involving three borings was conducted on 9 October 1980 about 1 week after material was deposited. Two settlement plates were also installed at the interface of the foundation and dredged material prior to filling; thus, good data on material settlement are available after 3 November 1980 when the plates were first read. Surface desiccation at the site was probably nonexistent before early spring 1981 but was probably a critical factor afterwards since the dike was breached in the summer of 1981 to aid in the removal of surface water from rainfall.

90. Table 2 lists the results of water content tests performed on samples taken during the boring survey. Corresponding void ratios for a specific gravity of solids of 2.70 are also listed. Using this void ratio and the sampling interval height, a total solids content can be calculated. Void ratios indicated by the borings also suggest that the dredged material was initially deposited at a void ratio of about 17.0 (which corresponds to a solids concentration of 150 g/ℓ). If it is assumed that the average height of solids is 0.4720 ft as shown in the table and the initial void ratio is 17.0, then the unconsolidated height of dredged material deposited is 8.50 ft.

Mobile Bay Test Basin

91. Hammer (1981) describes five test basins constructed in the Upper Polecat Bay disposal area near Mobile, Ala. Basically, the basins had 30-ft-square bottoms, 1 vertical to 2 horizontal side slopes, and depths from 8 to 10 ft. Four of the basins were subjected to various underdrainage techniques, but the one which will be analyzed here had dredged material deposited directly on an impermeable plastic liner.

Table 1

Annual Volumes and Height of Materials Deposited in Craney Island Disposal Area

Year	Dredged Volume @ e = 5.93 10^6 - yd^3	Total Solids 10^6 - yd^3	Dredged Fill Height* @ e = 12.0 ft	Height of Solids* ft	Dredged Fill Height** @ e = 12.0 ft	Height of Solids** ft
1956	0.98	0.14 (0.14)†	0.457 (0.457)	0.0352 (0.0352)	0.405 (0.405)	0.0311 (0.0311)
1957	4.19	0.60 (0.74)	1.947 (2.404)	0.1497 (0.1849)	1.724 (2.128)	0.1326 (0.1637)
1958	5.08	0.73 (1.48)	2.362 (4.766)	0.1817 (0.3666)	2.092 (4.220)	0.1609 (0.3246)
1959	10.29	1.49 (2.96)	4.786 (9.553)	0.3682 (0.7348)	4.238 (8.458)	0.3260 (0.6506)
1960	5.36	0.77 (3.74)	2.492 (12.045)	0.1917 (0.9265)	2.207 (10.665)	0.1698 (0.8204)
1961	3.37	0.49 (4.22)	1.569 (13.614)	0.1207 (1.0472)	1.389 (12.054)	0.1069 (0.9272)
1962	4.29	0.62 (4.84)	1.997 (15.611)	0.1536 (1.2009)	1.768 (13.822)	0.1360 (1.0633)
1963	1.41	0.20 (5.05)	0.656 (16.268)	0.0505 (1.2514)	0.581 (14.404)	0.0447 (1.1080)
1964	3.73	0.54 (5.59)	1.734 (18.002)	0.1334 (1.3847)	1.535 (15.939)	0.1181 (1.2261)
1965	6.23	0.90 (6.48)	2.897 (20.898)	0.2228 (1.6076)	2.565 (18.504)	0.1973 (1.4234)
1966	6.41	0.93 (7.41)	2.983 (23.882)	0.2295 (1.8370)	2.641 (21.145)	0.2032 (1.6266)
1967	10.93	1.58 (8.99)	5.086 (28.967)	0.3912 (2.2282)	4.503 (25.648)	0.3464 (1.9727)
1968	4.88	0.70 (9.69)	2.267 (31.235)	0.1744 (2.4027)	2.008 (27.656)	0.1544 (2.1274)

(Continued)

* Assumes 100 percent of solids are fine grained and area of deposition is 2500 acres.

** Assumes 85 percent of solids are fine grained and area of deposition is 2400 acres.

† Numbers in parentheses are cumulative totals.

Table 1 (Concluded)

Year	Dredged Volume @ e = 5.93 10^6 - yd^3	Total Solids 10^6 - yd^3	Dredged Fill Height @ e = 12.0 ft	Height of Solids ft	Dredged Fill Height @ e = 12.0 ft	Height of Solids ft
1969	5.31	0.77 (10.46)	2.470 (33.704)	0.1900 (2.5926)	2.187 (29.842)	0.1682 (2.2956)
1970	6.19	0.89 (11.35)	2.879 (36.583)	0.2214 (2.8141)	2.549 (32.391)	0.1961 (2.4916)
1971	20.59	2.97 (14.32)	9.574 (46.157)	0.7365 (3.5505)	8.477 (40.868)	0.6521 (3.1437)
1972	2.05	0.30 (14.62)	0.953 (47.110)	0.0733 (3.6239)	0.844 (41.712)	0.0647 (3.2086)
1973	4.18	0.60 (15.22)	1.945 (49.055)	0.1496 (3.7735)	1.722 (43.434)	0.1325 (3.3411)
1974	4.48	0.65 (15.87)	2.084 (51.139)	0.1603 (3.9338)	1.845 (45.279)	0.1419 (3.4830)
1975	5.04	0.73 (16.59)	2.345 (53 484)	0.1804 (4.1142)	2.076 (47.356)	0.1597 (3 6427)
1976	4.51	0.65 (17.25)	2.099 (55.583)	0.1615 (4.2756)	1.859 (49.214)	0.1430 (3.7857)
1977	2.13	0.31 (17.55)	0.990 (56.573)	0.0762 (4.3518)	0.877 (50.091)	0.0674 (3.8531)
1978	6.80	0.98 (18.53)	3.164 (59.737)	0.2434 (4.5952)	2.801 (52.892)	0.2155 (4.0686)
1979	1.33	0.19	0.616	0.0747	0.546	0.0420
TOTAL	129.8	18.73	60.353	4.6426	53.438	4.1106

Table 2

Boring Survey at Canaveral Harbor

Depth Below Water Surface ft	Boring L-1			Boring L-2			Boring L-3		
	Water Content %	Void Ratio	Height of Solids ft	Water Content %	Void Ratio	Height of Solids ft	Water Content %	Void Ratio	Height of Solids ft
1.5							622	16.8	0.0281
2.0				597	16.1	0.0292	571	15.4	0.0305
2.5				646	17.4	0.0271	609	16.4	0.0287
3.0				517	14.0	0.0334	555	15.0	0.0313
3.5				554	15.0	0.0313	537	14.5	0.0322
4.0	578	15.6	0.0301	439	11.9	0.0389	482	13.0	0.0357
4.5	541	14.6	0.0321	497	13.4	0.0346	449	12.1	0.0381
5.0	527	14.2	0.0328	529	14.3	0.0327	398	10.7	0.0426
5.5	492	13.3	0.0350	546	14.7	0.0318	375	10.1	0.0450
6.0	463	12.5	0.0371	556	15.0	0.0312	355	9.6	0.0472
6.5	501	13.5	0.0344	450	12.2	0.0380	333	9.0	0.050
7.0	452	12.2	0.0379	434	11.7	0.0393			
7.5	343	9.2	0.0488	392	10.6	0.0432			
8.0	363	9.8	0.0463	445	12.0	0.0384			
8.5	235	6.3	0.0682	501	13.5	0.0344			
9.0				459	12.4	0.0373			
9.5				422	11.4	0.0403			
10.0				394	10.6	0.0429			
TOTAL			0.4027			0.6040			0.4094

Average height of solids = 0.4720 ft.
Average unconsolidated height of fill (@ e = 17.0) = 8.50 ft.

It was reported that basin construction took place May through September 1976 and that dredged material was pumped into the basins during the month of October 1976 by a "Mud Cat" dredge through an 8-in. pipeline. There was no surface desiccation of material in the test basin until 10 March 1977 when an active surface drainage program was initiated.

92. It is important to note that this was not a typical dredged fill disposal operation, not only due to the site and shape of the disposal area, but also because of the filling procedure. Hammer (1981) states, "Since the slurry being pumped by dredge contained 15 to 25 percent solids it was necessary to fill each test section several times before the 6-ft desired depth of dredged material was attained. The general procedure for accomplishing this was to pump full, allow the solids to settle out (generally 24 hr was allowed for this), pump the clear water off, and fill again. This procedure was repeated until each test section contained sufficient solids for the experiment."

93. Figure 17 shows water content distribution within the deposited material at the beginning and end of the experiment. The "initial" curve is actually about 40 days after deposition started when all sedimentation and in fact some consolidation had probably taken place. Based on these measurements and a specific gravity of solids of 2.70, the height of solids can be calculated. The void ratio indicated by the uppermost "initial" water content and previous verbal description of the slurry percent solids suggest that the dredged material was initially deposited and sedimented to a void ratio of 10.0. If it is assumed that the average height of solids is 0.8711 ft as shown in the figure, the unconsolidated height of dredged material deposited is 9.58 ft.

PART IV: LABORATORY TESTING FOR SOIL PARAMETERS

94. The accuracy of any calculation of the consolidation behavior of fine-grained dredged material is only as good as the soil parameters used. It is therefore very important that the necessary time and resources be allocated to field sample testing and interpretation of the results. Detailed sampling procedures for obtaining sediment samples are found in Palermo, Montgomery, and Poindexter (1978). This part will review methods of consolidation testing, review a recommended oedometer test procedure for dredged material, discuss test data interpretation, and examine the results of several testing programs.

Consolidation Testing

95. There are essentially three methods of conducting consolidation tests on fine-grained dredged material. They are the self-weight settling test, the constant rate of strain (CRS) test, and the oedometer test. Each of these methods has its advantages and disadvantages and a combination is usually desirable.

Settling test

96. The self-weight settling test is advantageous in determining the void ratio-effective stress relationship at very low levels of effective stress. However, to cover the range of stresses encountered during the consolidation of a prototype dredged fill deposit, the settling column height must equal that of the prototype. If the settling column height equals that of the dredged fill layer, then the time required to complete the test could be on the order of years for typical layers. This is not practical in most situations and so for efficiency the settling test should be supplemented with one of the other type tests for the higher effective stresses.

Constant rate of strain test

97. The CRS test is probably best suited for the mid range of effective stresses where strains are still relatively large per unit of stress. This is probably the most efficient type test in terms of the

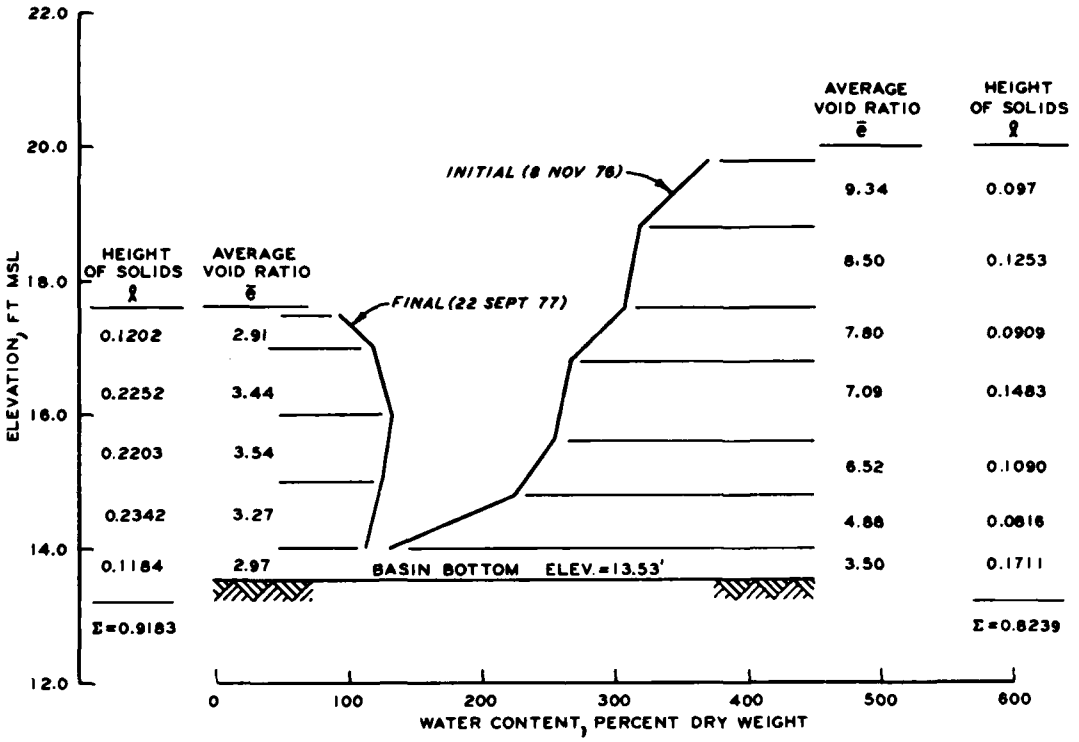

Figure 17. Initial and final water contents at Mobile test basin (after Hammer 1981)

time required for the test because, theoretically, it is applicable for any rate of strain. The only disadvantages to this test are that it requires a rather sophisticated apparatus capable of sustaining a known strain and monitoring stresses and pore pressures in the sample, and that it requires a rather complicated method of analysis. Because of these disadvantages, CRS devices are commonly found only in research facilities and are not readily accessible for routine use by Corps Districts. However, there is a preliminary study currently (March 1982) under way at the WES looking into the feasibility of constructing a large strain controlled rate of strain (LSCRS) device specifically for the purpose of testing fine-grained dredged material. When such a device is available, it is recommended that it be routinely used to define consolidation properties at the high void ratios common to dredged fill.

98. To demonstrate the type information obtainable from a CRS test and supplement the available consolidation properties of dredged material from Canaveral Harbor and Mobile test basin, CRS testing of material from each of these sites was contracted with the University of Colorado as part of this study. The testing apparatus and test data analysis are fully described by Znidarcic (1982). Basically, a 4.0-cm-high sample with one drained boundary is deformed at a constant rate; total stresses are measured at both ends; and pore pressure is measured at the undrained boundary. A modified finite strain theory of consolidation which neglects material self-weight and assumes a piecewise linear coefficient of consolidation g is used to analyze test measurements and produce the void ratio-effective stress and void ratio-permeability relationships. As an alternative, the void ratio-permeability relationship is also derived using a calculated excess pore pressure gradient at the drained boundary and Darcy's law. Results of these tests are given later in this Part.

Oedometer test

99. The most common type of consolidation testing currently available is the oedometer test. The apparatus required by this test is found in all well-equipped soils laboratories, and the test has been used successfully by the WES on numerous dredged fill materials.

Disadvantages of the test include:

a. The fact that void ratio-effective stress relationships at very low (<0.005 tsf) levels of effective stress are generally not possible.

b. The fact that the time required between load increments may sometimes be 2 weeks or more.

c. The fact that large strains during a given load increment add to the uncertainties of test data analysis for coefficients of consolidation and permeabilities.

d. The question of whether a thin oedometer sample with no initial excess pore pressure and subjected to a sudden load increment reacts the same as an underconsolidated thick sample whose excess pore pressure is slowly decreased.

Regardless of the disadvantages, the fact that it is the most common and readily available test is an advantage which makes the oedometer test the most attractive for dredged material today.

Recommended Oedometer Test Procedure

100. Oedometer testing of very soft dredged fill materials is accomplished essentially the same as is specified in EM 1110-2-1906 (Headquarters, Department of the Army 1970) for stiffer soils. The major difference is in the initial sample preparation and the size of the load increments. The majority of dredged fill samples will be in the form of a heavy liquid rather than a mass capable of being handled and trimmed.

101. Before testing begins, accurate weights and buoyant weights of the top porous stone and other items between the sample and dial gage stem should be determined because this will be a major part of the seating load. The force exerted by the dial indicator spring must also be determined for the range of readings initially expected because this will constitute the remainder of the seating load and will be considered the first consolidating load applied to the sample. Figure 18 shows how the dial gage force is determined using a common scale or balance. Samples are prepared for testing by placing a saturated bottom porous stone, filter paper, and consolidometer ring on the scale and recording their weights. Without removing this apparatus from the scale, material

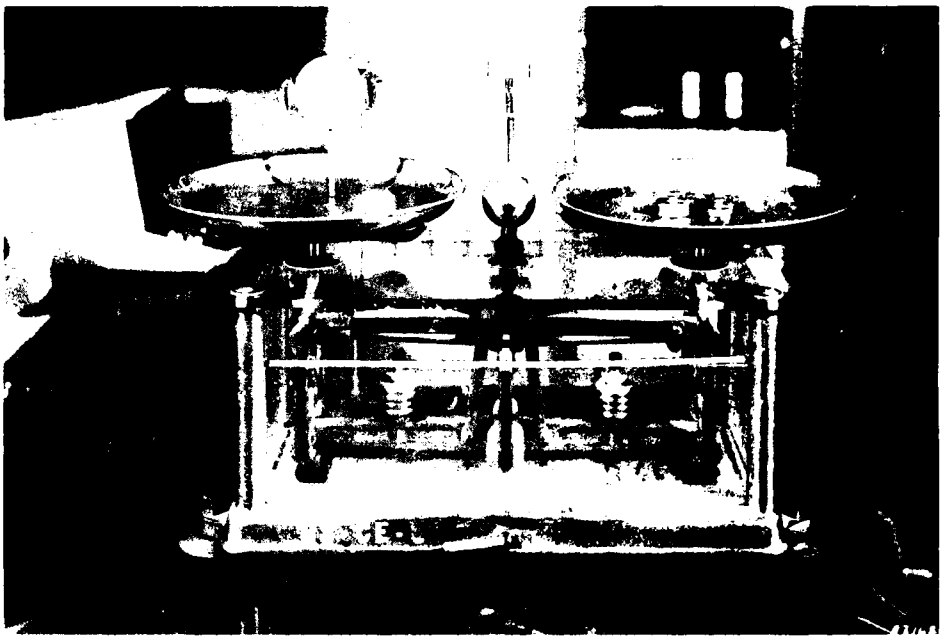

Figure 18. Determination of dial gage force for oedometer test on soft dredged material

is placed in the ring with a spatula. The material is placed and spread carefully to avoid trapping any air within the specimen. After slightly overfilling the ring with material, the excess is screeded with a straightedge, with care being taken not to permit excess material to fall onto the scale. After a level surface flush with the top of the ring is obtained, the ring top is wiped clean and a final weight recorded. Figure 19 shows material being placed in the consolidation ring. In Figure 20, the material is shown being screeded.

102. The ring with bottom stone is next assembled with the remainder of the consolidometer apparatus. Care must be taken not to jar or otherwise disturb the sample during this process. Figure 21 shows the assembled consolidometer and components of the seating load. Once the consolidometer is ready, it is placed on the loading platform and assembly completed. As soon as the seating load is placed, the water level in the consolidometer should be brought level with the top of the top porous stone and held there through at least the first three load

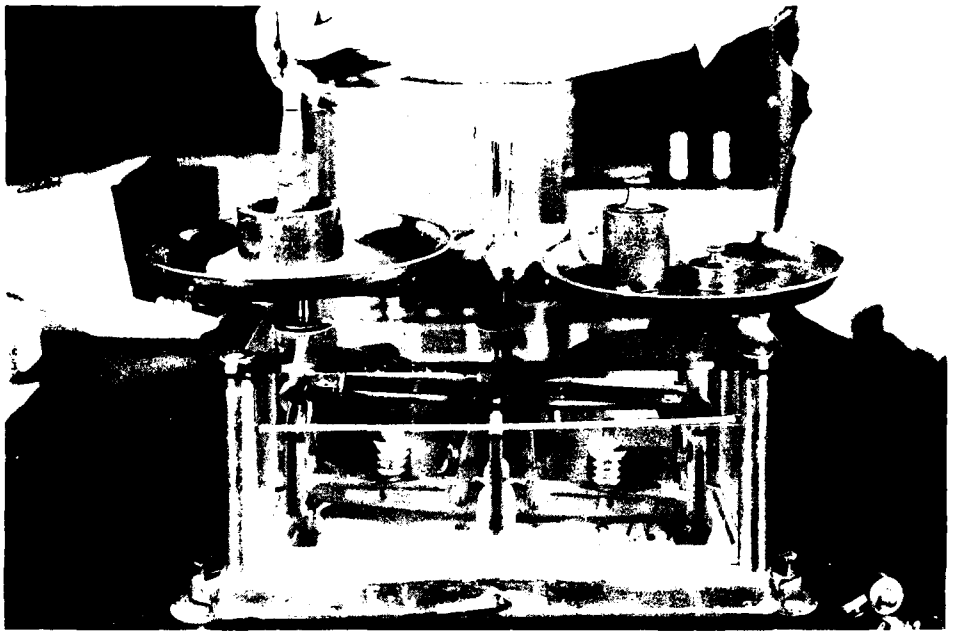

Figure 19. Placement of soft dredged material in consolidation ring

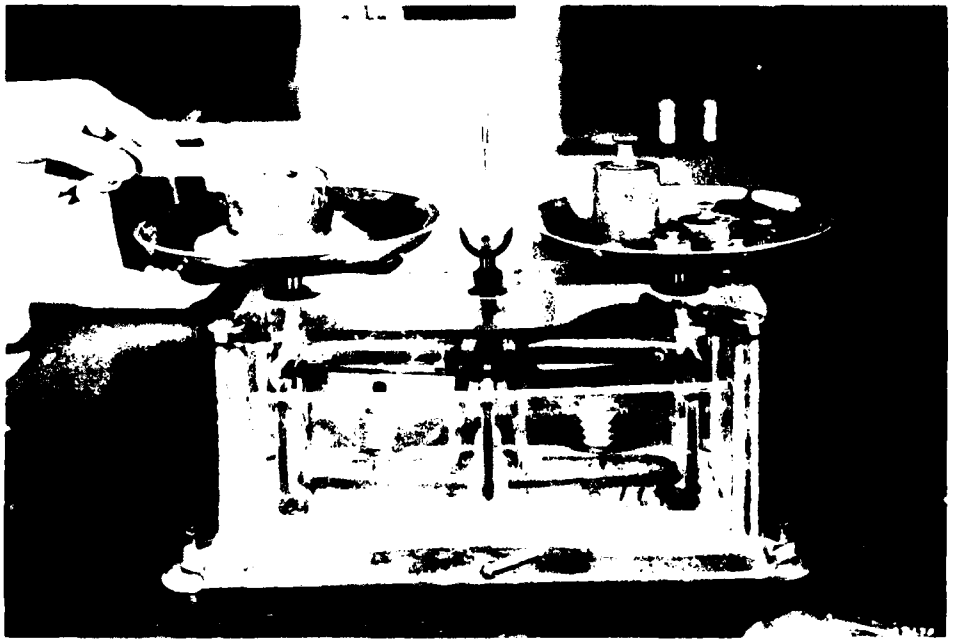

Figure 20. Material being screeded flush with top of consolidation ring

Figure 21. Assembled consolidometer and components of seating load

increments or until the difference in the actual weight and buoyant weight of the seating load is insignificant. Thereafter, the level of the water is not important so long as the sample is kept inundated.

103. Since some consolidation will normally occur very rapidly when the seating load is placed, it is important that this first load, to include the dial gage, is placed very quickly. If all induced settlement is not accounted for, later calculations may be inconsistent. It may be necessary to use a table level or some other measuring device to check the height of the top of the porous stone above the sample ring at some time during this first load increment. Of course, the thickness of the top porous stone and filter paper must have been previously measured. In this way, a reconciliation between deformation recorded by the dial gage and actual deformation can be made.

104. After the sample has been subjected to the seating load, dial gage readings are taken at times 0.1, 0.2, 0.5, 1.0, 2.0, 4.0, 8.0, 15.0, and 30.0 min; 1, 2, 4, 8, and 24 hr; and daily thereafter until

primary consolidation is complete as determined by the time-consolidation curve. The first series of readings is valid for determination of the first point of the e-log σ' curve and may be used in coefficient of consolidation or permeability determinations if the seating load is placed quickly and in a manner so as not to induce extraneous excess pore pressures. Figure 22 shows the sample loaded only by the seating load to include the dial gage.

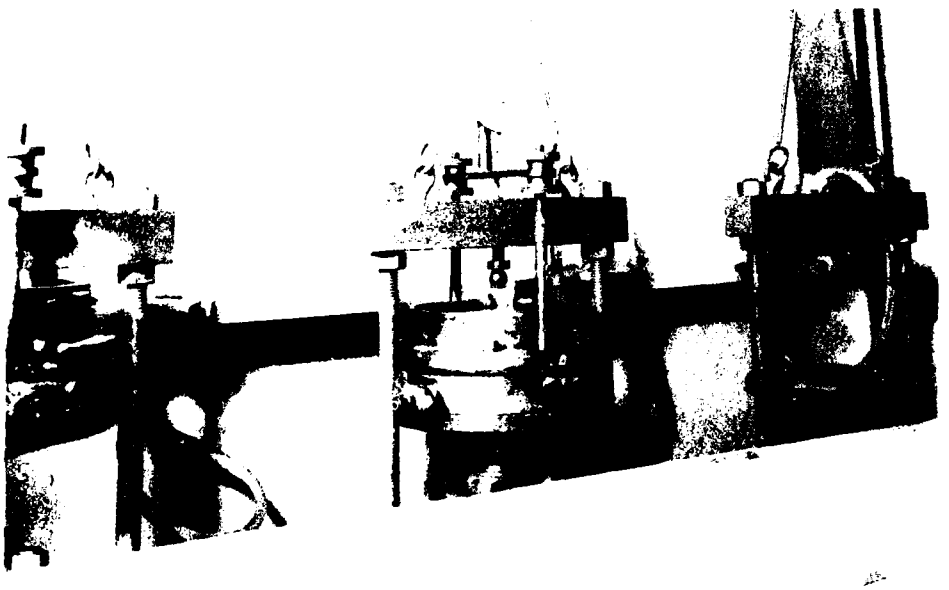

Figure 22. Fully assembled consolidometer loaded by the top porous stone, loading column, and dial gage spring

105. Consolidation of the sample is continued according to the following recommended loading schedule: 0.005, 0.01, 0.025, 0.05, 0.10, 0.25, 0.50, and 1.00 tsf. Exactly what the first load increment will equal depends on the weight of the top porous stone, loading column, and dial gage force. To keep the dial gage force relatively constant throughout testing, the dial gage may have to be reset periodically. If so, it should be reset just before the next load increment is placed and not during a load increment. If consolidation behavior at loads much

greater than about 1.0 tsf is required, it is recommended that samples which have been preconsolidated to 0.5 tsf be used since most typical dredged fill samples will have undergone more than 50 percent strain by the time the above loading schedule is completed. Experience has shown that extrapolation of the e-log σ' curve produced from the recommended loading schedule to lower void ratios should yield reasonably accurate results providing that the void ratios through the extrapolated range are greater than about 1.0.

106. When primary consolidation is completed under the final load of the schedule, the difference between the top of the top porous stone and the top of the sample ring should again be determined by a table level or other measuring device as a second check on final sample height as determined from dial gage readings. This check is considered important since the dial gage will probably have been reset several times during the loading schedule. Before the dial gage is removed, the sample should be unloaded and allowed to rebound under the seating load and dial gage force only. When the sample is fully rebounded, a final dial gage reading is made, and the sample is removed for water content and weight of solids measurements.

107. The preceding recommended test procedure is not meant to replace the more comprehensive treatment of EM 1110-2-1906 or other soils testing manuals. Its purpose is merely to point out where the conventional procedure must be modified or supplemented to handle extremely soft dredged fill material. A final recommendation is that a specific gravity of solids test always be accomplished for the actual material consolidated since calculations are very sensitive to this value and typical estimated values may lead to significant error.

Data Interpretation

108. The primary objectives of consolidation testing is determination of the void ratio-effective stress relationship and the variation of the coefficients of consolidation. The e-log σ' curve of the tested material is directly determined from measurements during the test.

However, the coefficient of consolidation must be deduced based on some consolidation theory in the absence of a direct measurement of the void ratio-permeability relationship.

109. Imai (1981) has shown that there can be considerable differences between the e-log σ' curves at the higher ranges of void ratio for the same fine-grained dredged material depending on the initial void ratio of the sample tested. However, the curves were found to merge at effective pressures around 0.001 tsf, which is usually less than the minimum obtainable in an oedometer test. Figure 23 shows e-log σ' curves constructed from Imai's data. Testing by Umehara and Zen (1982) on other fine-grained dredged material verifies Imai's findings. They also have shown that above an effective pressure of about 0.0001 tsf and for equal initial conditions there is a common curve upon which the virgin compression curves produced by the three main methods of consolidation testing all fall. Thus, it may be possible to extrapolate the virgin curve from an oedometer test to void ratios higher than possible in the test with some confidence if the sample tested has been consolidated from an initial condition similar to the initial condition of the dredged material in the disposal area.

110. Therefore, given the void ratio which the dredged material assumes upon initial sedimentation as determined in the column sedimentation test and a virgin compression curve from oedometer testing, an approximate compression curve covering the full range of possible void ratios can be constructed. However, since there is no 0.0 ordinate on an e-log σ' graph, it is proposed that the 0.0001 tsf ordinate be used for plotting the initial void ratio point as determined in the column sedimentation test. Examples of design curves obtained in this manner will be given in the following section.

111. Coefficients of consolidation, c_v and g, can be deduced from oedometer test compression-time curves and Figures 8 and 10, respectively, with appropriate layer heights. However, due to the fact that the coefficient needed must oftentimes be extrapolated to the applicable void ratio and the fact that the tendency of the required relationship cannot be accurately predicted for most materials, it is better to

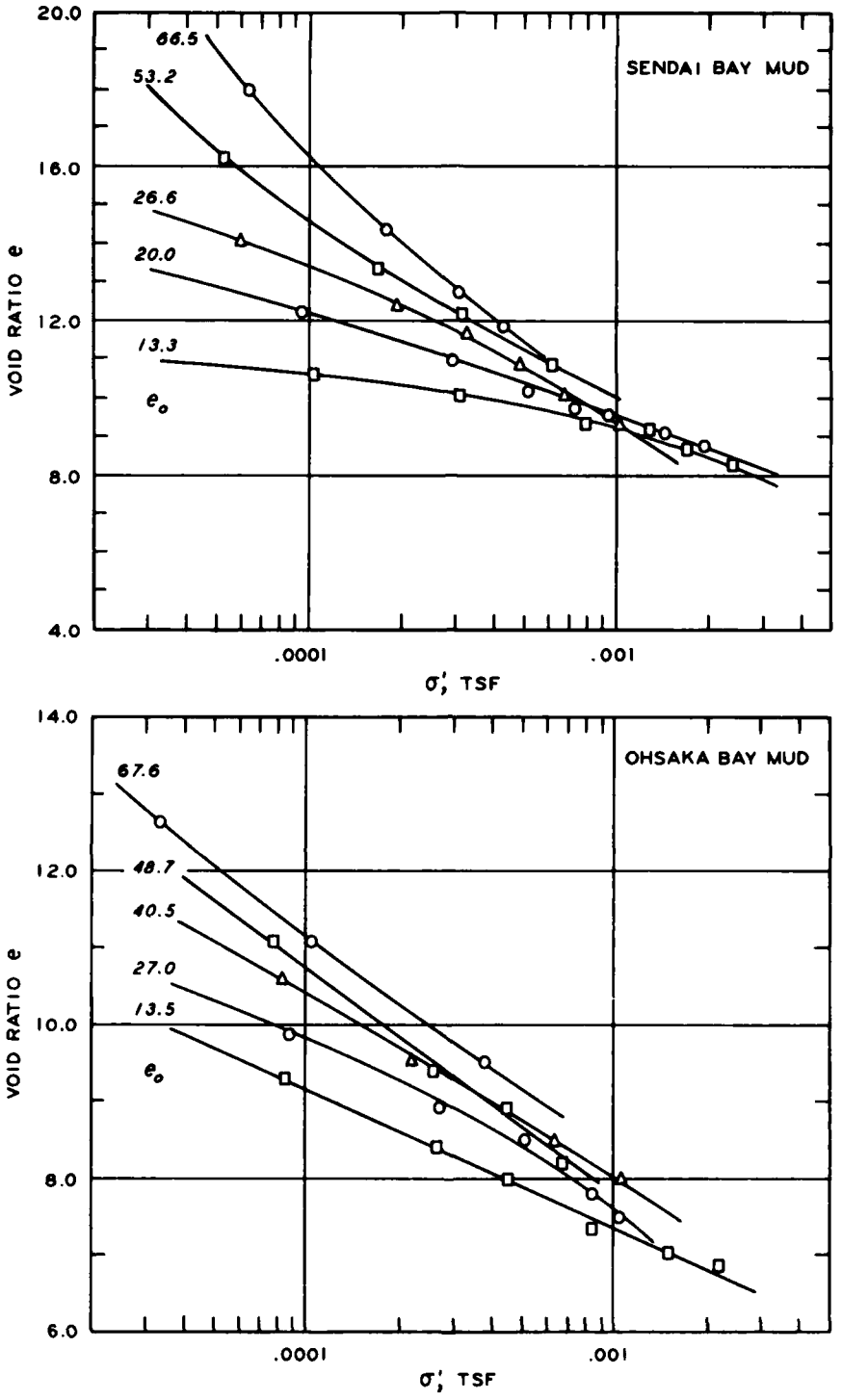

Figure 23. Void ratio-effective stress relationships for very soft, fine-grained materials deposited at various initial void ratios (after Imai 1981)

deduce permeability where tendency can be better predicted (i.e., permeability increases with increasing void ratio) and then calculate the coefficient of consolidation.

112. Since the conditions of the oedometer test correspond very closely with those assumed in small strain consolidation theory when data are analyzed for each load increment, there is probably no advantage in using the more complicated finite strain theory in deducing permeability. Then, using Equations 21 and 48, the expression

$$k = \frac{T_{ss}\bar{H}^2\gamma_w\bar{a}_v}{(1 + \bar{e})t} \tag{78}$$

can be written where the bar indicates average values during the load increment. If 50 percent consolidation is assumed to occur simultaneously with 50 percent settlement, the equation can be written

$$k = \frac{0.197\bar{H}^2\alpha_w\bar{a}_v}{(1 + \bar{e})t_{50}} \tag{79}$$

where t_{50} is the time required for 50 percent settlement from the compression-time curve for the particular load increment. The values for k are then plotted versus e, and a smooth curve drawn through the points. Plots of c_v and g versus e can then also be derived using Equation 21 which defines c_v, Equation 42 which defines g, and the e-log σ' curve for finding a_v at the particular value of e. Examples of these distributions are given in the next section.

Test Results

113. Results of oedometer and CRS testing of dredged fill and sediment samples from areas described in Part III of this report, permeability relationships, coefficients of consolidation, and the linearization constant λ are given next in Figures 24 through 35. Variables used in calculating the relationships between void ratio, permeability, and the coefficients of consolidation are tabulated in Appendix C.

Craney Island

114. The void ratio-effective stress relationship for Craney Island is based on oedometer testing of one channel sediment sample and four samples from the disposal area as shown in Figure 24. The test results have been corrected from the originally reported results (Palermo, Shields, and Hayes 1981) by assuming 100 percent saturation at test completion. This was necessary because direct measurements of the specific gravity of solids were not made and original results consistently indicated saturation greater than 100 percent when average specific gravity values were assumed. The solid line shown in the figure is the relationship to be used in later settlement calculations. This relationship is based on the virgin portion of the oedometer test curves and column

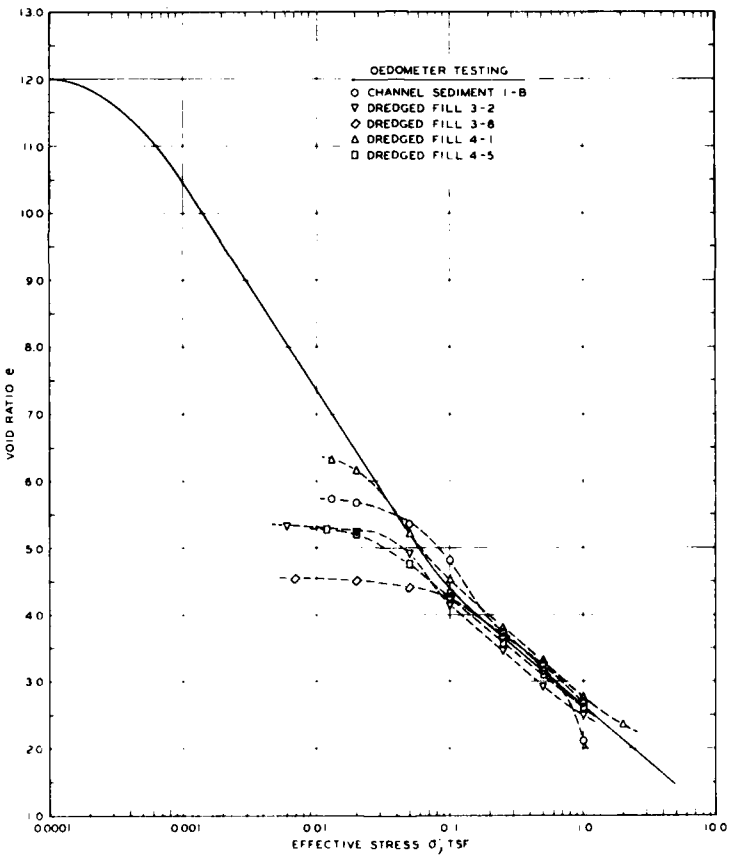

Figure 24. Void ratio-effective stress relationship for Craney Island material

sedimentation tests indicating that after one day of settling the material sediments to an average initial void ratio of 12.0 before consolidation begins. (In Figure 24, and other e-log σ' curves to follow, the 10^{-4} tsf ordinate is assumed to correspond to essentially zero effective stress and is used for plotting e_{oo}.)

115. Figure 25 shows the void ratio-permeability relationship for the Craney Island material as deduced from the oedometer testing data. Individual points were calculated from Equation 79 and variables from each oedometer test as tabulated in Table C1 found in Appendix C. There

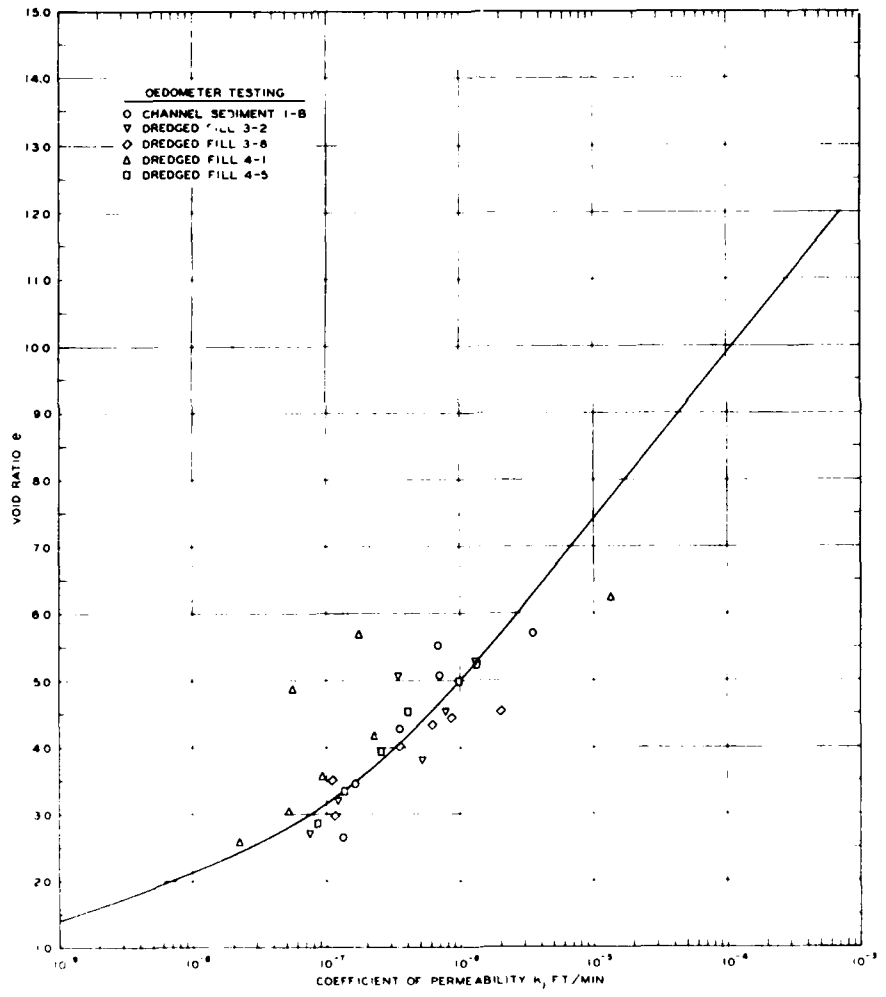

Figure 25. Void ratio-permeability relationship for Craney Island material

is some uncertainty associated with extrapolating the relationship to the higher void ratios but the general shape of the curve does conform to the shape of curves derived from direct measurements on other fine-grained material as reported here. Therefore, the solid line shown in Figure 25 is considered representative of the material and will be used in calculation of the coefficients of consolidation for use in later consolidation calculations.

116. Table C2 contains a listing of the variables used in calculating the small strain and finite strain coefficients of consolidation, c_v and g. In the table, a_v and k are determined from the solid curves in Figures 24 and 25, respectively, for corresponding void ratios. These values are then used in Equations 21 and 42 for calculation of c_v and g, respectively. Figure 26 shows smoothed curves through these calculated points.

117. The final soil variable necessary for the calculation of consolidation by linear finite strain theory is the linearization constant λ. To obtain this variable, the void ratio-effective stress relationship depicted in Figure 24 is plotted to an arithmetic scale over the range of effective stresses expected in the problem at hand. Then a curve corresponding to the exponential relationship of Equation 46 is drawn to approximate the laboratory-determined curve by choosing appropriate values for the constants e_{oo}, e_{∞}, and λ. Figure 27 shows such a curve fitted to the Craney Island data in the range of effective stresses expected.

Canaveral Harbor

118. Only one oedometer test had been conducted on the material from Canaveral Harbor. A CRS test on this material was also contracted as mentioned earlier. Figure 28 shows the results of both these tests and the void ratio-effective stress relationship to be used in the calculations to follow. It is interesting to note that the first point (highest void ratio) of the oedometer test points characterizes verifiable material behavior and is not merely a bad data point as would be suspected if the oedometer data were all that were available. The relationship is based on the average of the two test curves and the

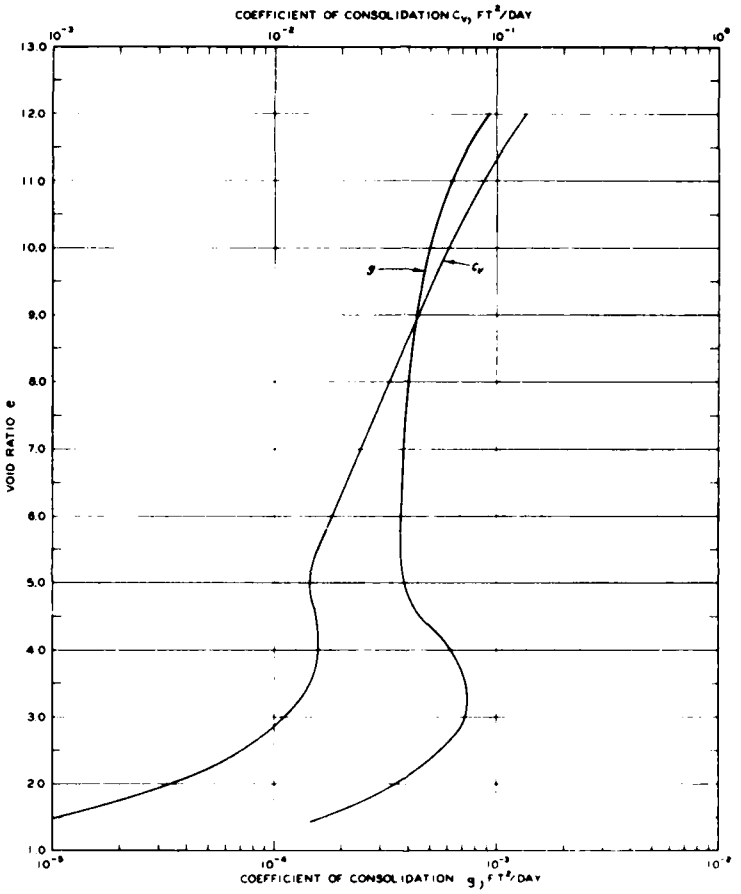

Figure 26. Coefficients of consolidation as functions of void ratio for Craney Island material

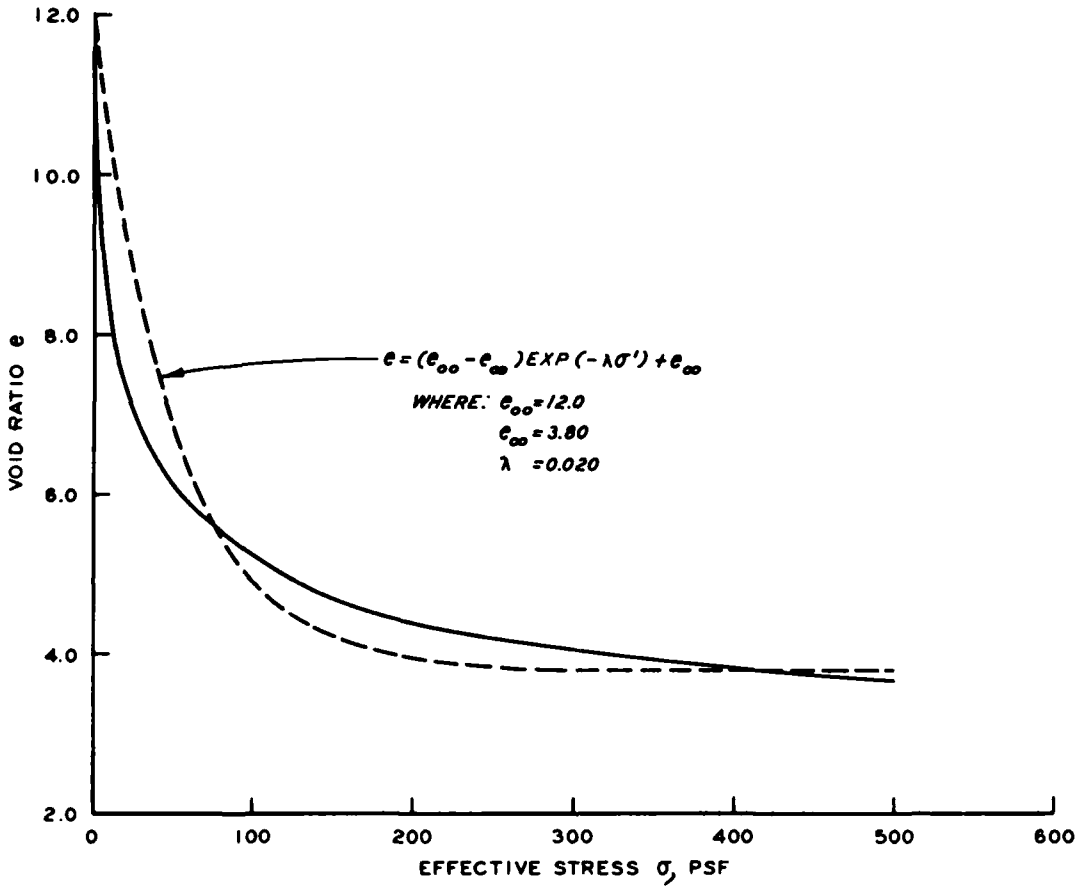

Figure 27. Exponential void ratio-effective stress relationship fitted to oedometer data for Craney Island material

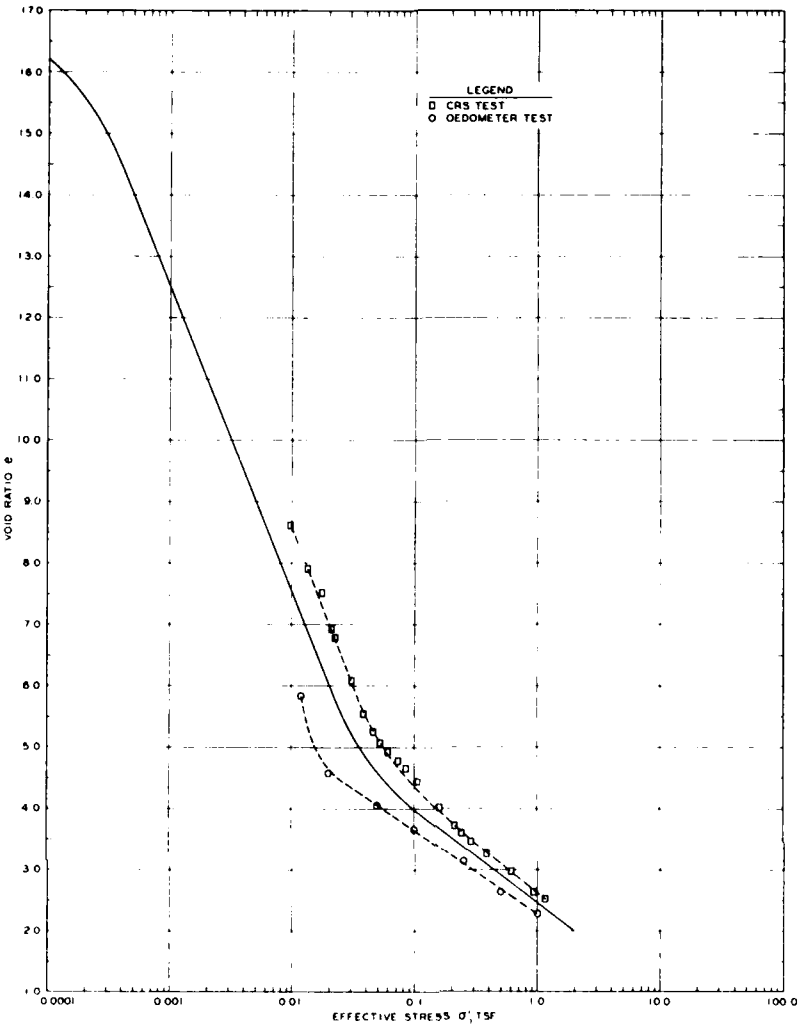

Figure 28. Void ratio-effective stress relationship for Canaveral Harbor material

previous data indicating the material sediments to an initial void ratio of about 17.0 before consolidation begins. (In Figure 28, the 10^{-4} tsf ordinate is not used to plot e_{oo} in order that a characteristic "S" shaped curve can be maintained, which means that there is a finite void ratio for zero effective stress.)

119. Figure 29 shows the void ratio-permeability relationship for the Canaveral Harbor material as deduced from the oedometer and CRS testing. Table C3 lists the calculation data from the oedometer test.

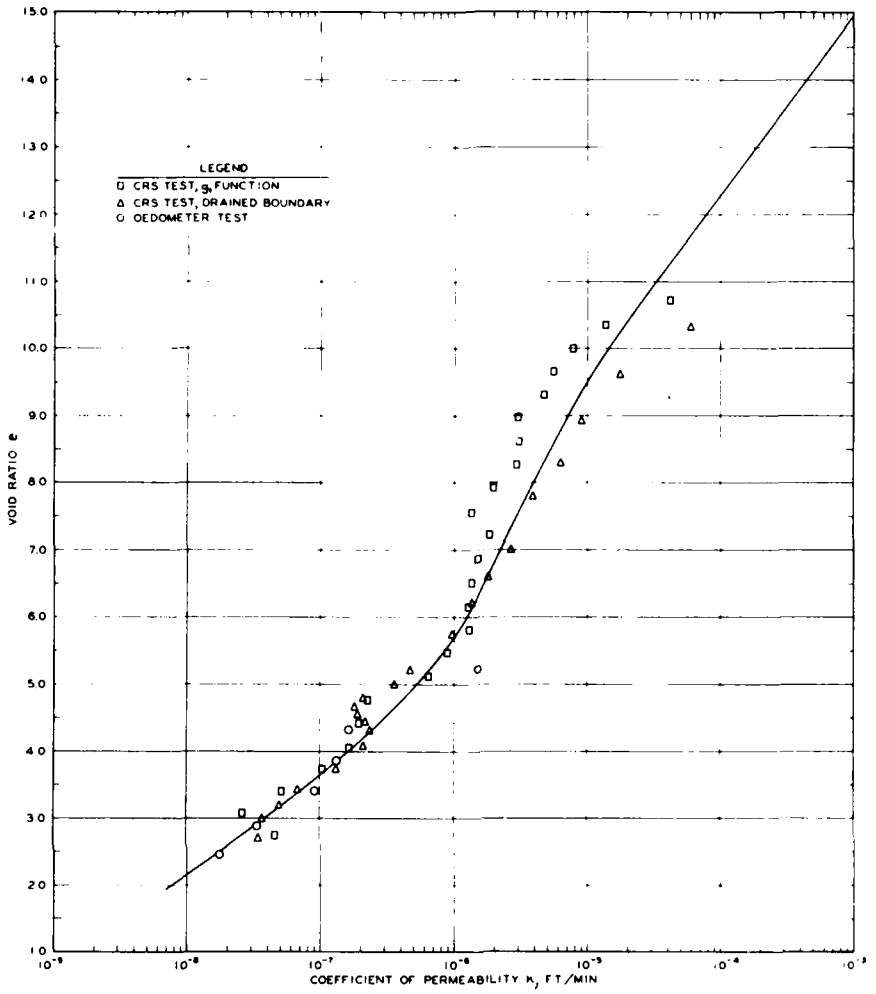

Figure 29. Void ratio-permeability relationship for Canaveral Harbor material

The data points resulting from the oedometer and CRS testing are virtually indistinguishable and provide a testimonial to the validity of the separate calculation procedures.

120. Figures 30 and 31 show curves of the coefficients of consolidation and a fitted curve for the chosen constant λ, respectively. The curves were derived as described previously for the Craney Island material. Table C4 contains a listing of the variables used in calculating the small strain and finite strain coefficients c_v and g.

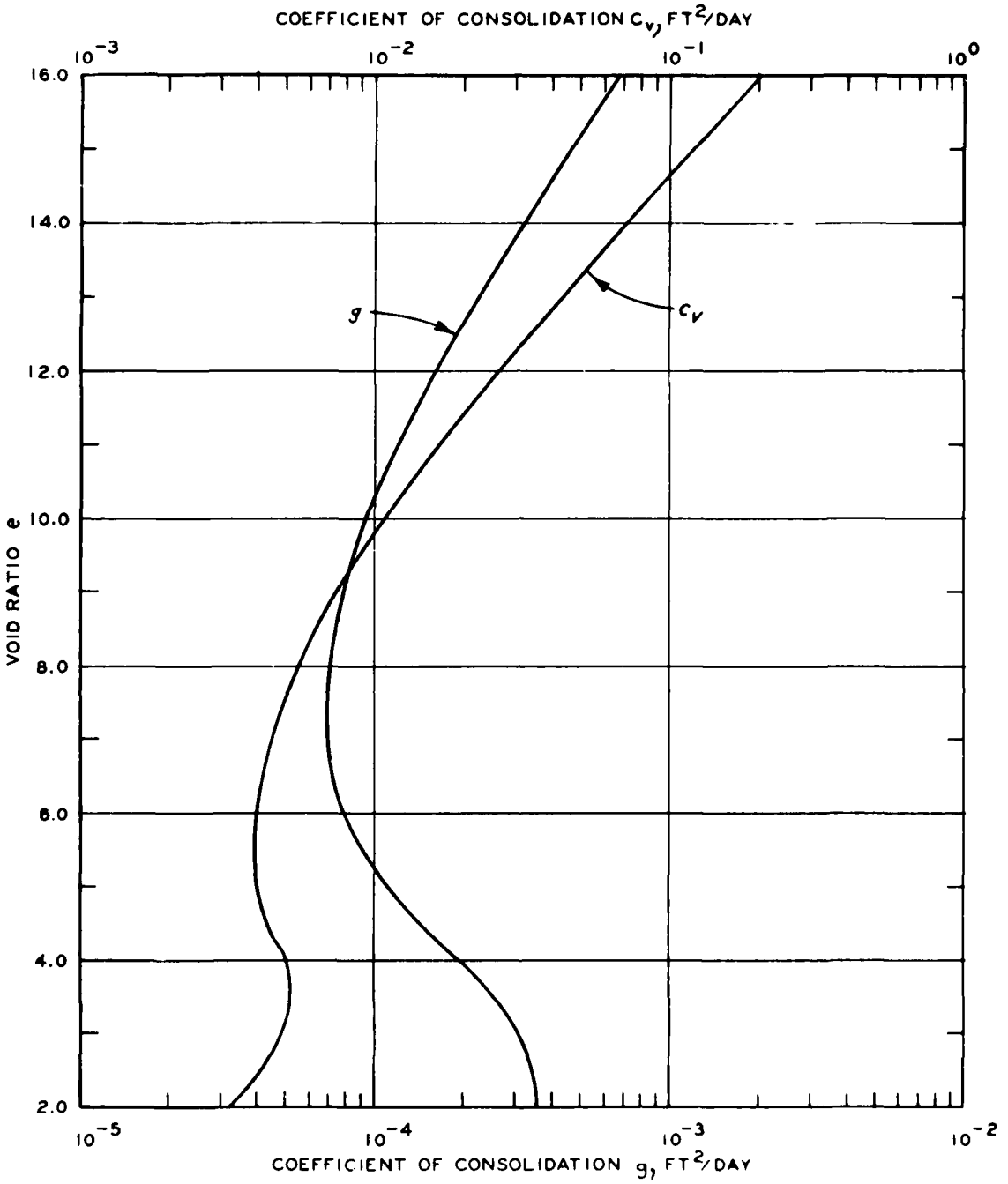

Figure 30. Coefficients of consolidation as functions of void ratio for Canaveral Harbor material

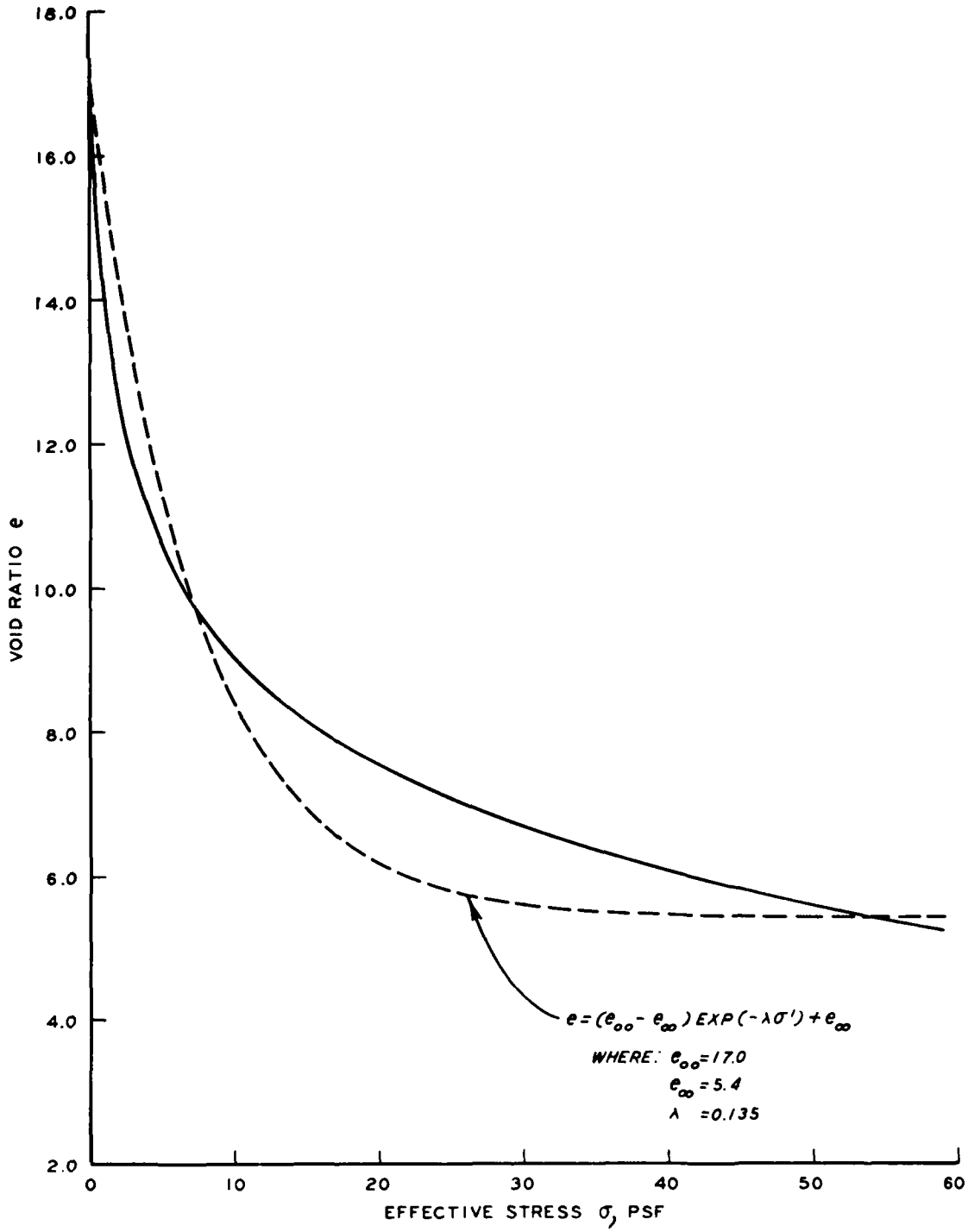

Figure 31. Exponential void ratio-effective stress relationship fitted to oedometer data for Canaveral Harbor material

Mobile test basin

121. Data available for determination of the void ratio-effective stress relationship for the Mobile test basin material consisted of three oedometer tests reported by Palermo (1977), one previously unreported oedometer test, a CRS test by the University of Colorado, and three points deduced from water content measurements reported by Hammer (1981) from test basin no. 1, which was continuously inundated and presumed to be nearly 100 percent consolidated when the measurements were taken. The solid curve shown in Figure 32 shows the primary relationship adopted for settlement calculations and conforms mainly to the curve as determined by the CRS test since oedometer test samples were obviously in an overconsolidated state when tested. The broken curve shown in the figure represents an attempt to average the results of the CRS test and the points from in situ water contents in test basin no. 1 and will be referred to as the secondary relationship.

122. Figure 33 shows the void ratio-permeability relationship for the Mobile test basin material as determined from CRS testing. As can be seen in the figure, data points from oedometer testing are not consistent with the CRS test data. Since the oedometer tests were conducted on overconsolidated dredged material, which had been in the disposal area for well over 2 years, these data points are ignored when arriving at the primary relationship for permeability used in consolidation calculation. However, since there was self-consistency in the oedometer data, a secondary relationship for permeability is also shown through the oedometer points and parallel to the primary relationship. A consolidation calculation will also be made using the secondary relationships. Table C5 lists the calculation data for oedometer tests.

123. Curves for the coefficients of consolidation for both the primary and secondary effective stress relationships are shown in Figure 34, and Table C6 lists the calculation data. Curves for determining the finite strain linearization constant λ are shown in Figure 35.

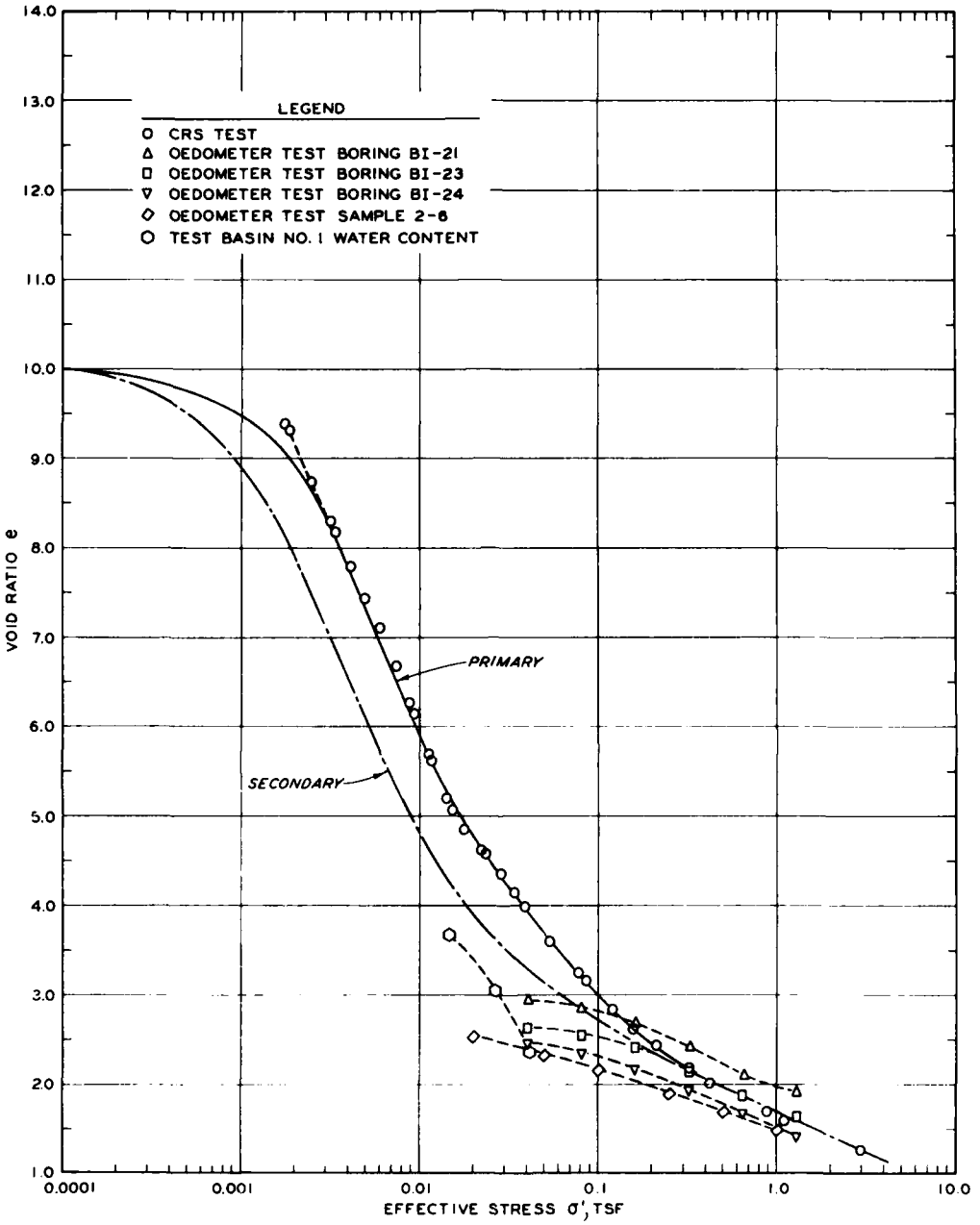

Figure 32. Void ratio-effective stress relationship for Mobile test basin material

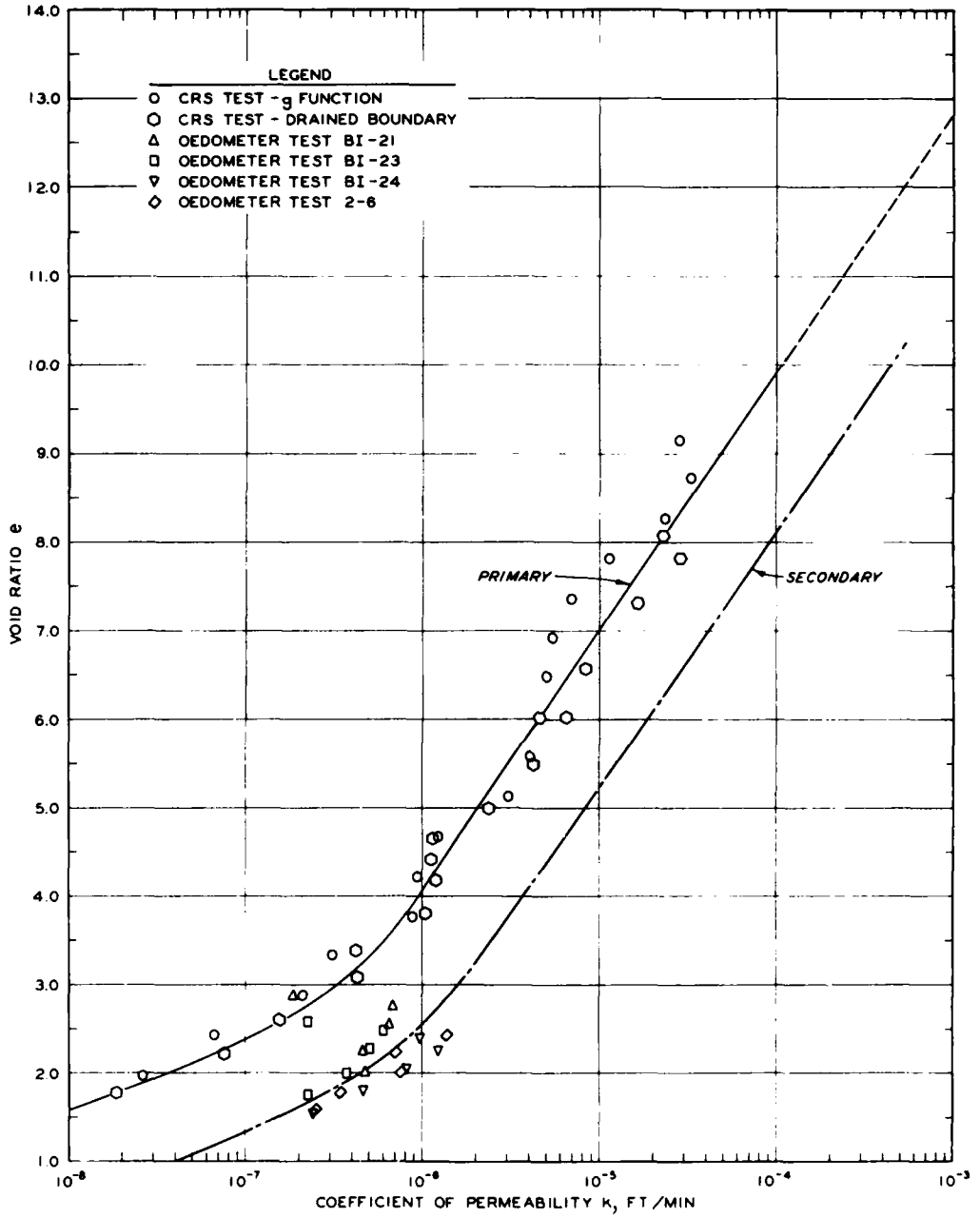

Figure 33. Void ratio-permeability relationships for Mobile test basin material

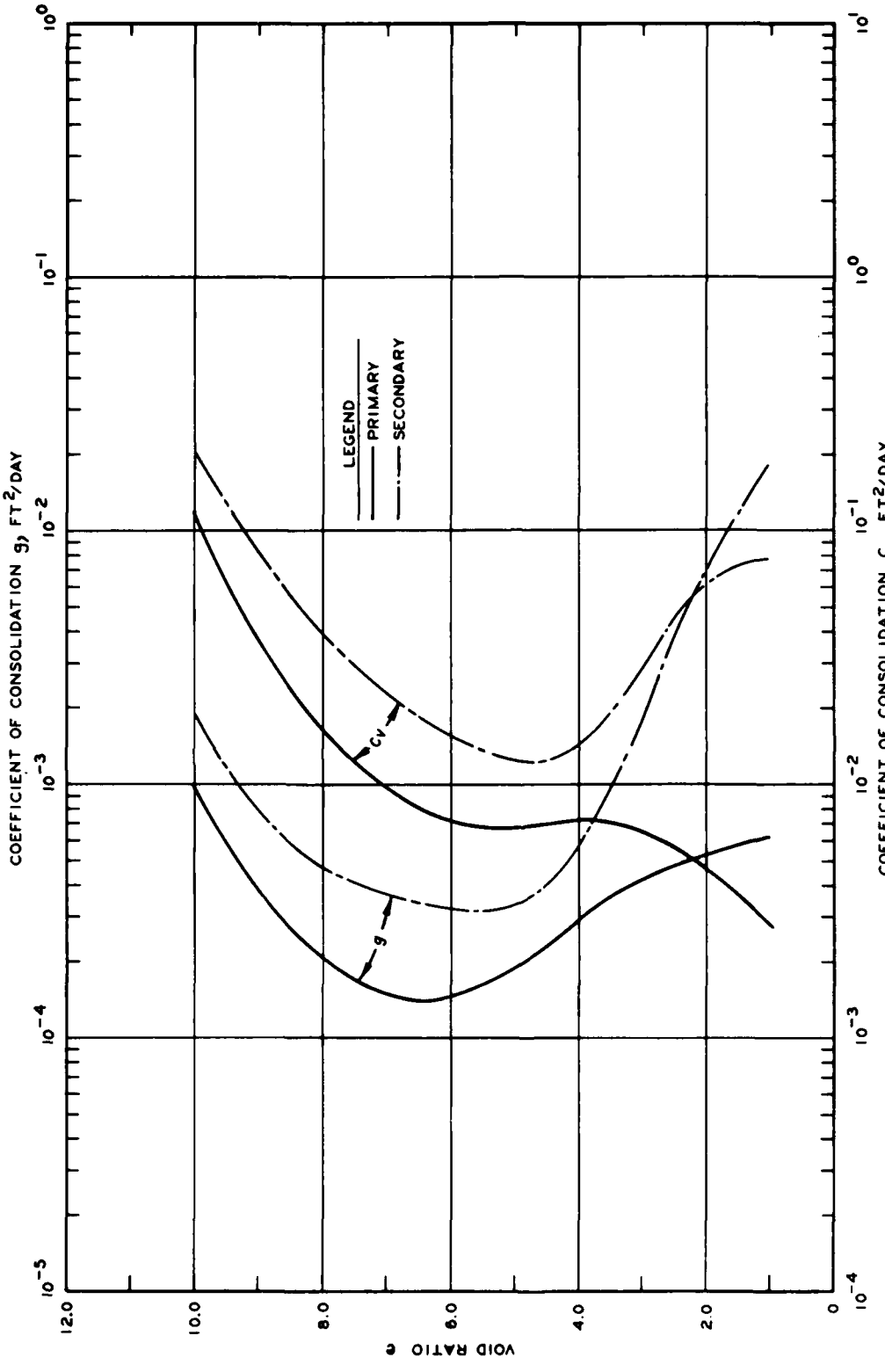

Figure 34. Coefficients of consolidation as functions of void ratio for Mobile test basin material

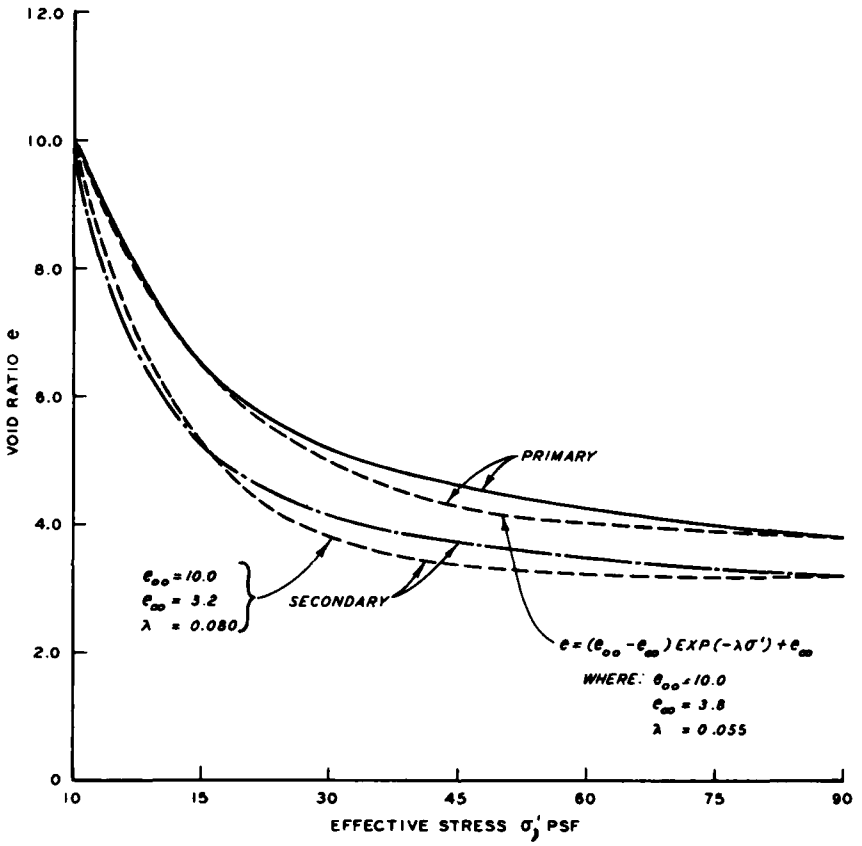

Figure 35. Exponential void ratio-effective stress relationship fitted to oedometer data for Mobile test basin material

PART V: CONSOLIDATION PREDICTION VERSUS FIELD BEHAVIOR

124. The final and most important test of any theoretical treatment of a physical problem is whether or not the theory can be used together with the basic material properties to predict how a material will actually perform in the field. In this part, both small strain and linear finite strain theories of consolidation as described in Part II will be used to predict the consolidation behavior of material at sites as described in Part III and having properties as described in Part IV.

125. It is important to remember that the analysis procedure presented in this report is applicable to primary one-dimensional consolidation only. While the procedure is useful in foundation settlement prediction as shown by the worked example problems, only self-weight consolidation of the dredged material will be considered. The procedure does not account for any settlement due to secondary consolidation or surface desiccation.

Craney Island

126. The predictions of the surface elevation in the Craney Island disposal area by both small strain and linear finite strain consolidation theories assuming the dredged material contains both no sand and 15 percent sand are shown in Figure 36. The survey data points also plotted in the figure represent the average surface elevation over the 2500-acre site as reported by Palermo, Shields, and Hayes (1981). Details of each prediction calculation are tabulated in Appendix D.

127. As shown in Figure 36, there are substantial differences in the consolidation behavior predicted by the two theories, and Appendix D shows that the finite strain theory has predicted almost 50 percent more settlement than the small strain theory. The figure also indicates the effect of accounting for the sand separately in a consolidation prediction based on gross dredged volumes. The surface elevations based on the assumption that the sand falls out immediately to a void ratio somewhat less than the fine-grained slurry are consistently less than those

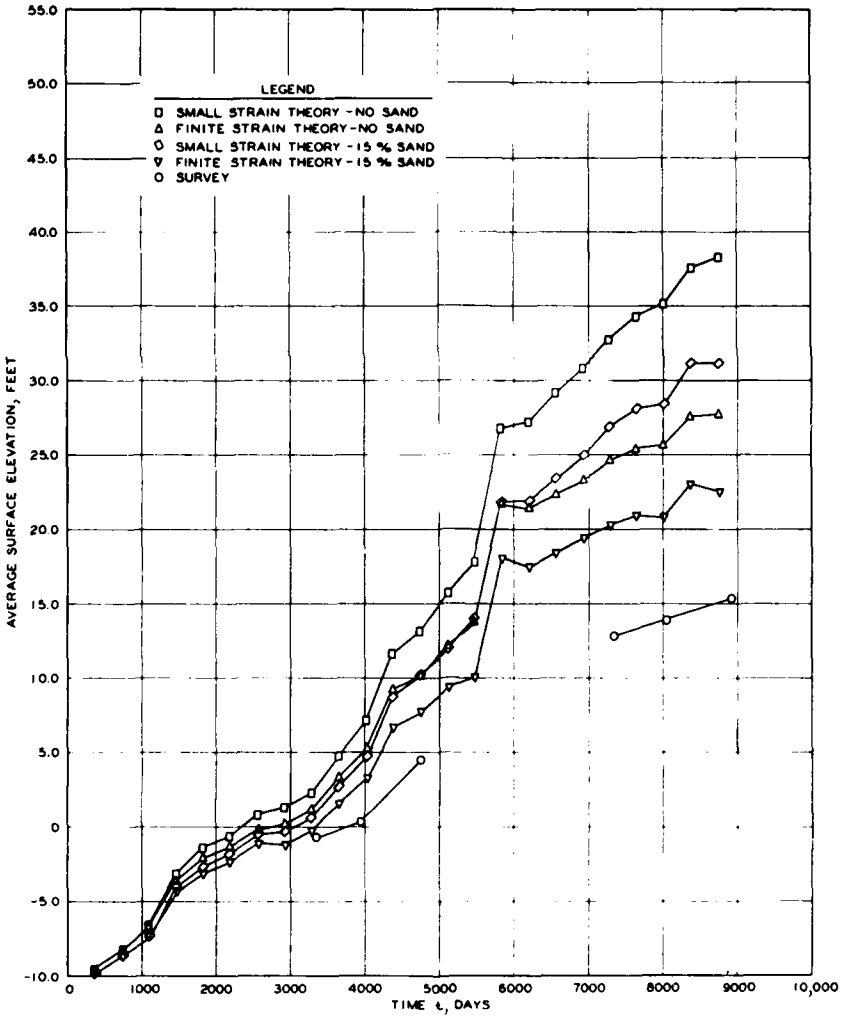

Figure 36. Predictions of surface elevations compared with survey data for the Craney Island disposal area

which treat the entire amount of solids as fine grained.

128. While all predictions apparently underestimate the amount of consolidation which actually took place in the disposal area, the linear finite strain theory with sand considered separately does come very close to correctly modeling the survey results. There are three main probable reasons for the difference between the prediction and measurement:

a. The theory has been simplified to a form suitable for hand calculation. These simplifications involve

assumptions which should approximate the actual material behavior in a conservative manner (i.e., estimate less settlement than is actually obtained). A more sophisticated solution technique programmed on a computer could result in predictions of faster settlement. A later report will deal with currently available and newly developed computer models for dredged fill settlement, and therefore further discussion of this topic will be deferred.

b. The Craney Island survey data include the effect of any foundation settlement while the predictions do not. Palermo, Shields, and Hayes (1981) report that the foundation is a highly plastic marine clay (CH) approximately 80 ft deep. Material properties are similar to those used for the foundation material used in the example problems of Appendices A and B. Very rough estimates indicate that the foundation may undergo an ultimate settlement of about 2 ft under the dredged fill loading and only about 1 ft would have occurred at the end of the disposal operation described herein. So, although the consideration of foundation settlement would lower the predicted dredged material surface elevation, it would not fully account for the differences, and the computational complexity is not warranted at this time.

c. Even though the least reported annual dredgings would have covered the entire site with from about 0.5 to 1.0 ft of slurry material, the site grade, as indicated by topographic survey, and interior diking have resulted in the periodic exposure of some material to desiccation which undoubtably has caused settlements in excess of those due strictly to self-weight consolidation. No attempt has been made here to estimate the amount of desiccation consolidation due to a lack of historical data, but the effect of such settlements would be to cause the predicted behavior to more closely approximate the observed behavior.

Canaveral Harbor

129. Predicted consolidation settlement for the Canaveral Harbor disposal area is shown in Figure 37 along with the measured data from two settlement plates installed in the area. Details of the prediction calculations are tabulated in Appendix E.

130. Since the settlement plates were set on the disposal area foundation, the resulting data do not include the effect of any

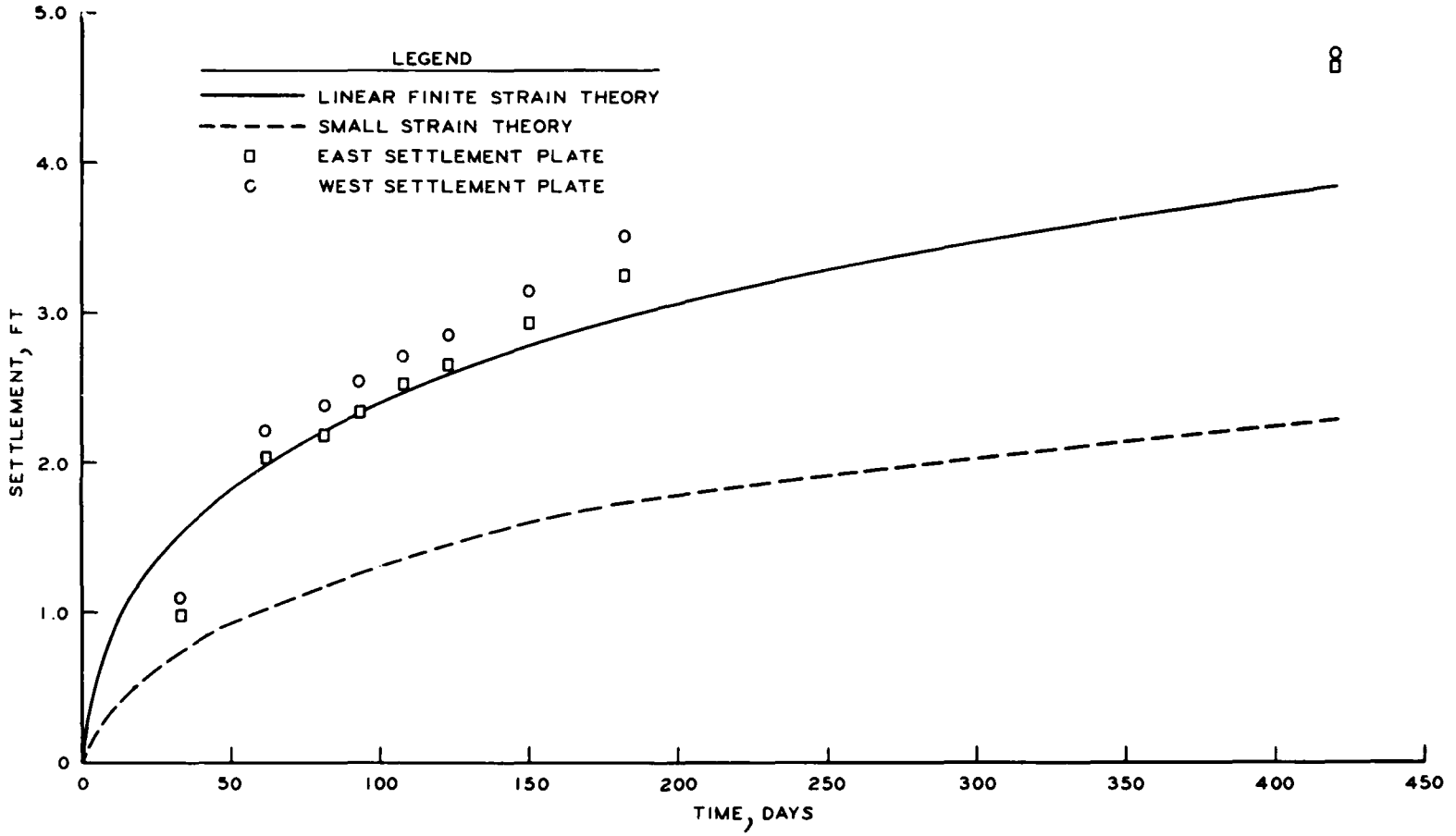

Figure 37. Predictions of dredged material settlement compared to settlement plate data for the Canaveral Harbor disposal area

foundation settlement. Area management would also have restricted surface desiccation to sometime after about day 180 during the consolidation period. Therefore, this site is considered a very good test of the consolidation calculation procedures presented in this report.

131. As shown in Figure 37, the linear finite strain theory predictions are in very close agreement with settlement plate data during the first 180 days of consolidation. Disagreement after 180 days is attributable to desiccation not accounted for in the calculation procedure. Again, there are substantial differences in the consolidation behavior predicted by the two theories. The small strain theory seriously underpredicts settlements even before desiccation effects are possible.

Mobile Test Basin

132. Figure 38 shows the consolidation prediction versus field behavior for the Mobile test basin. Measured settlement data shown on the figure do not conform to that reported by Hammer (1981) because his settlements were based on a layer height about 40 days after filling of the basin had begun. The measured settlements shown in the figure are based on measured surface elevations and the total unconsolidated lift thickness at a void ratio of 10.0 which was 9.58 ft. Separate predictions for both the primary and secondary void ratio-effective stress and permeability relationships by both theories are shown to indicate the effect of the different relationships. Tabulated calculation data along with other tabulations for the test basin are given in Appendix F.

133. As can be seen in the figure, all predictions seriously underestimate the amount of consolidation which actually took place in the test basin. Surface desiccation could not have been a factor before about day 160. Even though the finite strain theory is about 100 percent better than the small strain theory results, neither theory satisfactorily predicts settlements. There are two probable reasons for the discrepancy:

a. The physical aspects of the test basin geometry and method of material deposition may have led to very rapid

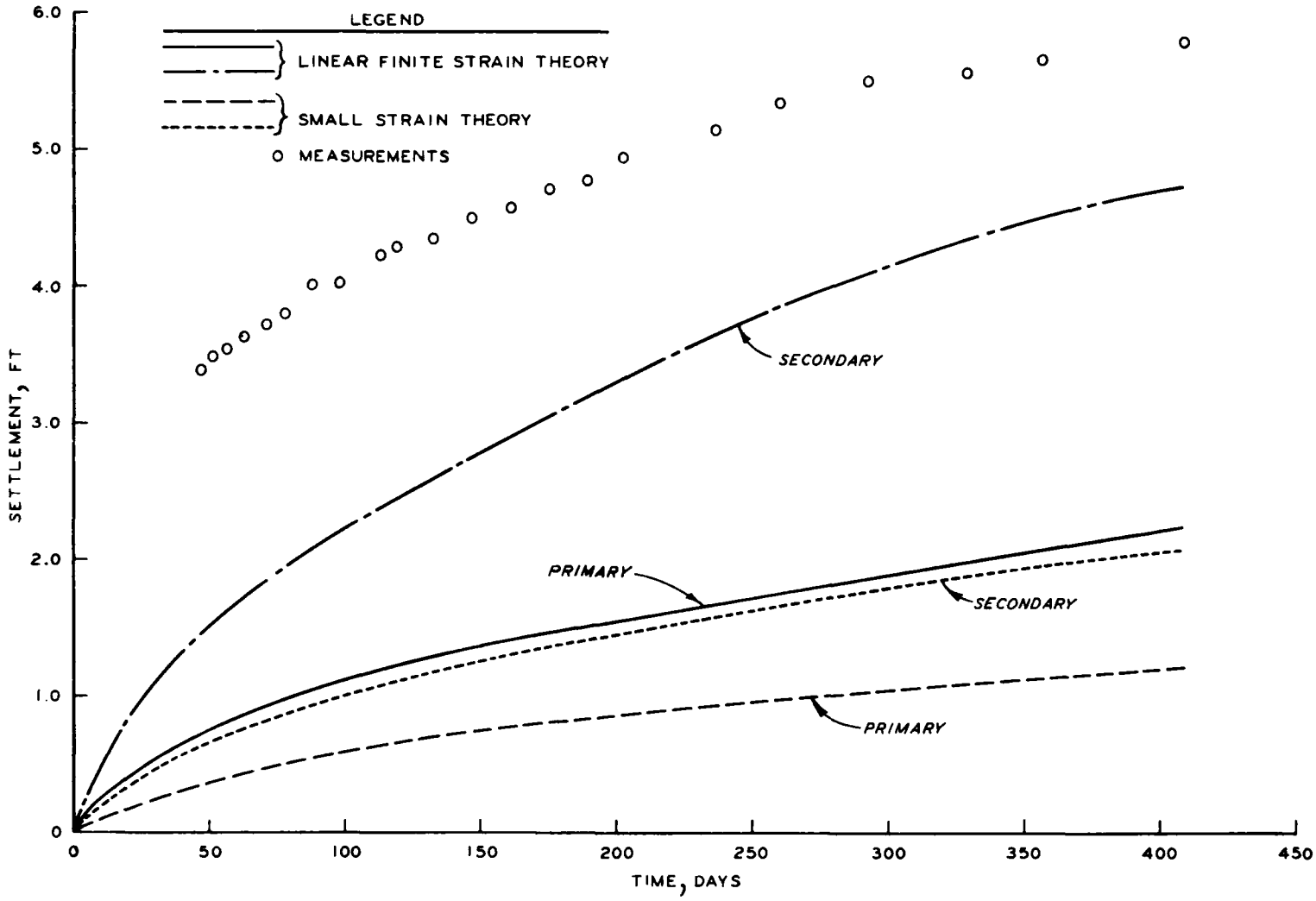

Figure 38. Predictions of dredged mater al settlement compared to settlements based on surface elevations for the Mobile test basin

consolidation during basin filling. The trapezoidal shape of the basin and plastic lining could have created drainage short-circuits which allowed excess pore pressure dissipation by routes other than one-dimensionally through the material. There also could have been drainage short-circuits created by impact loading on previously deposited material when new material was pumped into the basin. Since new material was dumped directly on material which usually had been allowed to settle for 24 hr, the shock waves created by this later dumping could also have acted as a consolidating load; and since material permeability is relatively high at the initial void ratios, there could have been consolidation induced which the material would normally not experience in the quiescent conditions away from the point of inflow in a conventional disposal area.

b. The second probable reason for the big difference between predicted settlements and actual settlements at any particular time is in the void ratio-permeability relationship used for determination of the coefficients of consolidation. As shown in Figure 33 there is considerable difference between permeabilities calculated from oedometer test results and those derived from the CRS testing which led to considerable differences in predicted consolidation. If the true permeability is higher than either the primary or secondary relationship used, the effect would be to calculate an even faster settlement from consolidation. This reinforces the contention that the method of deposition created drainage short-circuits and therefore a higher apparent permeability. As shown in the tabulations of Appendix F, the ultimate calculated settlement does approach that measured before surface desiccation became important; only the rate of settlement is in serious error.

PART VI: SUMMARY, CONCLUSIONS, AND RECOMMENDATIONS

134. In this report, state-of-the-art, one-dimensional consolidation theories have been developed in relatively concise and straightforward terms based on the laws of continuity, Darcy's law, force equilibrium, and fundamental material properties. The implications of simplifying assumptions during the development of the theories have been illustrated so that an appreciation for their limitations could be gained. The governing equations were reduced to nondimensional terms and solution charts developed to permit calculation of settlement as a function of time without the benefit of sophisticated computer programs. A complete set of percent consolidation-time factor figures based on the finite strain theory of consolidation was developed. Also, a here-to-fore unavailable technique to handle the case of multiple layers of consolidating material placed over a period of time has been proposed and used in the solution of field problems.

135. In terms of the original verification objectives stated in Part I, the following conclusions are drawn:

a. Accurate estimation of the ultimate settlement resulting from self-weight consolidation is possible by the procedures described herein. The most important aspect of the procedure is using a reliable void ratio-effective stress relationship which accurately reflects the material state at the lower effective stresses. In all the field problems considered, the ultimate settlement calculated compares favorably with ultimate settlement indicated by measurements when the effects of desiccation are ignored.

b. Calculation procedures based on small strain consolidation theory appear overly conservative (i.e., predict settlements much smaller than actually occur) in estimating settlement as a function of time for soft, fine-grained dredged material. Actually, this tendency for underestimation of settlements with time was anticipated due to inherent limitations of the theory as detailed in Part II. The fact that none of the predictions using small strain theory compared favorably with field measurements leads to the conclusion that small strain theory may not be an adequate method for calculation of consolidation in soft, fine-grained dredged material subjected to self-weight loading. This conclusion does

AD-A125 320 PROCEDURES FOR PREDICTION OF CONSOLIDATION IN SOFT FINE-GRAINED DREDGED MATERIAL(U) ARMY ENGINEER WATERWAYS EXPERIMENT STATION VICKSBURG MS K W CARGILL

2/2

UNCLASSIFIED JAN 83 WES-TR-D-83-1 F/G 13/2 NL

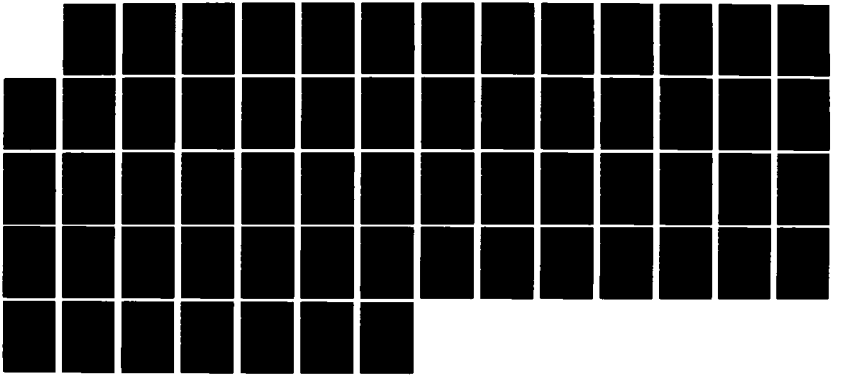

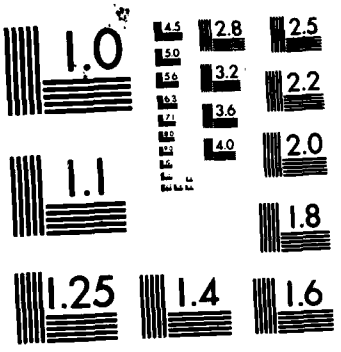

not imply that the simpler small strain theory is unsuitable for settlement prediction in thin, normally consolidated layers due to a relatively small increase in effective stress. However, when used for layers of underconsolidated dredged fill, the theory does tend to give unrealistically low settlements.

c. In two of the three field sites studied, the calculation procedures based on the finite strain theory of consolidation appear to provide very realistic estimates of settlement due to primary consolidation and conform well with field measurements. In the case of Mobile test basin where neither theory gave acceptable predictions, other factors were identified which could have led to the large discrepancies. Therefore, it is concluded that the finite strain theory provides an appropriate and adequate method for calculating settlements in soft, fine-grained dredged material. While the theory does appear to give conservative estimates of settlement when surface desiccation has been a factor, it does not give the overly conservative estimates of small strain theory. The finite strain theory predictions are then an effective lower bound on settlement predictions and represent the minimum amount of consolidation which can be expected in a newly constructed dredged material disposal area in a given time.

d. The proposed method of analysis for estimating settlements for any number of dredged material lifts deposited over a period of time is deemed an appropriate hand calculation technique. Unlike other methods which recommend treating all previously placed layers as a foundation soil, this technique accounts for the interaction between layers which could be very important when lower layers undergo large volume changes and do not have a free draining boundary. The fact that the proposed method used in conjunction with the finite strain theory gave reasonable estimates of settlement due to primary consolidation at the Craney Island site through 24 years of dredged material disposal activity verifies its adequacy.

e. The use of oedometer testing for the determination of consolidation parameters for fine-grained dredged material proved only partially adequate for the sites studied herein. For both Canaveral Harbor and the Mobile test basin, the relationships initially extrapolated had to be revised when the results of CRS testing became available. In the case of the Craney Island material where only oedometer test results were available, the extrapolation was apparently adequate since finite strain predictions did correlate with field measurements

to a good degree. Agreement between oedometer and CRS tests in the deduced void ratio-permeability relationship for Canaveral Harbor material at the lower void ratio is noteworthy and suggests that perhaps carefully conducted oedometer tests could be used routinely if an acceptable extrapolation technique could be devised. However, until such time, CRS tests are the only way of providing dependable material properties at the higher void ratios common to dredged material.

136. As a result of this study, it is recommended that, where a hand calculation is appropriate, primary self-weight consolidation used in the design of confined dredged material disposal areas be calculated by procedures outlined in this report for the finite strain theory of consolidation. This procedure is only slightly more mathematically complex than conventional small strain formulations and gives considerably more accurate and realistic results. The technique contained herein for handling multiple lifts deposited over a period to time is also recommended due to the successful calculation involving the 24 annual depositions at Craney Island. If oedometer testing data must be used for consolidation prediction of very soft dredged material, care should be taken to ensure that the sample is tested at an initial void ratio as near that of the unconsolidated dredge slurry as possible, and it is recommended that the data be supplemented with some form of CRS testing whenever possible to define properties at the higher void ratios.

REFERENCES

Cargill, K. W. 1982. "Consolidation of Soft Layers by Finite Strain Analysis," Miscellaneous Paper GL-82-3, U. S. Army Engineer Waterways Experiment Station, CE, Vicksburg, Miss.

Cargill, K. W., and Schiffman, R. L. 1980. "FSCON1-I, Version 1, Level A, One-Dimensional Finite Strain Consolidation, Dimensionless Void Ratio for a Thick, Normally Consolidated Homogeneous Layer," Geotechnical Engineering, Software Activity Department of Civil Engineer, University of Colorado, Boulder, Colo.

Carslaw, H. S., and Jaeger, J. C. 1959. Conduction of Heat in Solids, 2nd ed., Clarendon Press, Oxford.

Gibson, R. E., England, G. L., and Hussey, M. J. L. 1967. "The Theory of One-Dimensional Consolidation of Saturated Clays. I. Finite Non-Linear Consolidation of Thin Homogeneous Layers," Geotechnique, Vol 17, No. 3, pp 261-273.

Gibson, R. E., Schiffman, R. L., and Cargill, K. W. 1981. "The Theory of One-Dimensional Consolidation of Saturated Clays. II. Finite Non-Linear Consolidation of Thick Homogeneous Layers," Canadian Geotechnical Journal, Vol 18, No. 2, pp 280-293.

Haliburton, T. A. 1978. "Guidelines for Dewatering/Densifying Confined Dredged Material," Technical Report DS-78-11, U. S. Army Engineer Waterways Experiment Station, CE, Vicksburg, Miss.

Hammer, D. P. 1981. "Evaluation of Underdrainage Techniques for the Densification of Fine-Grained Dredged Material," Technical Report EL-81-3, U. S. Army Engineer Waterways Experiment Station, CE, Vicksburg, Miss.

Headquarters, Department of the Army. 1980. "Guidelines for Designing, Operating, and Managing Dredged Material Containment Areas," Engineer Manual EM 1110-2-5006, Washington, D. C.

_____. 1970. "Laboratory Soils Testing," Engineer Manual EM 1110-2-1906, Washington, D. C.

Imai, G. 1981. "Experimental Studies on Sedimentation Mechanism and Sediment Formation of Clay Materials," Soils and Foundations, Vol 21, No. 1, Japanese Society of Soil Mechanics and Foundation Engineering, pp 7-20.

Montgomery, R. L. 1978. "Methodology for Design of Fine-Grained Dredged Material Containment Areas for Solids Retention," Technical Report D-78-56, U. S. Army Engineer Waterways Experiment Station, CE, Vicksburg, Miss.

Ortenblad, A. 1930. "Mathematical Theory of the Process of Consolidation of Mud Deposits," Journal of Mathematics and Physics, Vol 9, No. 2, pp 73-149.

Palermo, M. R. 1977. Characteristics of the Upper Polecat Bay Disposal Area as Related to Potential Dredged Material Shrinkage and Consolidation Properties, M. S. Thesis, Department of Civil Engineering, Mississippi State University, Mississippi State, Miss.

Palermo, M. R., Montgomery, R. L., and Poindexter, M. E. 1978. "Guidelines for Designing, Operating, and Managing Dredged Material Containment Areas," Technical Report DS-78-10, U. S. Army Engineer Waterways Experiment Station, CE, Vicksburg, Miss.

Palermo, M. R., Shields, F. D., and Hayes, D. F. 1981. "Development of a Management Plan for Craney Island Disposal Area," Technical Report EL-81-11, U. S. Army Engineer Waterways Experiment Station, CE, Vicksburg, Miss.

Terzaghi, K. 1924. "Die Theorie der Hydrodynamishen Spanungserscheinungen und ihr Erdbautechnisches Answendungsgebeit," Proceedings, First International Congress of Applied Mechanics, Vol 1, Delft, The Netherlands, pp 288-294.

Terzaghi, K., and Peck, R. B. 1967. Soil Mechanics in Engineering Practice, 2nd ed., Wiley, New York, pp 173-182.

Umehara, Y., and Zen, K. 1982. "Consolidation and Settling Characteristics of Very Soft Contaminated Sediments," Management of Bottom Sediments Containing Toxic Substances; Proceedings of the 6th U. S./Japan Experts Meeting, U. S. Army Engineer Waterways Experiment Station, CE, Vicksburg, Miss.

Znidarcic, D. 1982. Laboratory Determination of Consolidation Properties of Cohesive Soil, Ph.D. Thesis, Department of Civil Engineering, University of Colorado, Boulder, Colo.

APPENDIX A: PRACTICAL EXAMPLE OF SINGLE CONSOLIDATING LAYER

1. In this appendix, the practical problem of a single dredged fill layer deposited on a compressible foundation will be solved for settlement as a function of time by both small strain and linear finite strain theories. The solutions will involve only hand calculations and the appropriate percent consolidation curves given previously in this report. A generalized flow diagram showing the principal steps of the calculation procedure is shown in Figure A1.

Problem Statement

2. It is required to determine the time rate of surface settlement of a 10.0-ft-thick fine-grained dredged fill material having a uniform initial void ratio after sedimentation of 7.0 deposited on a normally consolidated compressible foundation 10.0 ft thick which overlies an impermeable bedrock. Laboratory oedometer testing of the dredged material resulted in the σ'-e relationship shown in Figure 5 and k-e , c_v-e , and g-e relationships as shown in Figure 6 of the main text. Laboratory oedometer testing of the foundation material resulted in the relationships shown in Figure A2 and Figure A3. Laboratory testing also revealed specific gravity of solids $G_s = 2.75$ in the dredged material and $G_s = 2.65$ in the foundation material.

Void Ratio Distributions

3. For the most accurate calculations, it is necessary to know the distribution of void ratios throughout the consolidating layers both before consolidation begins and after it ends. As an aid in this and later calculations, Table A1 is set up where the layers are subdivided into ten increments each. Entries in the table correspond to average conditions at the center of each sublayer.

4. Completion of the table is a straightforward exercise for the dredged fill layer. The column for $e_{i,o}$ is given in the problem

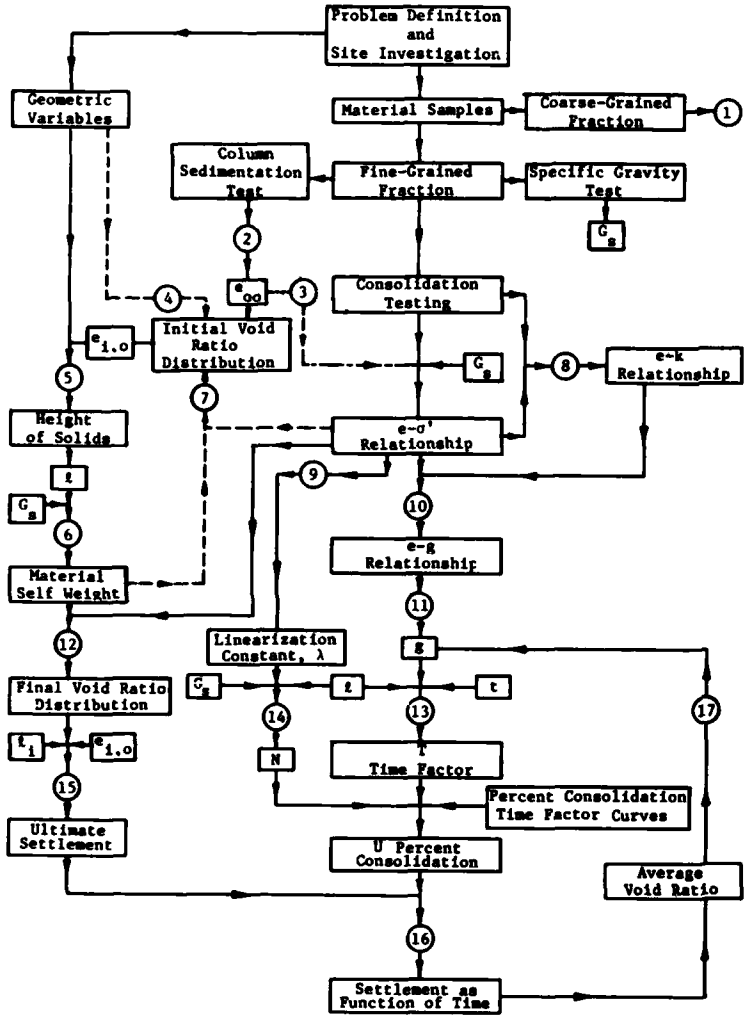

For all fine-grained materials

For dredged fill material only

For normally consolidated material only

NOTES

1. This procedure for fine-grained material only. Coarse-grained material must be considered separately and the area required deleted from that available for dredged fill.
2. Engineering judgment must be used in the interpretation of the test to insure that a good value for the zero effective stress void ratio is obtained.
3. Knowledge of e_{oo} is needed to complete the $e - \sigma'$ relationship.
4. An initial void ratio distribution must be assumed to start the iterative process for normally consolidated material.
5. Calculated by Equation 68.
6. Calculated by Equation 71 for each increment of layer.
7. Initial void ratio distribution is reevaluated based on calculated effective stress and $e - \sigma'$ relationship. Loop is repeated until desired accuracy is obtained.
8. Calculated by Equation 79.
9. Determined by fitting curve of the form of Equation 46 to $e - \sigma'$ relationship from consolidation testing.
10. Calculated by Equation 42.
11. Coefficient of consolidation chosen based on estimate of void ratio when consolidation is carried to chosen time.
12. With effective stress due to self-weight plus any surcharge, final void ratio is read from $e - \sigma'$ relationship.
13. Calculated by Equation 53.
14. Calculated by Equation 54.
15. Calculated by Equation 70.
16. Calculated by Equation 75.
17. From calculated settlement, average void ratio is computed by transposing Equation 77. Coefficient of consolidation is adjusted to account for any difference from original assumption and process repeated until desired degree of accuracy is obtained.

Figure A1. Generalized flow diagram of calculation procedure for consolidation of fine-grained materials

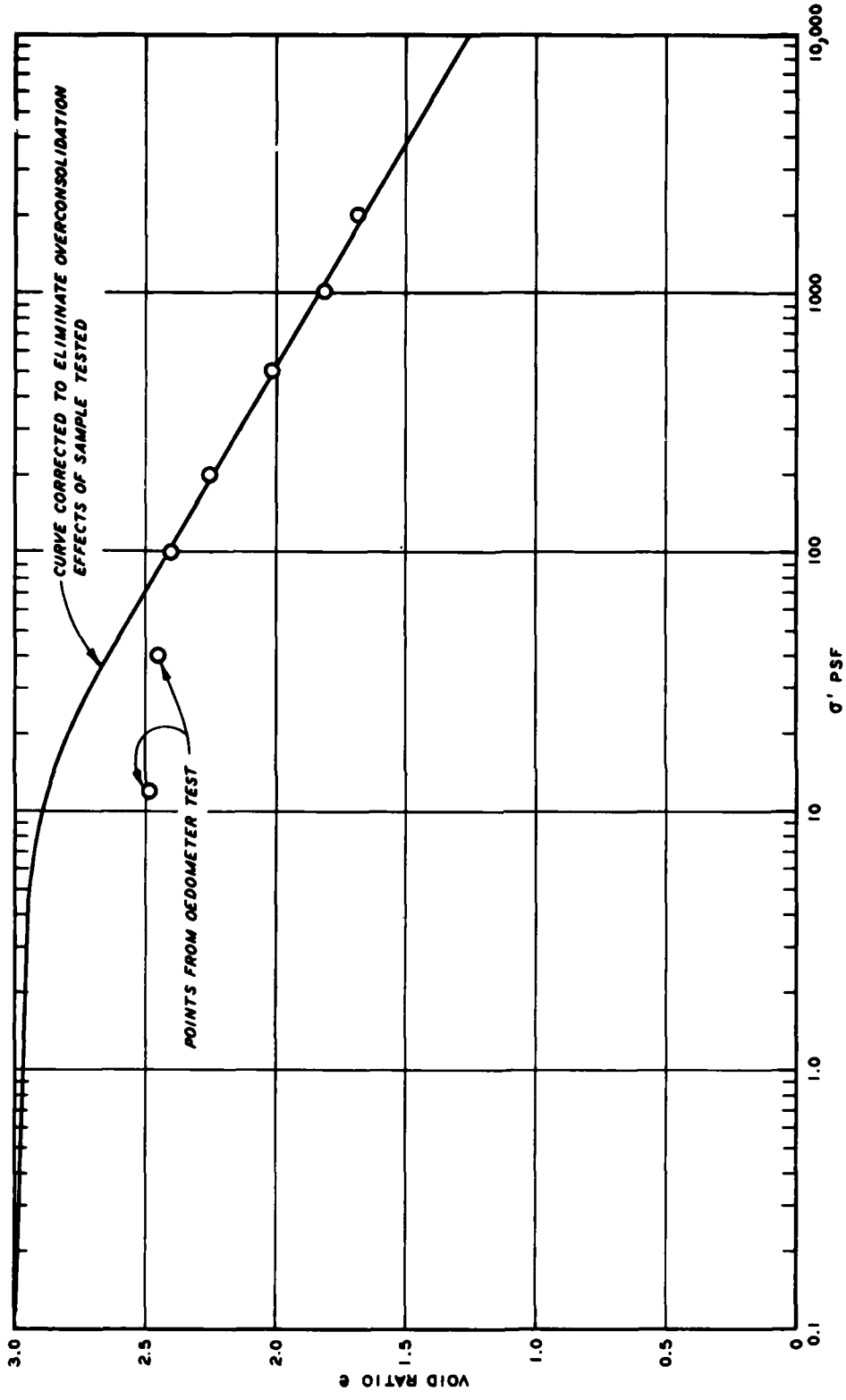

Figure A2. Relationship between void ratio and effective stress, e-log σ' curve, for compressible foundation from oedometer testing

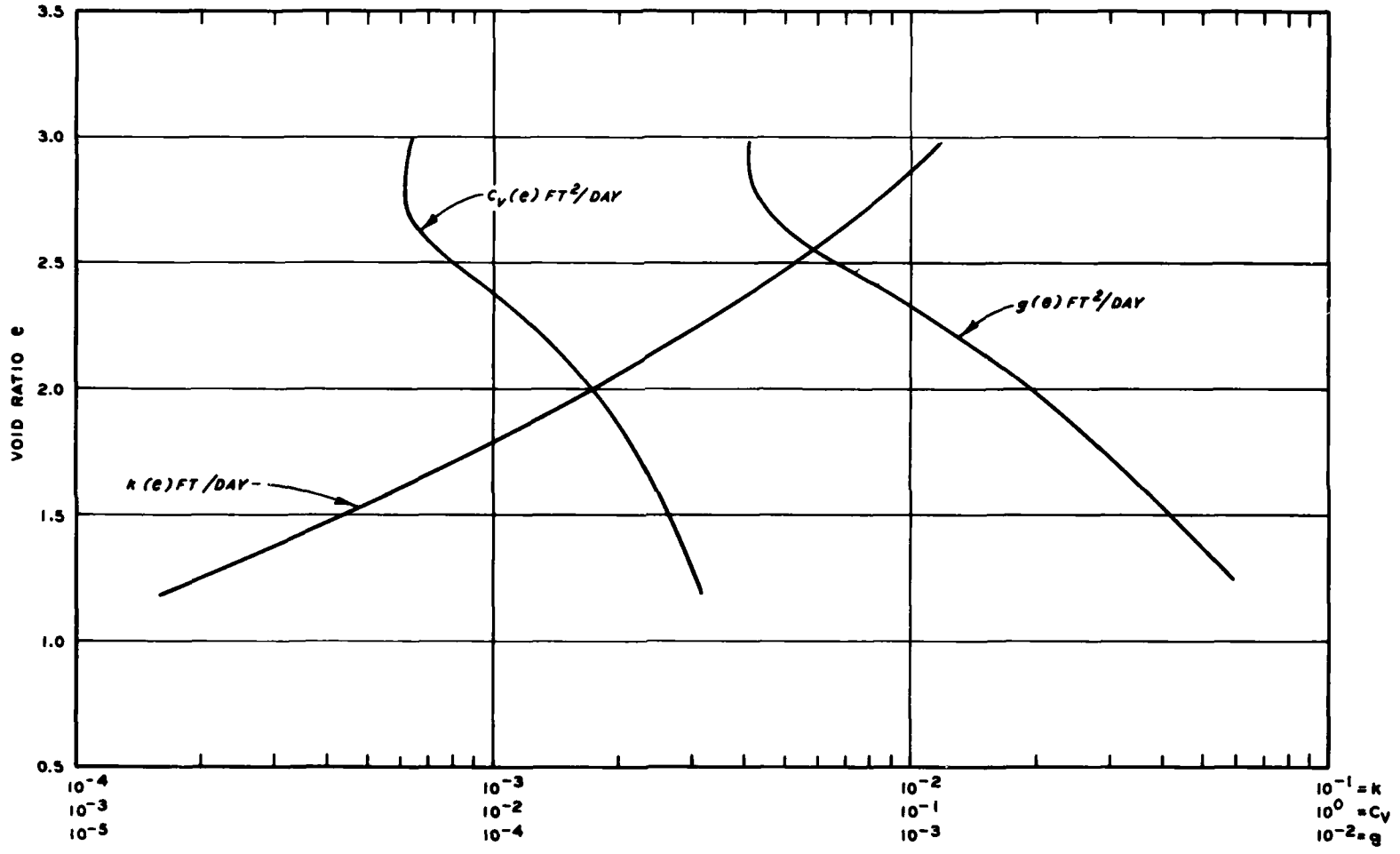

Figure A3. Permeability and coefficients of consolidation as a function of void ratio for a compressible foundation

Table A1

Void Ratio Distribution and Ultimate Settlement Calculations*

i	$h_{i,o}$ ft	ℓ_i ft	$\sigma'_{i,o}$ psf	$e_{i,o}$	$\sigma'_{i,\infty}$ psf	$e_{i,\infty}$	$h_{i,\infty}$ ft	$\delta_{i,\infty}$ ft
				Dredged Fill				
1	1.0	0.125	0.0	7.00	6.8	6.52	0.94	0.06
2	1.0	0.125	0.0	7.00	20.5	5.93	0.87	0.13
3	1.0	0.125	0.0	7.00	34.1	5.57	0.82	0.18
4	1.0	0.125	0.0	7.00	47.8	5.34	0.79	0.21
5	1.0	0.125	0.0	7.00	61.4	5.14	0.77	0.23
6	1.0	0.125	0.0	7.00	75.1	4.98	0.75	0.25
7	1.0	0.125	0.0	7.00	88.7	4.86	0.73	0.27
8	1.0	0.125	0.0	7.00	102.4	4.75	0.72	0.28
9	1.0	0.125	0.0	7.00	116.0	4.65	0.71	0.29
10	1.0	0.125	0.0	7.00	129.7	4.57	0.70	0.30
	$\Sigma = 10.0$	$\Sigma = 1.250$					$\Sigma = 7.80$	$\Sigma = 2.20$
				Foundation				
1	1.0	0.259	13.3	2.86	149.8	2.31	0.86	0.14
2	1.0	0.275	40.9	2.64	177.4	2.26	0.90	0.10
3	1.0	0.286	69.7	2.50	206.2	2.23	0.92	0.08
4	1.0	0.293	99.5	2.41	236.0	2.20	0.94	0.06
5	1.0	0.299	130.0	2.35	266.5	2.17	0.95	0.05
6	1.0	0.305	161.1	2.28	297.6	2.14	0.96	0.04
7	1.0	0.308	192.6	2.25	329.1	2.11	0.96	0.04
8	1.0	0.312	224.6	2.21	361.1	2.09	0.96	0.04
9	1.0	0.314	256.8	2.18	393.3	2.07	0.96	0.03
10	1.0	0.317	289.2	2.15	425.7	2.05	0.97	0.03
	$\Sigma = 10.0$	$\Sigma = 2.968$					$\Sigma = 9.38$	$\Sigma = 0.61$

* Symbols are defined in the main text.

statement and the initial effective stress $\sigma'_{i,o}$ will always be zero by definition. The sublayer depth in reduced coordinates is calculated directly from Equation 68.

$$\ell_i = \frac{h_{i,o}}{1 + e_{i,o}} = \frac{1.0}{1 + 7.0} = 0.125 \text{ ft}$$

The ultimate effective stress $\sigma'_{i,\infty}$ column is computed from Equation 71. Thus

$$\sigma'_{1,\infty} = \frac{1}{2}\ell_1(\gamma_s - \gamma_w) = \frac{0.125}{2}\left[(2.75 - 1.0)62.4\right] = 6.8 \text{ psf}$$

and

$$\sigma'_{2,\infty} = \frac{1}{2}\ell_2(\gamma_s - \gamma_w) + \ell_1(\gamma_s - \gamma_w) = 20.5 \text{ psf}$$

etc.

The final void ratio $e_{i,\infty}$ is read from the laboratory oedometer test curve. The usual e-log σ' curve is more accurate for this purpose than the curve given in Figure 5. The final sublayer height $h_{i,\infty}$ is also calculated by substitution into Equation 68

$$h_{1,\infty} = \ell_1(1 + e_{1,\infty}) = 0.125(1 + 6.52) = 0.94 \text{ ft}$$

5. Completion of the table for the compressible foundation layer is not quite as simple since the initial void ratio is not usually known. However, it can be calculated given its e-log σ' curve in the normally consolidated state as shown in Figure A1. An iterative process is required. First assume an initial void ratio for the first layer, $e_{1,o}$ Based on this void ratio, calculate ℓ from Equation 68. Thus, assuming $e_{1,o} = 3.0$

$$\ell_1 = \frac{h_1}{1 + e_{1,o}} = \frac{1.0}{1 + 3.0} = 0.250 \text{ ft}$$

Using this value of ℓ_1, $\sigma'_{1,o}$ is calculated from Equation 71 as

$$\sigma'_{1,o} = \frac{1}{2}\ell_1(\gamma_s - \gamma_w) = \frac{0.250}{2}\left[(2.65 - 1.0)62.4\right] = 12.9 \text{ psf}$$

Based on this value of $\sigma'_{1,o}$, a new estimate of $e_{1,o}$ is made from Figure A1 and the process repeated until no further iterations are

required. (Usually three iterations are required for an accuracy ±0.01 in the void ratio.) Using the total effective weight of the first layer, a first estimate of the void ratio in the second layer is made from Figure A1 and its true average void ratio determined as was done with the first sublayer. The first estimate of each following sublayer is based on the effective weight of those above it.

6. Once the initial void ratios and effective stresses have been determined throughout the compressible foundation, the final void ratios and effective stresses are easily found. The final effective stress $\sigma'_{i,\infty}$ is its initial value plus the effective weight of the dredged fill layer. Thus, if

$$\sigma'_{\text{dredged fill}} = \ell_{\text{d.f.}}(\gamma_s - \gamma_w) = 136.5 \text{ psf}$$

then

$$\sigma'_{i,\infty} = \sigma'_{i,o} + 136.5$$

for the foundation. The final sublayer void ratio can then be read from the e-log σ' curve and the final sublayer height $h_{i,\infty}$ can be calculated from Equation 68.

Ultimate Settlement

7. Ultimate settlements for the compressible layers are calculated directly from Equation 70. Alternately, it could have been calculated from the difference in the sum of the sublayer heights initially and finally. As shown in Table A1, for the dredged fill, $\delta_\infty = 2.20$ ft, and for the foundation, $\delta_\infty = 0.61$ ft. The fact that ultimate settlement plus total sublayer final heights in the foundation does not equal the initial total sublayer heights is due to round-off errors in the calculations.

Settlement as a Function of Time

8. A prerequisite to determining settlement as a function of time is the selection of an appropriate coefficient of consolidation during

the course of consolidation, and in the case of linear finite strain theory, appropriate values for λ and N.

9. For the dredged fill layer, a look at Table A1 shows the void ratio will vary between the extremes 7.00 to 4.57. Figure 6 is used to determine the appropriate coefficient of consolidation for the average void ratio during consolidation. For the foundation, where the void ratio extremes are 2.86 to 2.05, Figure A3 is used.

10. The value of λ must be determined by approximating the laboratory-determined curve with one of the form of Equation 46. Figure A4 shows that an appropriate value for the dredged fill is

$$\lambda = 0.026 \text{ ft}^3/\text{lb}$$

and Figure A5 shows that for the foundation

$$\lambda = 0.009 \text{ ft}^3/\text{lb}$$

is appropriate. These curves were fitted in the range of expected void ratios only and should not be used in computations outside those ranges.

11. Next, from the previously derived data, N can be calculated by Equation 54. For the dredged fill

$$N = 3.55$$

and for the foundation

$$N = 2.75$$

12. All that remains is to calculate the dimensionless time factor from either Equation 48 where $H = 10.0$ ft initially for both layers or by Equation 53 with appropriate constants. By small strain theory, Figure 8 is used to determine percent consolidation. Curve type I is used for the foundation and type III for the dredged fill. By linear finite strain theory, Figure 9 is used for the foundation and Figure 11 for the dredged fill. The calculations are organized in Table A2 and results plotted in Figures A6 and A7.

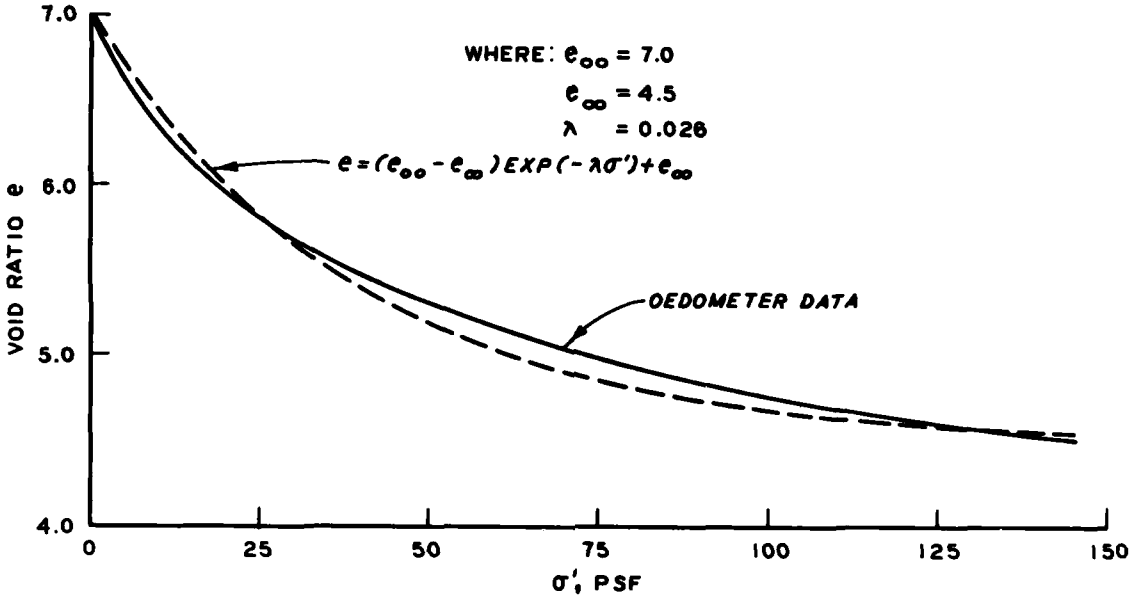

Figure A4. Exponential void ratio-effective stress relationship fitted to oedometer data for dredged fill

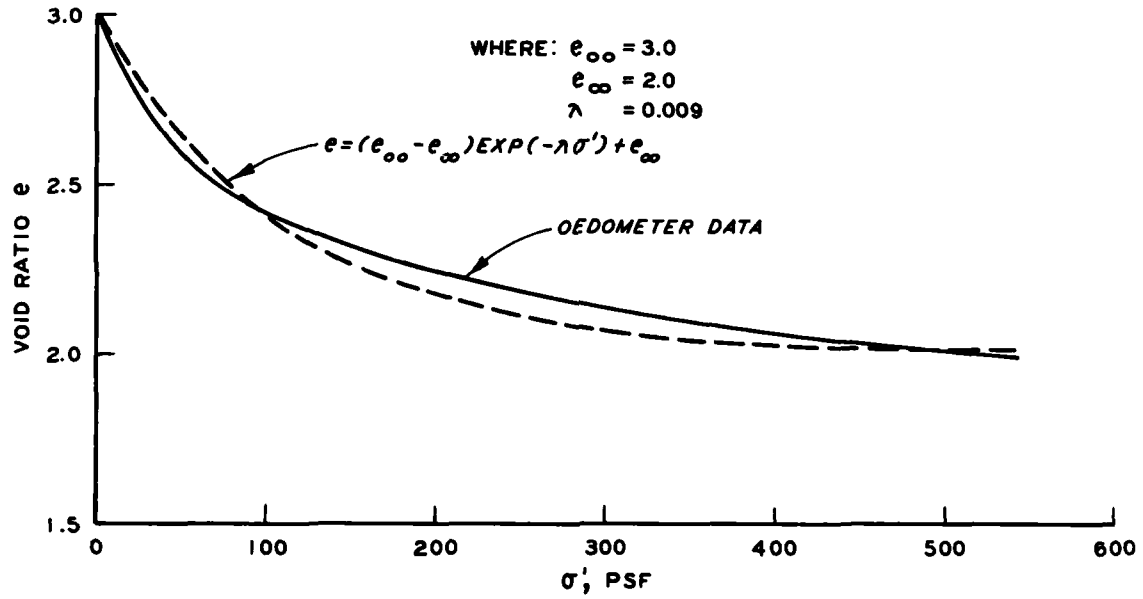

Figure A5. Exponential void ratio-effective stress relationship fitted to oedometer data for foundation

Table A2

Percent Consolidation and Settlement Calculations

t				Small Strain Theory						Linear Finite Strain Theory		
	$\bar{e}$	$\bar{H}$	c_v		U	δ	$\bar{e}$	$\bar{H}$	g		U	δ
days		ft	ft^2/day	T	%	ft		ft	ft^2/day	T	%	ft
						Dredged Fill						
500	6.8	9.75	1.25×10^{-2}	0.066	14	0.31	6.4	9.25	2.16×10^{-4}	0.069	33	0.73
1000	6.5	9.38	1.20×10^{-2}	0.136	26	0.57	5.9	8.63	2.410×10^{-4}	0.154	64	1.41
1500	6.3	9.13	1.17×10^{-2}	0.211	39	0.86	5.5	8.13	2.73×10^{-4}	0.262	85	1.87
2000	6.1	8.88	1.15×10^{-2}	0.292	50	1.10	5.3	7.87	2.96×10^{-4}	0.379	94	2.07
2500	5.9	8.63	1.14×10^{-2}	0.383	60	1.32	5.3	7.87	2.96×10^{-4}	0.474	97	2.13
3000	5.8	8.50	1.13×10^{-2}	0.469	68	1.50	5.3	7.87	2.96×10^{-4}	0.57	99	2.18
3500	5.7	8.38	1.13×10^{-2}	0.56	74	1.63	5.3	7.87	2.96×10^{-4}	0.66	100	2.20
4000	5.6	8.25	1.13×10^{-2}	0.66	80	1.76					100	2.20
4500	5.5	8.13	1.13×10^{-2}	0.77	85	1.87					100	2.20
5000	5.4	8.00	1.14×10^{-2}	0.89	89	1.96					100	2.20
						Foundation						
500	2.30	9.79	1.15×10^{-2}	0.060	28	0.17	2.25	9.65	1.19×10^{-3}	0.068	62	0.38
1000	2.30	9.79	1.15×10^{-2}	0.120	40	0.24	2.20	9.50	1.30×10^{-3}	0.148	78	0.48
1500	2.25	9.65	1.24×10^{-2}	0.200	51	0.31	2.20	9.50	1.30×10^{-3}	0.221	87	0.53
2000	2.25	9.65	1.24×10^{-2}	0.266	58	0.35	2.15	9.35	1.45×10^{-3}	0.329	93	0.57
2500	2.25	0.65	1.24×10^{-2}	0.333	65	0.40	2.15	9.35	1.45×10^{-3}	0.412	96	0.59
3000	2.20	9.50	1.32×10^{-2}	0.439	73	0.45	2.15	9.35	1.45×10^{-3}	0.494	98	0.60
3500	2.20	9.50	1.32×10^{-2}	0.51	77	0.47	2.15	9.35	1.45×10^{-3}	0.58	99	0.60
4000	2.20	9.50	1.32×10^{-2}	0.59	81	0.49	2.15	9.35	1.45×10^{-3}	0.66	100	0.61
4500	2.20	9.50	1.32×10^{-2}	0.66	84	0.51					100	0.61
5000	2.20	9.50	1.32×10^{-2}	0.73	87	0.53					100	0.61

Dredged material: $\delta_\infty = 2.20$ ft ; N = 3.55

Foundation: $\delta_\infty = 0.61$ ft ; N = 2.75

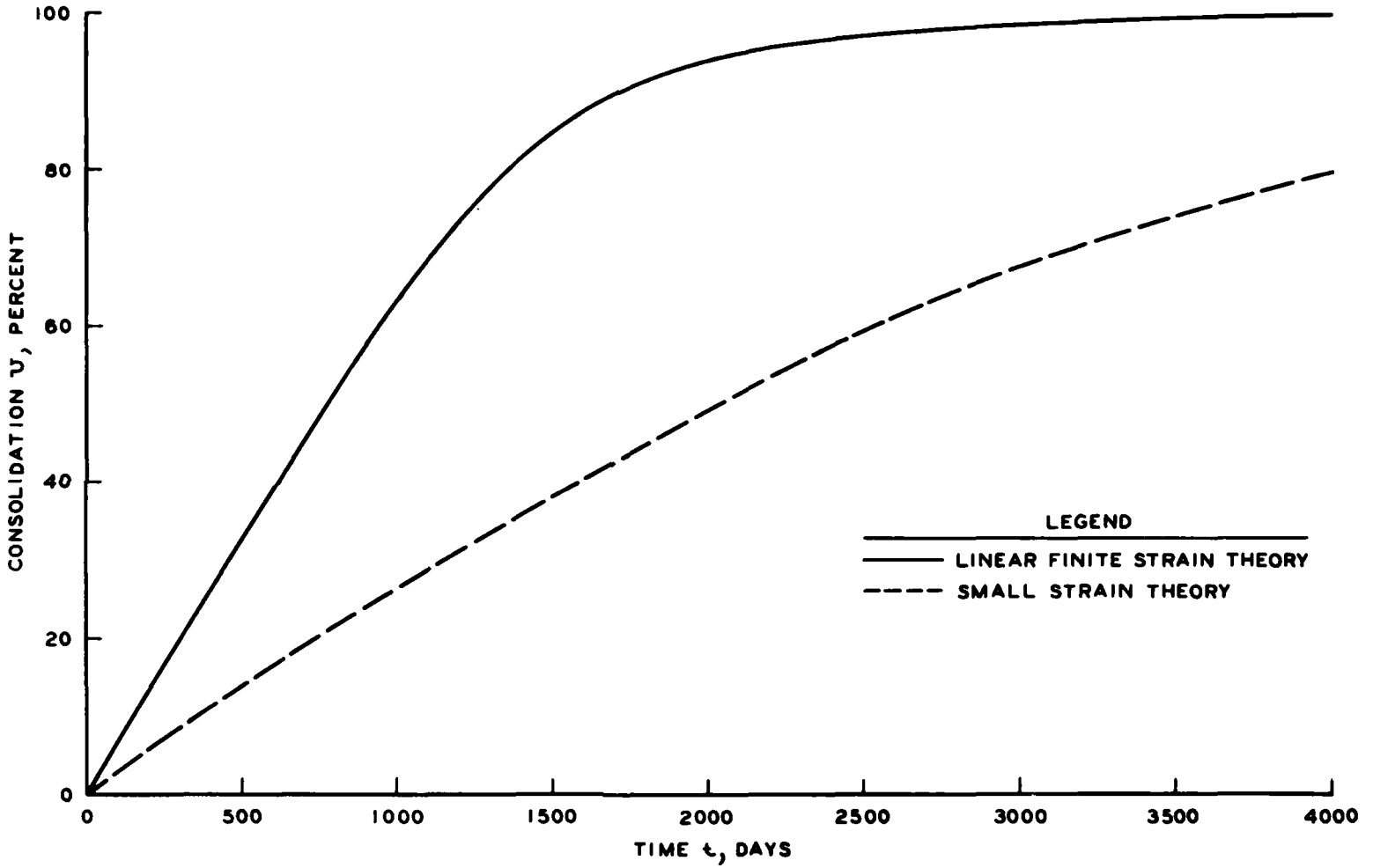

Figure A6. Comparison of consolidation percentages in the dredged fill layer as a function of time

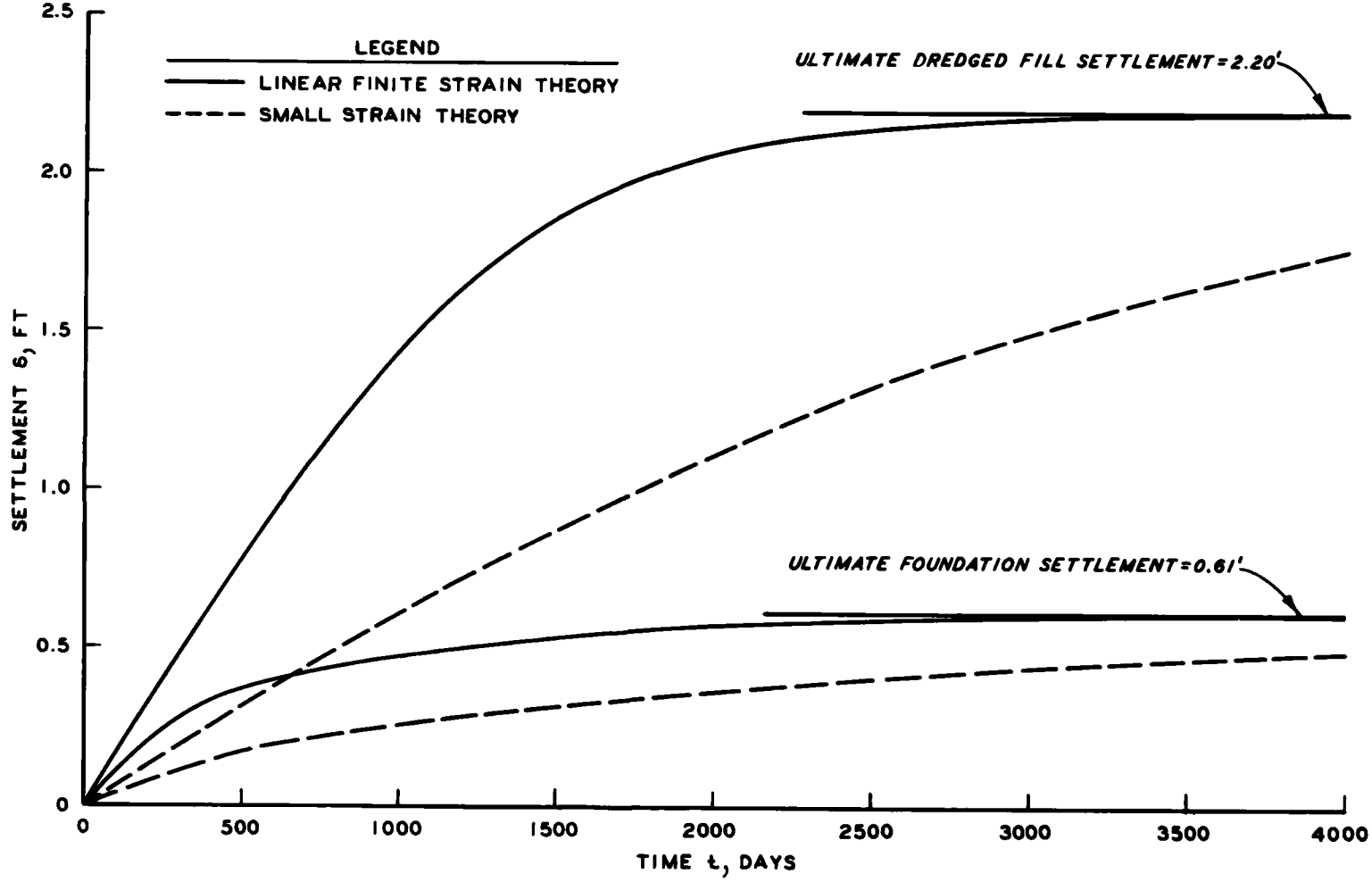

Figure A7. Comparison of settlement predictions by small strain and linear finite strain theories

APPENDIX B: PRACTICAL EXAMPLE OF MULTIPLE CONSOLIDATING LAYERS

1. This appendix solves the practical problem of multiple dredged fill layers deposited on a compressible foundation. Again, the object is settlement as a function of time and both small strain and linear finite strain theories will be used so that a comparison can be made. The procedure involves hand calculations and the appropriate percent consolidation curves previously given.

Problem Statement

2. In this problem it is required to determine the time rate of settlement of a dredged fill deposited in three layers. The first deposit is 4.0 ft thick, the second is 3.0 ft thick deposited at the beginning of the second year, and the third is 3.0 ft thick deposited at the beginning of the fifth year. The compressible foundation is again 10.0 ft thick, normally consolidated, and overlies impermeable bedrock. All material properties are as given in the previous problem solved in Appendix A.

Void Ratio Distributions

3. Table B1 shows the results of initial and final void ratio calculations. These void ratios were calculated in exactly the same way as was done for the problem in Appendix A, and indeed the initial conditions and final conditions after the entire 10.0 ft of dredged fill has been placed are exactly the same since indentical material properties and total depths of material are used.

Ultimate Settlement

4. Ultimate settlements were again calculated from Equation 70 and the information from Table B1. The summations in the table are respectively for the first, second, and third dredged fill layers. As

Table B1

Void Ratio Distribution and Ultimate Settlement Calculations

					First Dredged Fill Layer				Second Dredged Fill Layer				Third Dredged Fill Layer			
i	$h_{i,o}$ ft	ℓ_i ft	$\sigma'_{i,o}$ psf	$e_{i,o}$	$\sigma'_{i,\infty}$ psf	$e_{i,\infty}$	$h_{i,\infty}$ ft	$\delta_{i,\infty}$ ft	$\sigma'_{i,\infty}$ psf	$e_{i,\infty}$	$h_{i,\infty}$ ft	$\delta_{i,\infty}$ ft	$\sigma_{i,\infty}$ psf	$e_{i,\infty}$	$h_{i,\infty}$ ft	$\delta_{i,\infty}$ ft
								Dredged Fill								
1	[1.0]	[0.125]	[0.0]	[7.00]	--	--	--	--	--	--	--	--	6.8	6.52	0.94	0.06
2	[1.0]	[0.125]	[0.0]	[7.00]	--	--	--	--	--	--	--	--	20.5	5.93	0.87	0.13
3	[1.0]	[0.125]	[0.0]	[7.00]	--	--	--	--	--	--	--	--	34.1	5.57	0.82	0.18
4	(1.0)	(0.125)	(0.0)	(7.00)	--	--	--	--	6.8	6.52	0.94	0.06	47.8	5.34	0.79	0.21
5	(1.0)	(0.125)	(0.0)	(7.00)	--	--	--	--	20.5	5.93	0.87	0.13	61.4	5.14	0.77	0.23
6	(1.0)	(0.125)	(0.0)	(7.00)	--	--	--	--	34.1	5.57	0.82	0.18	75.1	4.98	0.75	0.25
7	1.0	0.125	0.0	7.00	6.8	6.52	0.94	0.06	47.8	5.34	0.79	0.21	88.7	4.86	0.73	0.27
8	1.0	0.125	0.0	7.00	20.5	5.93	0.87	0.13	61.4	5.14	0.77	0.23	102.4	4.75	0.72	0.28
9	1.0	0.125	0.0	7.00	34.1	5.57	0.82	0.18	75.1	4.98	0.75	0.25	116.0	4.65	0.71	0.29
10	1.0	0.125	0.0	7.00	47.8	5.34	0.79	0.21	88.7	4.86	0.73	0.27	129.7	4.57	0.70	0.30
								$\Sigma = 0.58$				$\Sigma = 1.33$				$\Sigma = 2.20$
								Foundation								
1	1.0	0.259	13.3	2.86	67.9	2.51	0.91	0.09	108.8	2.39	0.88	0.12	149.8	2.31	0.86	0.14
2	1.0	0.275	40.9	2.64	96.5	2.42	0.94	0.06	136.4	2.33	0.92	0.09	177.4	2.26	0.90	0.10
3	1.0	0.286	69.7	2.50	124.3	2.36	0.96	0.04	165.2	2.28	0.94	0.06	206.2	2.23	0.92	0.08
4	1.0	0.293	99.5	2.41	154.1	2.30	0.97	0.03	195.0	2.24	0.95	0.05	236.0	2.20	0.94	0.06
5	1.0	0.299	130.0	2.35	184.6	2.26	0.97	0.03	225.5	2.21	0.96	0.04	266.5	2.17	0.95	0.05
6	1.0	0.305	161.1	2.28	215.7	2.22	0.98	0.02	256.6	2.18	0.97	0.03	297.6	2.14	0.96	0.04
7	1.0	0.308	192.6	2.25	247.2	2.19	0.98	0.02	288.1	2.15	0.97	0.03	329.1	2.11	0.96	0.04
8	1.0	0.312	224.6	2.21	279.2	2.16	0.99	0.02	320.1	2.12	0.97	0.03	361.1	2.09	0.96	0.04
9	1.0	0.314	256.8	2.18	311.4	2.13	0.98	0.02	352.3	2.09	0.97	0.03	393.3	2.07	0.96	0.03
10	1.0	0.317	289.2	2.15	343.8	2.10	0.98	0.02	384.7	2.07	0.97	0.03	425.7	2.05	0.97	0.03
								$\Sigma = 0.35$				$\Sigma = 0.51$				$\Sigma = 0.61$

before, the ultimate settlement after the entire 10.0 ft of dredged fill is placed is the same as the previous problem.

Settlement as Function of Time

5. At the average void ratio during consolidation, Figure 6 and Figure A2 are used to determine variations in the coefficients of consolidation. The fitted curves shown in Figures B1, A3, and A4 are used to determine the linearization constant λ .

6. For consolidation under the first dredged fill layer:

	Dredged Fill	Foundation
λ =	0.031 ft^3/lb	0.009 ft^3/lb
N =	1.70	2.75

For consolidation under the first and second dredged fill layers:

	Dredged Fill	Foundation
λ =	0.031 ft^3/lb	0.009 ft^3/lb
N =	2.95	2.75

For consolidation under all dredged fill layers:

	Dredged Fill	Foundation
λ =	0.026 ft^3/lb	0.009 ft^3/lb
N =	3.55	2.75

7. Using the above constants and applicable figures from the report, Tables B2 and B3 are constructed from Equations 73, 74, 75, and 76. Figures B2 and B3 show the calculated data plotted on a time scale.

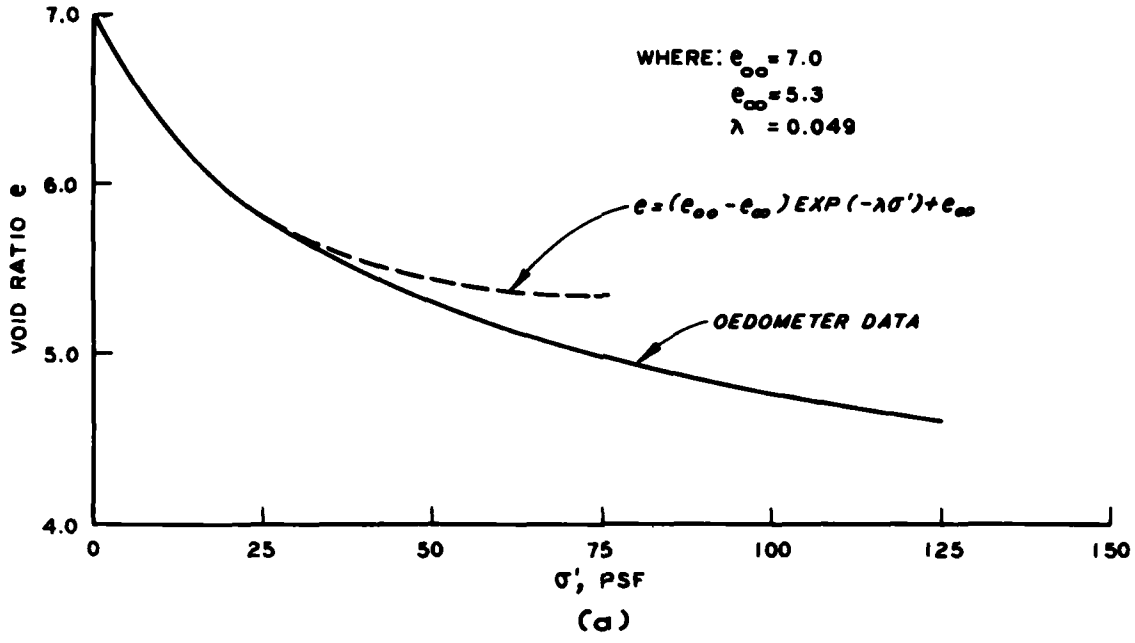

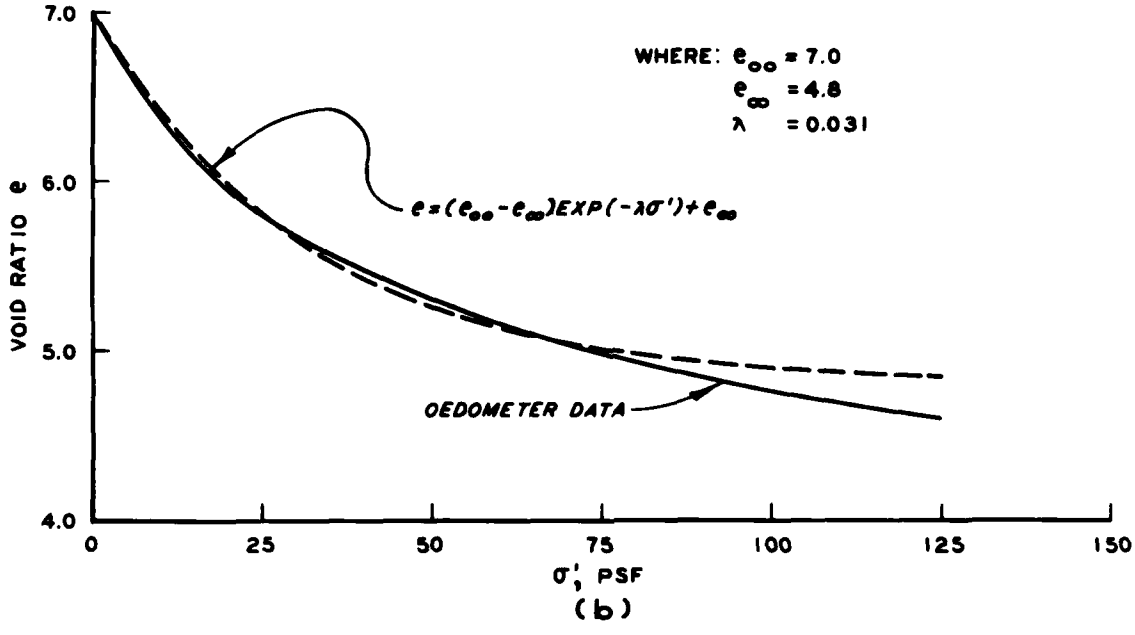

Figure B1. Exponential void ratio-effective stress relationships fitted to oedometer data for dredged fill

Table B2

Percent Consolidation and Settlement Calculations by Small Strain Theory

t days	$\Sigma h_{i,o}$ ft	t' days	$\bar{e}$	$\bar{H}$ ft	c_v ft^2/day	T'	U' %	δ'_∞ ft	δ'' ft	δ' ft	U %
					Dredged Fill						
300	4.0	300	6.5	3.75	1.20×10^{-2}	0.256	45	0.58	0.0	0.26	45
600	4.0	600	6.1	3.55	1.15×10^{-2}	0.55	73	0.58	0.0	0.43	73
730-	4.0	730	6.0	3.50	1.13×10^{-2}	0.67	80	0.58	0.0	0.46	80
730+	7.0	0	-	-	-	0.0	0	1.33	0.46	0.46	35
1000	7.0	270	6.3	6.39	1.17×10^{-2}	0.077	15	1.33	0.46	0.60	45
1500	7.0	770	6.0	6.13	1.13×10^{-2}	0.232	42	1.33	0.46	0.83	62
1825-	7.0	1095	5.9	6.04	1.13×10^{-2}	0.339	55	1.33	0.46	0.94	71
1825+	10.0	0	-	-	-	0.0	0	2.20	0.94	0.94	43
2500	10.0	675	6.0	8.75	1.13×10^{-2}	0.100	20	2.20	0.94	1.19	54
3000	10.0	1175	5.9	8.63	1.13×10^{-2}	0.178	33	2.20	0.94	1.36	62
3500	10.0	1675	5.8	8.50	1.12×10^{-2}	0.260	46	2.20	0.94	1.52	69
4000	10.0	2175	5.7	8.38	1.12×10^{-2}	0.347	56	2.20	0.94	1.65	75
4500	10.0	2675	5.6	8.25	1.12×10^{-2}	0.440	66	2.20	0.94	1.77	80
5000	10.0	3175	5.5	8.13	1.12×10^{-2}	0.54	72	2.20	0.94	1.85	84
					Foundation						
300	10.0	300	2.35	9.94	1.05×10^{-2}	0.032	20	0.35	0.0	0.07	20
600	10.0	600	2.35	9.94	1.05×10^{-2}	0.064	29	0.35	0.0	0.10	29
730-	10.0	730	2.35	9.94	1.05×10^{-2}	0.078	32	0.35	0.0	0.11	32
730+	10.0	0	-	-	-	0.0	0	0.51	0.11	0.11	22
1000	10.0	270	2.30	9.79	1.15×10^{-2}	0.032	20	0.51	0.11	0.19	37
1500	10.0	770	2.30	9.79	1.15×10^{-2}	0.092	34	0.51	0.11	0.25	49
1825-	10.0	1095	2.30	9.79	1.15×10^{-2}	0.131	41	0.51	0.11	0.27	53
1825+	10.0	0	-	-	-	0.0	0	0.61	0.27	0.27	44
2500	10.0	675	2.25	9.65	1.24×10^{-2}	0.090	34	0.61	0.27	0.39	64
3000	10.0	1175	2.20	9.50	1.32×10^{-2}	0.132	47	0.61	0.27	0.43	70
3500	10.0	1675	2.20	9.50	1.32×10^{-2}	0.245	56	0.61	0.27	0.46	75
4000	10.0	2175	2.20	9.50	1.32×10^{-2}	0.318	63	0.61	0.27	0.48	79
4500	10.0	2675	2.20	9.50	1.32×10^{-2}	0.391	70	0.61	0.27	0.51	84
5000	10.0	3175	2.20	9.50	1.32×10^{-2}	0.464	74	0.61	0.27	0.52	85

Table B3

Percent Consolidation and Settlement Calculations by Linear Finite Strain Theory

t days	$\Sigma h_{i,o}$ ft	t' days	$\bar{e}$	$\bar{H}$ ft	g ft^2/day	T'	N	U' %	δ'_∞ ft	δ'' ft	δ' ft	U %
					Dredged Fill							
300	4.0	300	6.1	3.55	2.30×10^{-4}	0.284	1.70	69	0.58	0.0	0.40	69
600	4.0	600	6.0	3.50	2.37×10^{-4}	0.57	1.70	91	0.58	0.0	0.53	91
730-	4.0	730	5.9	3.45	2.41×10^{-4}	0.70	1.70	95	0.58	0.0	0.55	95
730+	7.0	0	-	-	-	0.0	2.95	0	1.33	0.55	0.55	41
1000	7.0	270	6.0	6.13	2.37×10^{-4}	0.084	2.95	34	1.33	0.55	0.8[illegible]	62
1500	7.0	770	5.7	5.86	2.57×10^{-4}	0.258	2.95	80	1.33	0.55	1.17	88
1825-	7.0	1095	5.5	5.69	2.75×10^{-4}	0.393	2.95	92	1.33	0.55	1.27	95
1825+	10.0	0	-	-	-	0.0	3.55	0	2.20	1.27	1.27	58
2500	10.0	675	5.6	8.25	2.65×10^{-4}	0.114	3.55	51	2.20	1.27	1.74	79
3000	10.0	1175	5.4	8.00	2.85×10^{-4}	0.214	3.55	78	2.20	1.27	2.00	91
3500	10.0	1675	5.3	7.87	2.96×10^{-4}	0.317	3.55	90	2.20	1.27	2.11	96
4000	10.0	2175	5.3	7.87	2.96×10^{-4}	0.412	3.55	95	2.20	1.27	2.15	98
4500	10.0	2675	5.2	7.75	3.09×10^{-4}	0.53	3.55	99	2.20	1.27	2.19	99
5000	10.0	3175	5.2	7.75	3.09×10^{-4}	0.63	3.55	100	2.20	1.27	2.20	100
					Foundation							
300	10.0	300	2.30	9.79	1.05×10^{-3}	0.036	2.75	49	0.35	0.0	0.17	49
600	10.0	600	2.30	9.79	1.05×10^{-3}	0.072	2.75	63	0.35	0.0	0.22	63
730-	10.0	730	2.30	9.79	1.05×10^{-3}	0.087	2.75	67	0.35	0.0	0.23	67
730+	10.0	0	-	-	-	0.0	2.75	0	0.51	0.23	0.23	45
1000	10.0	270	2.25	9.65	1.19×10^{-3}	0.036	2.75	49	0.51	0.23	0.37	73
1500	10.0	770	2.20	9.50	1.30×10^{-3}	0.114	2.75	72	0.51	0.23	0.43	84
1825-	10.0	1095	2.20	9.50	1.30×10^{-3}	0.162	2.75	80	0.51	0.23	0.45	88
1825+	10.0	0	-	-	-	0.0	2.75	0	0.61	0.45	0.45	74
2500	10.0	675	2.20	9.50	1.30×10^{-3}	0.100	2.75	69	0.61	0.45	0.56	92
3000	10.0	1175	2.15	9.35	1.45×10^{-3}	0.193	2.75	84	0.61	0.45	0.58	95
3500	10.0	1675	2.15	9.35	1.45×10^{-3}	0.276	2.75	84	0.61	0.45	0.59	97
4000	10.0	2175	2.15	9.35	1.45×10^{-3}	0.358	2.75	90	0.61	0.45	0.60	98
4500	10.0	2675	2.15	9.35	1.45×10^{-3}	0.440	2.75	97	0.61	0.45	0.61	100
5000	10.0	3175	-	-	-		2.75	100	0.61	0.45	0.61	100

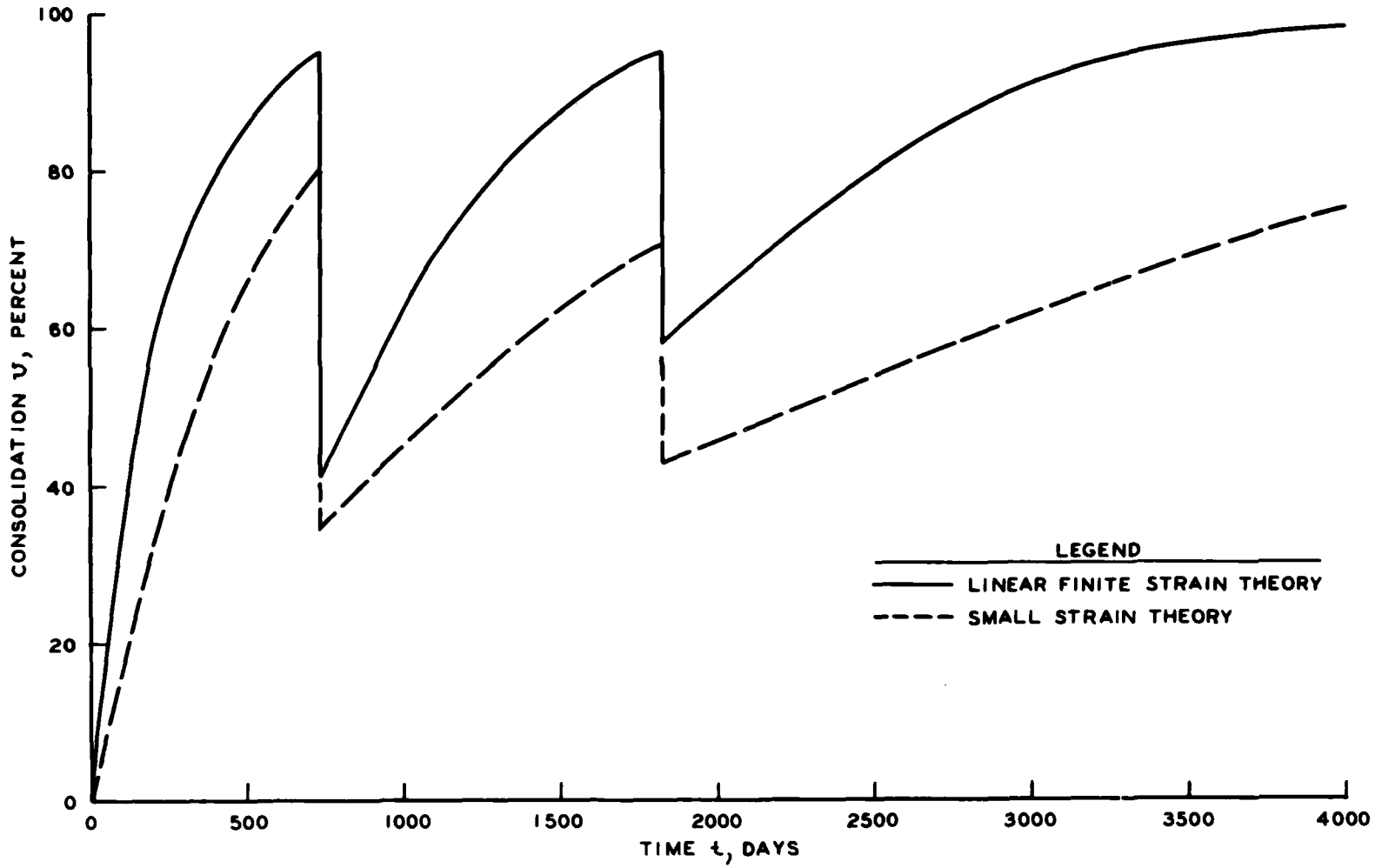

Figure B2. Comparison of consolidation percentages in the dredged fill for multiple layers as a function of time for small strain and linear finite strain theories

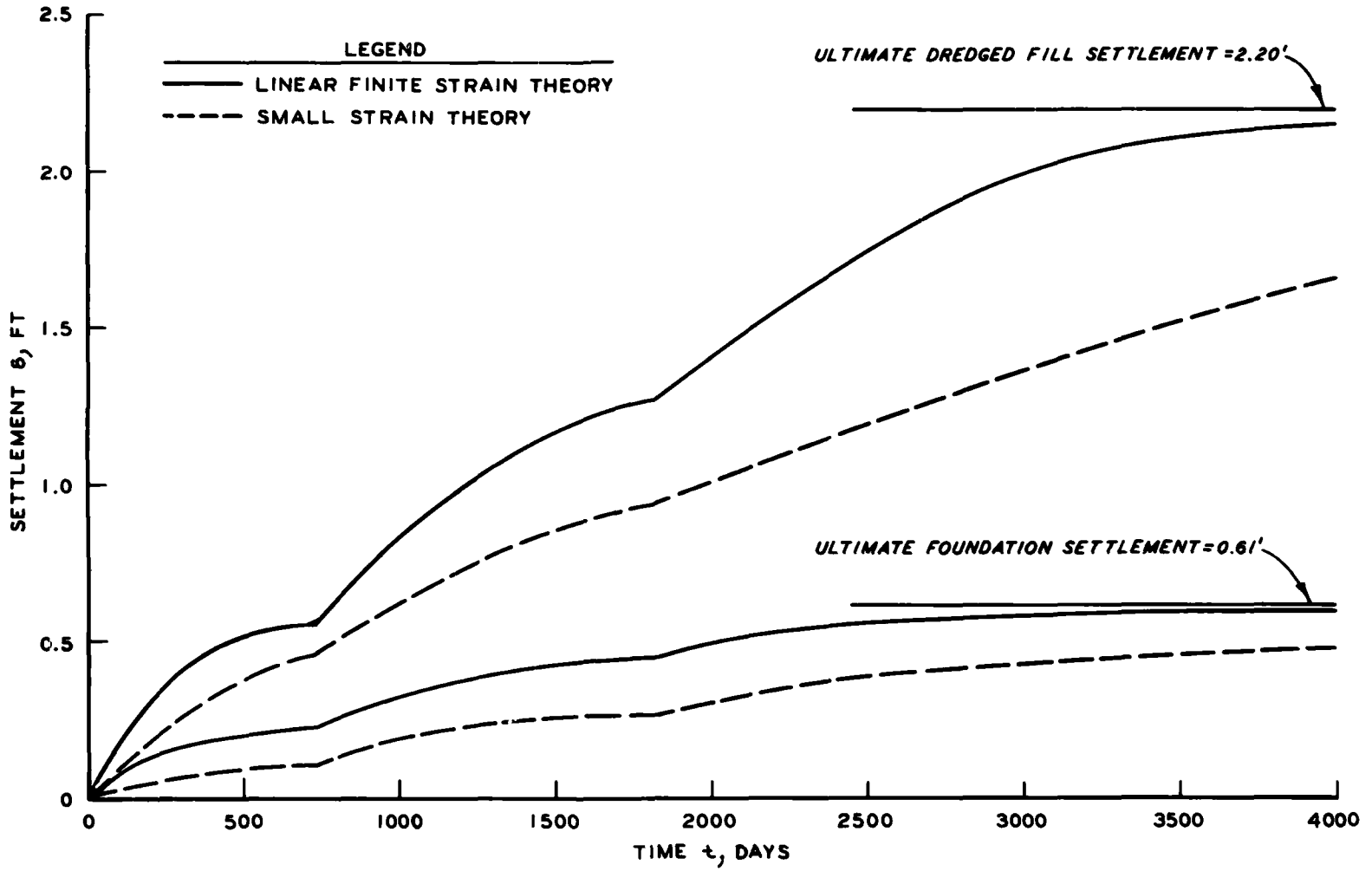

Figure B3. Comparison of settlement predictions for multiple layers by small strain and linear finite strain theories

APPENDIX C: CALCULATION DATA FOR PERMEABILITY AND COEFFICIENTS OF CONSOLIDATION

This appendix contains tabulated data used in the calculation of permeability and coefficients of consolidation for material from Craney Island, Canaveral Harbor, and Mobile test basin referred to in Part IV of the report.

Table C1

Data Used in Calculating Permeability from Oedometer Testing

Craney Island

Sample	σ' tsf	e	$\bar{e}$	$\bar{a}_v$ psf^{-1}	$\bar{H}^2$ $in.^2$	t_{50} min	k ft/min
	0.013	6.31					
			6.24	1.184×10^{-2}	0.3084	3.25	1.325×10^{-5}
	0.02	6.17					
			5.69	1.551×10^{-2}	0.2639	300	1.741×10^{-7}
	0.05	5.21					
			4.87	6.080×10^{-3}	0.2014	315	5.653×10^{-8}
$\left(e_o^{1-B} = 8.59\right)$	0.10	4.53					
			4.17	2.792×10^{-3}	0.1562	32	2.290×10^{-7}
	0.25	3.81					
			3.56	1.303×10^{-3}	0.1209	32	9.216×10^{-8}
	0.50	3.32					
			3.04	6.515×10^{-4}	0.0953	25	5.248×10^{-8}
	1.00	2.77					
			2.56	2.533×10^{-4}	0.0732	20	2.223×10^{-8}
	2.00	2.35					
	0.006	5.34					
			5.29	3.508×10^{-3}	0.5435	20	1.294×10^{-6}
	0.02	5.24					
			5.08	6.887×10^{-3}	0.5007	140	3.458×10^{-7}
	0.05	4.92					
			4.54	8.396×10^{-3}	0.4152	69	7.785×10^{-7}
$\left(e_o^{3.2} = 5.44\right)$	0.10	4.15					
			3.82	2.147×10^{-3}	0.3119	23	5.157×10^{-7}
	0.25	3.48					
			3.21	1.002×10^{-3}	0.2360	39	1.229×10^{-7}
	0.50	2.94					
			2.72	4.140×10^{-4}	0.1822	23	7.526×10^{-8}
	1.00	2.50					

(Continued)

Table C1 (Concluded)

Sample	σ' tsf	e	$\bar{e}$	$\bar{a}_v$ psf^{-1}	$\bar{H}^2$ in.^{2}	t_{50} min	k ft/min
	0.007	4.55					
			4.53	1.428×10^{-3}	0.5547	6	2.038×10^{-6}
	0.02	4.51					
			4.46	1.882×10^{-3}	0.5401	18	8.829×10^{-7}
	0.05	4.41					
			4.35	1.795×10^{-3}	0.5188	24	6.191×10^{-7}
(e_o = 4.56)	0.10	4.29					
			4.02	1.787×10^{-3}	0.4536	39	3.534×10^{-7}
	0.25	3.74					
			3.51	8.339×10^{-4}	0.3602	51	1.115×10^{-7}
	0.50	3.27					
			2.99	5.762×10^{-4}	0.2793	30	1.148×10^{-7}
	1.00	2.70					
	0.013	5.74					
			5.71	4.080×10^{-3}	0.5391	8	3.498×10^{-6}
	0.02	5.68					
			5.52	4.901×10^{-3}	0.5104	48	6.823×10^{-7}
	0.05	5.36					
			5.09	5.646×10^{-3}	0.4424	50	7.003×10^{-7}
(e_o = 5.84)	0.10	4.82					
			4.29	3.288×10^{-3}	0.3320	50	3.523×10^{-7}
	0.25	3.75					
			3.47	1.100×10^{-3}	0.2346	30	1.643×10^{-7}
	0.50	3.18					
			2.65	3.802×10^{-4}	0.1747	27	1.332×10^{-7}
	1.00	2.12					
	0.012	5.28					
			5.25	4.614×10^{-3}	0.5426	26	1.315×10^{-6}
	0.02	5.21					
			4.99	7.693×10^{-3}	0.4962	56	9.715×10^{-7}
	0.05	4.77					
			4.54	4.806×10^{-3}	0.4250	78	4.035×10^{-7}
(e_o = 5.35)	0.10	4.31					
			3.95	2.060×10^{-3}	0.3402	48	2.518×10^{-7}
	0.25	3.58					
			3.36	9.613×10^{-4}	0.2602	36	1.360×10^{-7}
	0.50	3.13					
			2.87	4.806×10^{-4}	0.2020	25	8.566×10^{-8}
	1.00	2.61					

Table C2

Data Used for Calculation of Coefficients of Consolidation

Craney Island

e	a_v^* psf^{-1}	k* ft/day	c_v ft^2/day	g ft^2/day
1.5	7.854×10^{-5}	2.059×10^{-6}	1.050×10^{-5}	1.681×10^{-4}
2.0	1.538×10^{-4}	1.008×10^{-5}	3.151×10^{-3}	3.501×10^{-4}
2.5	3.076×10^{-4}	3.816×10^{-5}	6.958×10^{-3}	5.680×10^{-4}
3.0	5.954×10^{-4}	1.109×10^{-4}	1.194×10^{-2}	7.462×10^{-4}
3.5	1.191×10^{-3}	2.448×10^{-4}	1.482×10^{-2}	7.320×10^{-4}
4.0	2.307×10^{-3}	4.752×10^{-4}	1.650×10^{-2}	6.602×10^{-4}
4.5	5.670×10^{-3}	6.568×10^{-4}	1.332×10^{-2}	4.403×10^{-4}
5.0	1.104×10^{-2}	1.440×10^{-3}	1.254×10^{-2}	3.484×10^{-4}
5.5	1.642×10^{-2}	2.419×10^{-3}	1.535×10^{-2}	3.632×10^{-4}
6.0	2.404×10^{-2}	3.888×10^{-3}	1.814×10^{-2}	3.703×10^{-4}
7.0	5.100×10^{-2}	9.792×10^{-3}	2.462×10^{-2}	3.846×10^{-4}
8.0	1.069×10^{-1}	2.448×10^{-2}	3.303×10^{-2}	4.078×10^{-4}
9.0	2.244×10^{-1}	6.764×10^{-2}	4.473×10^{-2}	4.473×10^{-4}
10.0	4.774 x 10-1	1.584×10^{-1}	5.849×10^{-2}	4.834×10^{-4}
11.0	8.185×10^{-1}	4.032×10^{-1}	9.475×10^{-2}	6.579×10^{-4}

* These values determined from curves shown in Figures 24 and 25.

Table C3

Data Used in Calculating Permeability from Oedometer Testing

Canaveral Harbor

	σ' tsf	e	$\bar{e}$	$\bar{a}_v$ psf^{-1}	$\bar{H}^2$ $in.^2$	t_{50} min	k ft/min
	0.012	5.84					
			5.22	5.836×10^{-2}	0.2452	130	1.511×10^{-6}
	0.02	4.59					
			4.52	5.956×10^{-3}	0.1889	110	1.641×10^{-7}
	0.05	4.05					
			3.86	3.445×10^{-5}	0.1585	72	1.332×10^{-7}
$(e_o = 8.13)$	0.10	3.67					
			3.40	1.836×10^{-3}	0.1301	50	9.269×10^{-8}
	0.75	3.14					
			2.88	9.207×10^{-4}	0.1000	60	3.376×10^{-8}
	0.50	2.63					
			2.46	3.619×10^{-4}	0.0799	41	1.740×10^{-8}
	1.00	2.28					

Table C4

Data Used for Calculation of Coefficients of Consolidation

Canaveral Harbor

e	a_v^* psf^{-1}	k* ft/day	c_v ft^2/day	g ft^2/day
2.0	1.686×10^{-4}	1.123×10^{-5}	3.202×10^{-3}	3.558×10^{-4}
3.0	7.638×10^{-4}	5.616×10^{-5}	4.713×10^{-3}	2.946×10^{-4}
4.0	3.716×10^{-3}	2.335×10^{-4}	5.031×10^{-3}	2.012×10^{-4}
5.0	1.864×10^{-2}	7.632×10^{-4}	3.937×10^{-3}	1.094×10^{-4}
6.0	5.429×10^{-2}	1.814×10^{-3}	3.748×10^{-3}	7.650×10^{-5}
8.0	1.371×10^{-1}	5.760×10^{-3}	6.060×10^{-3}	7.481×10^{-5}
10.0	3.427×10^{-1}	2.088×10^{-2}	1.074×10^{-2}	8.876×10^{-5}
12.0	8.501×10^{-1}	1.123×10^{-1}	2.752×10^{-2}	1.628×10^{-4}
14.0	2.150×10^{0}	6.336×10^{-1}	7.084×10^{-2}	3.148×10^{-4}

* These values determined from curves shown in Figures 28 and 29.

Table C5

Data Used in Calculating Permeability from Oedometer Testing

Mobile Test Basin

Sample	σ' tsf	e	$\bar{e}$	$\bar{a}_v$ psf^{-1}	$\bar{H}^2$ $in.^2$	t_{50} min	k ft/min
	0.04	2.94					
			2.89	1.086×10^{-3}	1.7745	230	1.839×10^{-7}
	0.08	2.85					
			2.77	1.068×10^{-3}	1.6675	60	6.721×10^{-7}
(B1-21, $e_o = 3.12$)	0.16	2.69					
			2.55	8.143×10^{-4}	1.4940	46	6.360×10^{-7}
	0.32	2.42					
			2.26	4.750×10^{-4}	1.2551	34	4.592×10^{-7}
	0.64	2.10					
			2.01	1.402×10^{-4}	1.0605	9	4.685×10^{-7}
	1.28	1.91					
	0.04	2.63					
			2.59	1.086×10^{-3}	1.7240	200	2.226×10^{-7}
	0.08	2.55					
			2.48	9.048×10^{-4}	1.6205	60	5.995×10^{-7}
(B1-2B, $e_o = 2.80$)	0.16	2.41					
			2.28	7.510×10^{-4}	1.4454	57	4.967×10^{-7}
	0.32	2.16					
			2.01	4.479×10^{-4}	1.2243	42	3.703×10^{-7}
	0.64	1.87					
			1.76	1.696×10^{-3}	1.0140	24	2.216×10^{-7}
	1.28	1.64					

(Continued)

Table C5 (Concluded)

Sample	σ' tsf	e	$\bar{e}$	$\bar{a}_v$ psf^{-1}	$\bar{H}^2$ in.^{2}	t_{50} min	k ft/min
	0.04	2.46					
			2.41	1.339×10^{-3}	1.8382	65	9.480×10^{-7}
	0.08	2.36					
			2.27	1.122×10^{-5}	1.6913	41	1.708×10^{-6}
(B1-24, $e_o = 2.57$)	0.16	2.18					
			2.06	7.691×10^{-4}	1.4872	40	7.977×10^{-7}
	0.32	1.94					
			1.81	3.845×10^{-4}	1.2455	32	4.546×10^{-7}
	0.64	1.68					
			1.55	1.923×10^{-4}	1.0221	28	2.350×10^{-7}
	1.25	1.41					
	0.02	2.54					
			2.43	5.285×10^{-3}	1.6654	100	1.363×10^{-6}
	0.05	2.32					
			2.23	1.535×10^{-3}	1.4702	85	7.017×10^{-7}
(2-6, $e_o = 2.98$)							
			2.02	8.438×10^{-4}	1.2905	41	7.507×10^{-7}
	0.25	1.88					
			1.78	3.938×10^{-4}	1.0899	39	3.379×10^{-7}
	0.50	1.69					
			1.59	1.969×10^{-4}	0.9467	25	2.458×10^{-7}
	1.00	1.49					

Table C6

Data Used for Calculation of Coefficients of Consolidation

Mobile Test Basin

	Primary				Secondary			
e	a_v^* psf^{-1}	k* ft/day	c_v ft^2/day	g ft^2/day	a_v^* psf^{-1}	k* ft/day	c_v ft^2/day	g ft^2/day
1.5	1.221×10^{-4}	1.109×10^{-5}	3.639×10^{-3}	5.822×10^{-4}	1.221×10^{-4}	2.189×10^{-4}	7.183×10^{-2}	1.149×10^{-2}
2.0	5.083×10^{-4}	5.04×10^{-5}	4.767×10^{-3}	5.297×10^{-4}	5.083×10^{-4}	6.624×10^{-4}	6.265×10^{-2}	6.961×10^{-3}
2.5	1.978×10^{-3}	1.872×10^{-4}	5.308×10^{-3}	4.333×10^{-4}	1.717×10^{-3}	1.397×10^{-3}	4.564×10^{-2}	3.725×10^{-3}
3.0	4.738×10^{-3}	4.752×10^{-4}	6.429×10^{-3}	4.018×10^{-4}	5.284×10^{-3}	2.318×10^{-3}	2.812×10^{-2}	1.758×10^{-3}
4.0	1.486×10^{-2}	1.354×10^{-3}	7.301×10^{-3}	2.920×10^{-4}	3.040×10^{-2}	5.472×10^{-3}	1.442×10^{-2}	5.769×10^{-4}
5.0	4.228×10^{-2}	2.981×10^{-3}	6.779×10^{-3}	1.883×10^{-4}	9.648×10^{-2}	1.224×10^{-2}	1.220×10^{-2}	3.389×10^{-4}
6.0	1.018×10^{-1}	6.48×10^{-3}	7.141×10^{-3}	1.457×10^{-4}	1.921×10^{-1}	2.707×10^{-2}	1.581×10^{-2}	3.226×10^{-4}
8.0	2.799×10^{-1}	3.168×10^{-2}	1.632×10^{-2}	2.015×10^{-4}	5.257×10^{-1}	1.325×10^{-1}	3.635×10^{-2}	4.488×10^{-4}
9.0	2.972×10^{-1}	7.013×10^{-2}	3.782×10^{-2}	3.782×10^{-4}	5.487×10^{-1}	2.844×10^{-1}	8.452×10^{-2}	8.452×10^{-4}

* These values determined from curves shown in Figures 32 and 33.

APPENDIX D: CALCULATION OF SETTLEMENTS AT CRANEY ISLAND

This appendix contains tables of data used for the calculation of settlements in the Craney Island disposal area. Ultimate settlement and consolidation as a function of time are included.

Table D1

Ultimate Settlement Calculations for Craney Island Disposal Area

(e_{oo} = 12.0 ; G_s = 2.75)

i	$h_{i,o}$ ft	$\Sigma h_{i,o}$ ft	ℓ_i ft	$\Sigma \ell_i$ ft	$\sigma'_{i,\infty}$ psf	$e_{i,\infty}$	$h_{i,\infty}$ ft	$\delta_{i,\infty}$ ft	$\Sigma \delta_{i,\infty}$ ft
1	0.50	0.50	0.0385	0.0385	2.1	10.40	0.4385	0.0615	0.0615
2	0.50	1.00	0.0385	0.0769	6.3	8.94	0.3823	0.1177	0.1792
3	0.50	1.50	0.0385	0.1154	10.5	8.26	0.3562	0.1438	0.3230
4	0.50	2.00	0.0385	0.1538	14.7	7.81	0.3350	0.1650	0.4880
5	0.50	2.50	0.0385	0.1923	18.9	7.47	0.3258	0.1742	0.6622
6	0.50	3.00	0.0385	0.2308	23.1	7.20	0.3154	0.1846	0.8468
7	0.50	3.50	0.0385	0.2692	27.3	6.97	0.3065	0.1935	1.0403
8	0.50	4.00	0.0385	0.3077	31.5	6.78	0.2292	0.2008	1.2411
9	0.50	4.50	0.0385	0.3462	35.7	6.63	0.2935	0.2065	1.4476
10	0.50	5.00	0.0385	0.3846	39.9	6.47	0.2873	0.2127	1.6603
11	0.50	5.50	0.0385	0.4231	44.1	6.33	0.2819	0.2181	1.8784
12	0.50	6.00	0.0385	0.4615	48.3	6.70	0.2769	0.2231	2.1015
13	0.50	6.50	0.0385	0.500	52.5	6.09	0.2727	0.2273	2.3288
14	0.50	7.00	0.0385	0.5385	56.7	5.99	0.2688	0.2312	2.5600
15	0.50	7.50	0.0385	0.5769	60.9	5.90	0.2654	0.2346	2.7946
16	0.50	8.00	0.0385	0.6154	65.1	5.81	0.2619	0.2381	3.0327
17	0.50	8.50	0.0385	0.6538	69.3	5.72	0.2585	0.2415	3.2742
18	0.50	9.00	0.0385	0.6923	73.5	5.64	0.2554	0.2446	3.5188
19	0.50	9.50	0.0385	0.7308	77.7	5.57	0.2527	0.2473	3.7661
20	0.50	10.00	0.0385	0.7692	81.9	5.50	0.2500	0.2500	4.0161
21	0.50	10.50	0.0385	0.8077	86.1	5.43	0.2473	0.2527	4.2688
22	0.50	11.00	0.0385	0.8462	90.3	5.37	0.2450	0.2550	4.5238
23	0.50	11.50	0.0385	0.8846	94.5	5.29	0.2419	0.2581	4.7819
24	0.50	12.00	0.0385	0.9231	98.7	5.24	0.2400	0.2600	5.0419
25	0.50	12.50	0.0385	0.9615	102.9	5.18	0.2377	0.2623	5.3042
26	0.50	13.00	0.0385	1.0000	107.1	5.12	0.2354	0.2646	5.5688
27	0.50	13.50	0.0385	1.0385	111.3	5.07	0.2335	0.2665	5.8353
28	0.50	14.00	0.0385	1.0769	115.5	5.02	0.2315	0.2685	6.1038
29	0.50	14.50	0.0385	1.1154	119.7	4.98	0.2300	0.2700	6.3738
30	0.50	15.00	0.0385	1.1538	123.9	4.93	0.2281	0.2719	6.6457

(Continued)

Table D1 (Continued)

i	$h_{i,o}$ ft	$\Sigma h_{i,o}$ ft	ℓ_i ft	$\Sigma \ell_i$ ft	$\sigma'_{i,\infty}$ psf	$e_{i,\infty}$	$h_{i,\infty}$ ft	$\delta_{i,\infty}$ ft	$\Sigma \delta_{i,\infty}$ ft
31	0.50	15.50	0.0385	1.1923	128.1	4.89	0.2265	0.2735	6.9192
32	0.50	16.00	0.0385	1.2308	132.3	4.85	0.2250	0.2750	7.1942
33	0.50	16.50	0.0385	1.2692	136.5	4.81	0.2235	0.2765	7.4707
34	0.50	17.00	0.0385	1.3077	140.7	4.77	0.2219	0.2781	7.7488
35	0.50	17.50	0.0385	1.3462	144.9	4.73	0.2204	0.2796	8.0284
36	0.50	18.00	0.0385	1.3846	149.1	4.70	0.2192	0.2808	8.3092
37	0.50	18.50	0.0385	1.4231	153.3	4.67	0.2181	0.2819	8.5911
38	0.50	19.00	0.0385	1.4615	157.5	4.64	0.2169	0.2831	8.8742
39	0.50	19.50	0.0385	1.5000	161.7	4.61	0.2158	0.2842	9.1584
40	0.50	20.00	0.0385	1.5385	165.9	4.58	0.2146	0.2854	9.4438
41	0.50	20.50	0.0385	1.5769	170.1	4.55	0.2135	0.2865	9.7303
42	0.50	21.00	0.0385	1.6154	174.3	4.53	0.2127	0.2873	10.0176
43	0.50	21.50	0.0385	1.6538	178.5	4.51	0.2119	0.2881	10.3057
44	0.50	22.00	0.0385	1.6923	182.7	4.49	0.2112	0.2888	10.5945
45	0.50	22.50	0.0385	1.7308	186.9	4.47	0.2104	0.2896	10.8841
46	0.50	23.00	0.0385	1.7692	191.1	4.45	0.2096	0.2904	11.1745
47	0.50	23.50	0.0385	1.8077	195.3	4.43	0.2088	0.2912	11.4657
48	0.50	24.00	0.0385	1.8462	199.5	4.41	0.2081	0.2919	11.7576
49	0.50	24.50	0.0385	1.8846	203.7	4.39	0.2073	0.2927	12.0503
50	0.50	25.00	0.0385	1.9231	207.9	4.37	0.2065	0.2935	12.3438
51	0.50	25.50	0.0385	1.9615	212.1	4.35	0.2058	0.2942	12.6380
52	0.50	26.00	0.0385	2.000	216.3	4.33	0.2050	0.2950	12.9330
53	0.50	26.50	0.0385	2.0385	220.5	4.31	0.2042	0.2958	13.2288
54	0.50	27.00	0.0385	2.0769	224.7	4.29	0.2035	0.2965	13.5253
55	0.50	27.50	0.0385	2.1154	228.9	4.27	0.2027	0.2973	13.8226
56	0.50	28.00	0.0385	2.1538	233.1	4.26	0.2073	0.2977	14.1203
57	0.50	28.50	0.0385	2.1923	237.3	4.24	0.2015	0.2985	14.4188
58	0.50	29.00	0.0385	2.2308	241.5	4.22	0.2008	0.2992	14.7180
59	0.50	29.50	0.0385	2.2692	245.7	4.20	0.2000	0.3000	15.0180
60	0.50	30.00	0.0385	2.3077	249.9	4.19	0.1996	0.3004	15.3184

(Continued)

Table D1 (Continued)

i	$h_{i,o}$ ft	$\Sigma h_{i,o}$ ft	ℓ_i ft	$\Sigma \ell_i$ ft	$\sigma'_{i,\infty}$ psf	$e_{i,\infty}$	$h_{i,\infty}$ ft	$\delta_{i,\infty}$ ft	$\Sigma \delta_{i,\infty}$ ft
61	0.50	30.50	0.0385	2.3462	254.1	4.18	0.1992	0.3008	15.6192
62	0.50	31.00	0.0385	2.3846	258.3	4.16	0.1985	0.3015	15.9207
63	0.50	31.50	0.0385	2.4231	262.5	4.14	0.1977	0.3023	16.2230
64	0.50	32.00	0.0385	2.4615	266.7	4.13	0.1973	0.3027	16.5257
65	0.50	32.50	0.0385	2.5000	270.9	4.12	0.1969	0.3031	16.8288
66	0.50	33.00	0.0385	2.5385	275.1	4.11	0.1965	0.3035	17.1323
67	0.50	33.50	0.0385	2.5769	279.3	4.09	0.1958	0.3042	17.4365
68	0.50	34.00	0.0385	2.6154	283.5	4.03	0.1954	0.3046	17.7411
69	0.50	34.50	0.0385	2.6538	287.7	4.07	0.1950	0.3050	18.0461
70	0.50	35.00	0.0385	2.6923	291.9	4.06	0.1946	0.3054	18.3515
71	0.50	35.50	0.0385	2.7308	296.1	4.05	0.1942	0.3058	18.6573
72	0.50	36.00	0.0385	2.7692	300.3	4.04	0.1938	0.3062	18.9635
73	0.50	36.50	0.0385	2.8077	304.5	4.03	0.1935	0.3065	19.2700
74	0.50	37.00	0.0385	2.8462	308.7	4.02	0.1931	0.3069	19.5769
75	0.50	37.50	0.0385	2.8846	312.9	4.01	0.1927	0.3073	19.8842
76	0.50	38.00	0.0385	2.9231	317.1	4.00	0.1923	0.3077	20.1919
77	0.50	38.50	0.0385	2.9615	321.3	3.99	0.1919	0.3081	20.5000
78	0.50	39.00	0.0385	3.0000	325.5	3.98	0.1915	0.3085	20.8085
79	0.50	39.50	0.0385	3.0385	329.7	3.97	0.1912	0.3088	21.1173
80	0.50	40.00	0.0385	3.0769	333.9	3.96	0.1908	0.3092	21.4265
81	0.50	40.50	0.0385	3.1154	338.1	3.95	0.1904	0.3096	21.7361
82	0.50	41.00	0.0385	3.1538	342.3	3.94	0.1900	0.3100	22.0461
83	0.50	41.50	0.0385	3.1923	346.5	3.95	0.1896	0.3104	22.3565
84	0.50	42.00	0.0385	3.2308	350.7	3.92	0.1892	0.3108	22.6673
85	0.50	42.50	0.0385	3.2692	354.9	3.92	0.1892	0.3108	22.9781
86	0.50	43.00	0.0385	3.3077	359.1	3.91	0.1888	0.3112	23.2893
87	0.50	43.50	0.0385	3.3462	363.3	3.90	0.1885	0.3115	23.6008
88	0.50	44.00	0.0385	3.3846	367.5	3.89	0.1881	0.3119	23.9127
89	0.50	44.50	0.0385	3.4231	371.7	3.88	0.1877	0.3123	24.2250
90	0.50	45.00	0.0385	3.4615	375.9	3.87	0.1873	0.3127	24.5377

(Continued)

Table D1 (Concluded)

i	$h_{i,o}$ ft	$\Sigma h_{i,o}$ ft	ℓ_i ft	$\Sigma \ell_i$ ft	$\sigma'_{i,\infty}$ psf	$e_{i,\infty}$	$h_{i,\infty}$ ft	$\delta_{i,\infty}$ ft	$\Sigma \delta_{i,\infty}$ ft
91	0.50	45.50	0.0385	3.5000	380.1	3.86	0.1869	0.3131	24.8508
92	0.50	46.00	0.0385	3.5385	384.3	3.86	0.1869	0.3131	25.1639
93	0.50	46.50	0.0385	3.5769	388.5	3.85	0.1865	0.3135	25.4774
94	0.50	47.00	0.0385	3.6154	392.7	3.85	0.1865	0.3135	25.7909
95	0.50	47.50	0.0385	3.6538	396.9	3.84	0.1862	0.3138	26.1047
96	0.50	48.00	0.0385	3.6923	401.1	3.83	0.1858	0.3142	26.4189
97	0.50	48.50	0.0385	3.7308	405.3	3.82	0.1854	0.3146	26.7335
98	0.50	49.00	0.0385	3.7692	409.5	3.81	0.1850	0.3150	27.0485
99	0.50	49.50	0.0385	3.8077	413.7	3.80	0.1846	0.3154	27.3639
100	0.50	50.00	0.0385	3.8462	417.9	3.79	0.1842	0.3158	27.6797
101	0.50	50.50	0.0385	3.8846	422.1	3.78	0.1838	0.3162	27.9959
102	0.50	51.00	0.0385	3.9231	426.3	3.77	0.1835	0.3165	28.3124
103	0.50	51.50	0.0385	3.9615	430.5	3.76	0.1831	0.3169	28.6793
104	0.50	52.00	0.0385	4.0000	434.7	3.75	0.1827	0.3173	28.9466
105	0.50	52.50	0.0385	4.0385	438.9	3.75	0.1827	0.3173	29.7639
106	0.50	53.00	0.0385	4.0769	443.1	3.74	0.1823	0.3177	29.5816
107	0.50	53.50	0.0385	4.1154	447.3	3.73	0.1819	0.3181	29.8997
108	0.50	54.00	0.0385	4.1538	451.5	3.72	0.1815	0.3185	30.2182
109	0.50	54.50	0.0385	4.1923	455.7	3.72	0.1815	0.3185	30.5367
110	0.50	55.00	0.0385	4.2308	459.9	3.71	0.1812	0.3188	30.8555
111	0.50	55.50	0.0385	4.2692	464.1	3.71	0.1812	0.3188	31.1743
112	0.50	56.00	0.0385	4.3077	468.3	3.70	0.1808	0.3192	31.4935
113	0.50	56.50	0.0385	4.3462	472.5	3.70	0.1808	0.3192	31.8127
114	0.50	57.00	0.0385	4.3846	476.7	3.69	0.1804	0.3196	32.1323
115	0.50	57.50	0.0385	4.4231	480.9	3.68	0.1800	0.3200	32.4523
116	0.50	58.00	0.0385	4.4615	485.1	3.68	0.1800	0.3200	32.7723
117	0.50	58.50	0.0385	4.5000	489.3	3.67	0.1796	0.3204	33.0927
118	0.50	59.00	0.0385	4.5385	493.5	3.67	0.1796	0.3204	33.4131
119	0.50	59.50	0.0385	4.5769	497.7	3.66	0.1792	0.3208	33.7339
120	0.50	60.00	0.0385	4.6154	501.9	3.66	0.1792	0.3208	34.0547
121	0.50	60.50	0.0385	4.6538	506.1	3.65	0.1788	0.3212	34.3759

Table D2

Calculation of Consolidation by Linear Finite Strain Theory for Craney Island Disposal Area (15% Sand)

t days	$\Sigma h_{i,o}$ ft	t' days	$\bar{e}$	$\bar{H}$ ft	g ft^2/day	T'	N	U' %	δ'_∞ ft	δ'' ft	δ' ft	U %
0	0.5	0	-	-	-	0	-	0	0.0615	0	0	0
365	0.5	365	10.5	0.44	5.6×10^{-4}	138	0.1	100	0.0615	0	0.0615	100
365+	2.0	0	-	-	-	-	-	0	0.4880	0.0615	0.0615	13
730-	2.0	365	8.8	1.51	4.3×10^{-4}	6.64	0.3	100	0.4880	0.0615	0.4880	100
730+	4.0	0	-	-	-	0	-	0	1.2411	0.4880	0.4880	39
1095	4.0	365	8.0	2.77	4.0×10^{-4}	1.542	0.7	100	1.2411	0.4880	1.2411	100
1095+	8.5	0	-	-	-	0	-	0	3.2742	1.2411	1.2411	38
1460-	8.5	365	7.8	5.75	4.0×10^{-4}	0.342	1.4	76	3.2742	1.2411	2.7863	85
1460+	10.5	0	-	-	-	0	-	0	4.2688	2.7863	2.7863	65
1825-	10.5	365	7.5	6.87	3.9×10^{-4}	0.218	1.8	61	4.2688	2.7863	3.6906	86
1825+	12.0	0	-	-	-	0	-	0	5.0419	3.6906	3.6906	73
2190-	12.0	365	7.2	7.57	3.9×10^{-4}	0.167	2.0	52	5.0419	3.6906	4.3933	87
2190+	14.0	0	-	-	-	0	-	0	6.1038	4.3933	4.3933	72
2555-	14.0	365	7.2	8.83	3.9×10^{-4}	0.123	2.4	46	6.1038	4.3933	5.1801	85
2555+	14.5	0	-	-	-	0	-	0	6.3738	5.1801	5.1801	81
2920-	14.5	365	6.9	8.81	3.8×10^{-4}	0.111	2.4	42	6.3738	5.1801	5.6815	89
2920+	16.0	0	-	-	-	0	-	0	7.1942	5.6815	5.6815	80
3285-	16.0	365	6.9	9.72	3.8×10^{-4}	0.092	2.7	36	7.1942	5.6815	6.2261	87

(Continued)

Table D2 (Continued)

t days	$\Sigma h_{i,o}$ ft	t' days	$\bar{e}$	$\bar{H}$ ft	g ft^2/day	T'	N	U' %	δ'_∞ ft	δ'' ft	δ' ft	U %
3285+	18.5	0	-	-	-	0	-	0	8.5911	6.2261	6.2261	72
3650-	18.5	365	7.1	11.53	3.8×10^{-4}	0.068	3.1	30	8.5911	6.2261	6.9356	81
3650+	21.0	0	-	-	-	0	-	0	10.0176	6.9356	6.9396	69
4015-	21.0	365	7.2	13.24	3.9×10^{-4}	0.055	3.5	26	10.0176	6.9356	7.7369	77
4015+	25.5	0	-	-	-	0	-	0	12.6380	7.7369	7.7369	61
4380-	25.5	365	7.5	16.67	3.9×10^{-4}	0.0370	4.3	20	12.6380	7.7369	8.7171	69
4380+	27.5	0	-	-	-	0	-	0	13.8226	8.7171	8.7171	63
4745-	27.5	365	7.4	17.77	3.9×10^{-4}	0.0318	4.6	18	13.8226	8.7171	9.6361	70
4745+	30.0	0	-	-	-	0	-	0	15.3184	9.6361	9.6361	63
5110-	30.0	365	7.4	19.38	3.9×10^{-4}	0.0267	5.0	17	15.3184	9.6361	10.6021	69
5110+	32.5	0	-	-	-	0	-	0	16.8288	10.6021	10.6021	63
5475-	32.5	365	7.4	20.00	3.9×10^{-4}	0.0228	5.5	16	16.8288	10.6021	11.5984	69
5475+	41.0	0	-	-	-	0	-	0	22.0461	11.5984	11.5984	53
5840-	41.0	365	7.9	28.07	4.0×10^{-4}	0.0147	6.9	12	22.0461	11.5984	12.8521	58
5840+	41.5	0	-	-	-	0	-	0	22.3565	12.8521	12.8521	57
6205-	41.5	365	7.6	27.45	3.9×10^{-4}	0.0140	7.0	12	22.3565	12.8521	13.9926	63
6205+	43.5	0	-	-	-	0	-	0	23.6008	13.9926	13.9926	59
6570-	43.5	365	7.5	28.44	3.9×10^{-4}	0.0127	7.3	12	23.6008	13.9926	15.1456	64
6570+	45.5	0	-	-	-	0	-	0	24.8508	15.1456	15.1456	61

(Continued)

Table D2 (Concluded)

t days	$\Sigma h_{i,o}$ ft	t' days	$\bar{e}$	$\bar{H}$ ft	g ft^2/day	T'	N	U' %	δ'_∞ ft	δ'' ft	δ' ft	U %
6935-	45.5	365	7.4	29.40	3.9×10^{-4}	0.0116	7.6	11	24.8508	15.1456	16.2132	65
6935+	47.5	0	-	-	-	0	-	0	26.1047	16.2132	16.2132	62
7300-	47.5	365	7.3	30.33	3.9×10^{-4}	0.017	8.0	10	26.1047	16.2132	17.2023	66
7300+	49.0	0	-	-	-	0	-	0	27.0485	17.2023	17.2023	64
7655-	49.0	365	7.2	30.91	3.9×10^{-4}	0.0100	8.2	10	27.0485	17.2023	18.1869	67
7655+	50.0	0	-	-	-	0	-	0	27.6797	18.1869	18.1869	66
8030-	50.0	365	7.0	30.77	3.8×10^{-4}	0.0094	8.4	10	27.6797	18.1869	19.1362	69
8030+	53.0	0	-	-	-	0	-	0	29.5816	19.1362	19.1362	65
8395-	53.0	365	7.1	33.02	3.9×10^{-4}	0.0086	8.9	9	29.5816	19.1362	20.0763	68
8395+	53.0	0	-	-	-	0	-	0	29.8997	20.0763	20.0763	67
8760	53.5	365	6.9	32.51	3.8×10^{-4}	0.0082	9.0	9	29.8997	20.0763	20.9604	70

Table D3

Calculation of Consolidation by Linear Finite Strain Theory for Craney Island Disposal Area (No Sand)

t days	$\Sigma h_{i,o}$ ft	t' days	$\bar{e}$	$\bar{H}$ ft	g ft^2/day	T'	N	U' %	δ'_∞ ft	δ'' ft	δ' ft	U %
0	0.5	0	-	-	-	0	-	0	0.0615	0	0	0
365-	0.5	365	10.5	0.44	5.6×10^{-4}	138	0.1	100	0.0615	0	0.0615	100
365+	2.5	0	-	-	-	0	-	0	0.6622	0.0615	0.0615	9
730-	2.5	365	8.5	1.83	4.2×10^{-4}	4.14	0.4	100	0.6622	0.0615	0.6622	100
730+	5.0	0	-	-	-	0	-	0	1.6603	0.6622	0.6622	40
1095-	5.0	365	7.8	3.38	4.0×10^{-4}	0.987	0.8	96	1.6603	0.6622	1.6204	98
1095+	9.5	0	-	-	-	0	-	0	3.7661	1.6204	1.6204	43
1460-	9.5	365	7.8	6.43	4.0×10^{-4}	0.273	1.6	68	3.7661	1.6204	3.0795	82
1460+	12.0	0	-	-	-	0	-	0	5.0419	3.0795	3.0795	61
1825-	12.0	365	7.6	7.94	3.9×10^{-4}	0.167	2.0	53	5.0419	3.0795	4.1196	82
1825+	13.5	0	-	-	-	0	-	0	5.8353	4.1196	4.1196	71
2190-	13.5	365	7.3	8.62	3.9×10^{-4}	0.132	2.3	47	5.8353	4.1196	4.9260	84
2190+	15.5	0	-	-	-	0	-	0	6.9192	4.9260	4.9260	71
2555-	15.5	365	7.2	9.78	3.9×10^{-4}	0.100	2.6	39	6.9192	4.9260	5.7033	82
2555+	16.5	0	-	-	-	0	-	0	7.4707	5.7033	5.7033	76
2920-	16.5	365	7.0	10.15	3.8×10^{-4}	0.086	2.8	35	7.4707	5.7033	6.3219	85
2920+	18.0	0	-	-	-	0	-	0	8.3092	6.3219	6.3219	76
3285-	18.0	365	7.0	11.08	3.8×10^{-4}	0.072	3.0	30	8.3092	6.3219	6.9181	83

(Continued)

Table D3 (Continued)

t days	$\Sigma h_{i,o}$ ft	t' days	$\bar{e}$	$\bar{H}$ ft	g ft^2/day	T'	N	U' %	δ'_∞ ft	δ'' ft	δ' ft	U %
3285+	21.0	0	-	-	-	0	-	0	10.0176	6.9181	6.9181	69
3650-	21.0	365	7.2	13.25	3.9×10^{-4}	0.055	3.5	26	10.0176	6.9181	7.7240	77
3650+	24.0	0	-	-	-	0	-	0	11.7576	7.7240	7.7240	66
4015-	24.0	365	7.3	15.32	3.9×10^{-4}	0.0418	4.0	22	11.7576	7.7240	8.6114	73
4015+	29.0	0	-	-	-	0	-	0	14.7180	8.6114	8.6114	59
4380-	29.0	365	7.6	19.18	3.9×10^{-4}	0.0286	4.9	18	14.7180	8.6114	9.7106	66
4380+	31.0	0	-	-	-	0	-	0	15.9207	9.7106	9.7106	61
4745-	31.0	365	7.5	20.27	3.9×10^{-4}	0.0250	5.2	16	15.9207	9.7106	10.7042	67
4745+	34.0	0	-	-	-	0	-	0	17.7411	10.7042	10.7042	60
5110-	34.0	365	7.5	23.23	3.9×10^{-4}	0.0208	5.7	15	17.7111	10.7042	11.7597	66
5110+	36.5	0	-	-	-	0	-	0	19.2700	11.7597	11.7597	61
5475-	36.5	365	7.5	23.87	3.9×10^{-4}	0.0181	6.1	13	19.2700	11.7597	12.7360	66
5475+	46.0	0	-	-	-	0	-	0	25.1639	12.7360	12.7360	51
5840-	46.0	365	8.0	31.85	4.0×10^{-4}	0.0117	7.7	11	25.1639	12.7360	14.1031	56
5840+	47.0	0	-	-	-	0	-	0	25.7909	14.1031	14.1031	55
6205-	47.0	365	7.7	31.45	4.0×10^{-4}	0.0112	7.9	11	25.7909	14.1031	15.3888	60
6205+	49.0	0	-	-	-	0	-	0	27.0485	15.3888	15.3888	57
6570-	49.0	365	7.6	32.41	3.9×10^{-4}	0.0100	8.2	10	27.0485	15.3888	16.5548	61
6570+	51.0	0	-	-	-	0	-	0	28.3124	16.5548	16.5548	58

(Continued)

Table D3 (Concluded)

t days	$\Sigma h_{i,o}$ ft	t' days	$\bar{e}$	$\bar{H}$ ft	g ft^2/day	T'	N	U' %	δ'_∞ ft	δ'' ft	δ' ft	U %
6935-	51.0	365	7.5	33.35	3.9×10^{-4}	0.0092	8.6	10	28.3124	16.5548	17.7306	63
6935+	53.5	0	-	-	-	0	-	0	29.8997	17.7306	17.7306	59
7300-	53.5	365	7.4	34.57	3.9×10^{-4}	0.0084	9.0	9	29.8997	17.7306	18.8258	63
7300+	55.5	0	-	-	-	0	-	0	31.1743	18.8258	18.8258	60
7655-	55.5	365	7.3	35.43	3.9×10^{-4}	0.0078	9.3	9	31.1743	18.8258	19.9372	64
7655+	56.5	0	-	-	-	0	-	0	31.8127	19.9372	18.9372	63
8030-	56.5	365	7.2	35.64	3.9×10^{-4}	0.0075	9.5	8	31.8127	19.9372	20.8872	66
8030+	59.5	0	-	-	-	0	-	0	33.7339	20.8872	20.8872	62
8395-	59.5	365	7.2	37.53	3.9×10^{-4}	0.0068	10.0	8	33.7339	20.8872	21.9149	65
8395+	60.5	0	-	-	-	0	-	0	34.3759	21.9149	21.9149	64
8760	60.5	365	7.1	37.70	3.8×10^{-4}	0.0064	10.2	8	34.3759	21.9149	22.9118	67

Table D4

Calculation of Consolidation by Small Strain Theory for

Craney Island Disposal Area (15% Sand)

t days	$\Sigma h_{i,o}$ ft	t' days	$\bar{e}$	$\bar{H}$ ft	c_v ft^2/day	T'	U' %	δ'_∞ ft	δ'' ft	δ' ft	U %
0	0.5	0	-	-	-	0	0	0.0615	0	0	0
365-	0.5	365	10.5	0.44	7.2×10^{-2}	135	100	0.0615	0	0.0615	100
365+	2.0	0	-	-	-	0	0	0.4880	0.0615	0.0615	13
730-	2.0	365	8.8	1.51	4.2×10^{-2}	6.72	100	0.4880	0.0615	0.4880	100
730+	4.0	0	-	-	-	0	0	1.2411	0.4880	0.4880	37
1095-	4.0	365	8.0	2.77	3.3×10^{-2}	1.570	96	1.2411	0.4880	1.2110	98
1095+	8.5	0	-	-	-	0	0	3.2742	1.2110	1.2110	37
1460-	8.5	365	8.3	6.08	3.6×10^{-2}	0.355	57	3.2742	1.2110	2.3870	73
1460+	10.5	0	-	-	-	0	0	4.2688	2.3870	2.3870	56
1825-	10.5	365	8.1	7.35	3.4×10^{-2}	0.230	42	4.2688	2.3870	3.1774	74
1825+	12.0	0	-	-	-	0	0	5.0419	3.1774	3.1774	63
2190-	12.0	365	7.9	8.22	3.2×10^{-2}	0.173	32	5.0419	3.1774	3.7740	75
2190+	14.0	0	-	-	-	0	0	6.1038	3.7740	3.7740	62
2555-	14.0	365	8.0	9.69	3.3×10^{-2}	0.128	25	6.1038	3.7740	4.3564	71
2555+	14.5	0	-	-	-	0	0	6.3738	4.3564	4.3564	68
2920-	14.5	365	7.7	9.70	3.0×10^{-2}	0.116	23	6.3738	4.3564	4.8204	76
2920+	16.0	0	-	-	-	0	0	7.1942	4.8204	4.8204	67

(Continued)

Table D4 (Continued)

t days	$\Sigma h_{i,o}$ ft	t' days	$\bar{e}$	$\bar{H}$ ft	c_v ft^2/day	T'	U' %	δ'_∞ ft	δ'' ft	δ' ft	U %
3285-	16.0	365	7.7	10.71	3.0×10^{-2}	0.095	19	7.1942	4.8204	5.2714	73
3285+	18.5	0	-	-	-	0	0	8.5911	5.2714	5.2714	61
3650-	18.5	365	7.9	12.67	3.2×10^{-2}	0.073	15	8.5911	5.2714	5.7694	67
3650+	21.0	0	-	-	-	0	0	10.0176	5.7694	5.7694	58
4015-	21.0	365	8.1	14.70	3.4×10^{-2}	0.057	12	10.0176	5.7694	6.2792	63
4015+	25.5	0	-	-	-	0	0	12.6380	6.2792	6.2792	50
4380-	25.5	365	8.5	18.63	3.8×10^{-2}	0.0400	9	12.6380	6.2792	6.8515	54
4380+	27.5	0	-	-	-	0	0	13.8226	6.8515	6.8515	50
4745-	27.5	365	8.5	20.10	3.8×10^{-2}	0.0343	8	13.8226	6.8515	7.4092	54
4745+	30.0	0	-	-	-	0	0	15.3184	7.4092	7.4092	48
5110-	30.0	365	8.6	22.15	4.0×10^{-2}	0.0298	7	15.3184	7.4092	7.9628	52
5110+	32.5	0	-	-	-	0	0	16.8288	7.9628	7.9628	47
5475-	32.5	365	8.6	24.00	4.0×10^{-2}	0.0253	6	16.8288	7.9628	8.4948	50
5475+	41.0	0	-	-	-	0	0	22.0461	8.4948	8.4948	39
5840-	41.0	365	9.1	31.85	4.6×10^{-2}	0.0166	4	22.0461	8.4948	9.0369	41
5840+	41.5	0	-	-	-	0	0	22.3565	9.0369	9.0369	40
6205-	41.5	365	9.0	31.92	4.4×10^{-2}	0.0158	4	22.3565	9.0369	9.5697	43
6205+	43.5	0	-	-	-	0	0	23.6008	9.5697	9.5697	41
6570-	43.5	365	9.0	33.46	4.4×10^{-2}	0.0143	3	23.6008	9.5697	9.9906	42

(Continued)

Table D4 (Concluded)

t days	$\Sigma h_{i,o}$ ft	t' days	$\bar{e}$	$\bar{H}$ ft	c_v ft^2/day	T'	U' %	δ'_∞ ft	δ'' ft	δ' ft	U %
6570+	45.5	0	-	-	-	0	0	24.8508	9.9906	9.9906	40
6935-	45.5	365	9.0	35.00	4.4×10^{-2}	0.0131	3	24.8508	9.9906	10.4364	42
6935+	47.5	0	-	-	-	0	0	26.1047	10.4364	10.4364	40
7300-	47.5	365	9.1	36.90	4.6×10^{-2}	0.0123	2	26.1047	10.4364	10.7498	41
7300+	49.0	0	-	-	-	0	0	27.0485	10.4364	10.7498	40
7655-	49.0	365	9.1	38.07	4.6×10^{-2}	0.0116	2	27.0485	10.7498	11.0758	41
7655+	50.0	0	-	-	-	0	0	27.6797	11.0758	11.0758	40
8030-	50.0	365	9.0	38.46	4.4×10^{-2}	0.0109	2	27.6797	11.0758	11.4079	41
8030+	53.0	0	-	-	-	0	0	29.5816	11.4079	11.4079	39
8395-	53.0	365	9.1	41.18	4.6×10^{-2}	0.0099	2	29.5816	11.4079	11.7714	40
8395+	53.5	0	-	-	-	0	0	29.8997	11.7714	11.7714	39
8760	53.5	365	9.0	41.15	4.4×10^{-2}	0.0095	2	29.8997	11.7714	12.1340	41

Table D5

Calculation of Consolidation by Small Strain Theory for

Craney Island Disposal Area (No Sand)

t days	$\Sigma h_{i,o}$ ft	t' days	$\bar{e}$	$\bar{H}$ ft	c_v ft^2/day	T'	U' %	δ'_∞ ft	δ'' ft	δ' ft	U %
0	0.5	0	-	-	-	0	0	0.0615	0	0	0
365-	0.5	365	10.5	0.44	7.2×10^{-2}	135	100	0.0615	0	0.0615	100
365+	2.5	0	-	-	-	0	0	0.6622	0.0615	0.0615	9
730-	2.5	365	8.7	1.86	4.1×10^{-2}	4.32	99	0.6622	0.0615	0.6562	99
730+	5.0	0	-	-	-	0	0	1.6603	0.6562	0.6562	40
1095-	5.0	365	7.9	3.42	3.2×10^{-2}	1.00	91	1.6603	0.6562	1.5699	94
1095+	9.5	0	-	-	-	0	0	3.7661	1.5699	1.5699	42
1460-	9.5	365	8.4	6.87	3.7×10^{-2}	0.286	49	3.7661	1.5699	2.6460	70
1460+	12.0	0	-	-	-	0	0	5.0419	2.6460	2.6460	52
1825-	12.0	365	8.3	8.58	3.6×10^{-2}	0.178	34	5.0419	2.6460	3.4606	69
1825+	13.5	0	-	-	-	0	0	5.8353	3.4606	3.4606	59
2190-	13.5	365	8.1	9.45	3.4×10^{-2}	0.139	27	5.8353	3.4606	4.1018	70
2190+	15.5	0	-	-	-	0	0	6.9192	4.1018	4.1018	59
2555-	15.5	365	8.1	10.85	3.4×10^{-2}	0.105	21	6.9192	4.1018	4.6935	68
2555+	16.5	0	-	-	-	0	0	7.4707	4.6935	4.6935	63
2920-	16.5	365	7.9	11.30	3.2×10^{-2}	0.091	18	7.4707	4.6935	5.1934	70
2920+	18.0	0	-	-	-	0	0	8.3092	5.1934	5.1934	63

(Continued)

Table D5 (Continued)

t days	$\Sigma h_{i,o}$ ft	t' days	$\bar{e}$	$\bar{H}$ ft	c_v ft^2/day	T'	U' %	δ'_∞ ft	δ'' ft	δ' ft	U %
3285-	18.0	365	7.9	12.32	3.2×10^{-2}	0.077	16	8.3092	5.1934	5.6919	69
3285+	21.0	0	-	-	-	0	0	10.0176	5.6919	5.6919	57
3650-	21.0	365	8.1	14.70	3.4×10^{-2}	0.057	12	10.0176	5.6919	6.2110	62
3650+	24.0	0	-	-	-	0	0	11.7576	6.2110	6.2110	53
4015-	24.0	365	8.3	17.17	3.6×10^{-2}	0.0446	10	11.7576	6.2110	6.7657	58
4015+	29.0	0	-	-	-	0	0	14.7180	6.7657	6.7657	46
4380-	29.0	365	8.7	21.64	4.1×10^{-2}	0.0320	7	14.7180	6.7657	7.3224	50
4380+	31.0	0	-	-	-	0	0	15.9207	7.3224	7.3224	46
4745-	31.0	365	8.7	23.13	4.1×10^{-2}	0.0280	6	15.9207	7.3224	7.8383	49
4745+	34.0	0	-	-	-	0	0	17.7411	7.8383	7.8383	44
5110-	34.0	365	8.8	25.63	4.2×10^{-2}	0.0233	5	17.7411	7.8383	8.3334	47
5110+	36.5	0	-	-	-	0	0	19.2700	8.3334	8.3334	43
5475-	36.5	365	8.9	27.80	4.3×10^{-2}	0.0203	4	19.2700	8.3334	8.7709	46
5475+	46.0	0	-	-	-	0	0	25.1639	8.7709	8.7709	35
5840-	46.0	365	9.4	36.80	5.0×10^{-2}	0.0135	3	25.1639	8.7709	9.2627	37
5840+	47.0	0	-	-	-	0	0	25.7909	9.2627	9.2627	36
6205-	47.0	365	9.3	37.24	4.8×10^{-2}	0.0126	2	25.7909	9.2627	9.5933	37
6205+	49.0	0	-	-	-	0	0	27.0485	9.5933	9.5933	35
6570-	49.0	365	9.4	39.20	5.0×10^{-2}	0.0119	2	27.0485	9.5933	9.9424	37

(Continued)

Table D5 (Concluded)

t days	$\Sigma h_{i,o}$ ft	t' days	$\bar{e}$	$\bar{H}$ ft	c_v ft^2/day	T'	U' %	δ'_∞ ft	δ'' ft	δ' ft	U %
6570+	51.0	0	-	-	-	0	0	28.3124	9.9424	9.9424	35
6935-	51.0	365	9.4	40.80	5.0×10^{-2}	0.0110	2	28.3124	9.9424	10.3098	36
6935+	53.5	0	-	-	-	0	0	29.8997	10.3098	10.3098	34
7300-	53.5	365	9.4	42.80	5.0×10^{-2}	0.0100	2	29.8997	10.3098	10.7016	36
7300+	55.5	0	-	-	-	0	0	31.1743	10.7016	10.7016	34
7655-	55.5	365	9.4	44.04	5.0×10^{-2}	0.0093	2	31.1743	10.7016	11.1111	36
7655+	56.5	0	-	-	-	0	0	31.8127	11.1111	11.1111	35
8030-	56.5	365	9.4	45.20	5.0×10^{-2}	0.0089	2	31.8127	11.1111	11.5251	36
8030+	59.5	0	-	-	-	0	0	33.7339	11.5251	11.5251	34
8395-	59.5	365	9.4	47.60	5.0×10^{-2}	0.0081	2	33.7339	11.5251	11.9693	35
8395+	60.5	0	-	-	-	0	0	34.3759	11.9693	11.9693	35
8760	60.5	365	9.4	48.40	5.0×10^{-2}	0.0078	2	34.3759	11.9693	12.4174	36

APPENDIX E: CALCULATION OF SETTLEMENTS AT CANAVERAL HARBOR

This appendix contains tables of data used for the calculation of settlements in the Canaveral Harbor disposal area. Ultimate settlement and consolidation as a function of time are included.

Table E1

Ultimate Settlement Calculations for Canaveral Harbor

Disposal Area (e_{oo} = 17.0 ; G_s = 2.70)

i	$h_{i,o}$ ft	$\Sigma h_{i,o}$ ft	ℓ_i ft	$\Sigma \ell_i$ ft	$\sigma'_{i,\infty}$ psf	$e_{i,\infty}$	$h_{i,\infty}$ ft	$\delta_{i,\infty}$ ft	$\Sigma \delta_{i,\infty}$ ft
1	0.85	0.85	0.0472	0.0472	2.50	12.05	0.6162	0.2338	0.2338
2	0.85	1.70	0.0472	0.0944	7.51	9.67	0.5039	0.3461	0.5799
3	0.85	2.55	0.0472	0.1417	12.52	8.55	0.4510	0.3990	0.9789
4	0.85	3.40	0.0472	0.1889	17.53	7.81	0.4160	0.4340	1.4129
5	0.85	4.25	0.0472	0.2361	22.54	7.27	0.3905	0.4595	1.8724
6	0.85	5.10	0.0472	0.2833	27.55	6.83	0.3697	0.4803	2.3527
7	0.85	5.95	0.0472	0.3306	32.56	6.48	0.3532	0.4968	2.8495
8	0.85	6.80	0.0472	0.3778	37.57	6.18	0.3391	0.5109	3.3604
9	0.85	7.65	0.0472	0.4250	42.58	5.89	0.3254	0.5246	3.8850
10	0.85	8.50	0.0472	0.4722	47.59	5.66	0.3145	0.5355	4.4205

Table E2

Calculation of Consolidation by Linear Finite Strain Theory

for Canaveral Harbor Disposal Area

t days	$\Sigma h_{i,o}$ ft	t' days	$\bar{e}$	$\bar{H}$ ft	g ft^2/day	T'	N	U' %	δ'_∞ ft	δ'' ft	δ' ft	U %
7	8.50	7	15.6	7.84	5.8×10^{-4}	0.0182	6.76	15	4.4205	0.0	0.6631	15
15	8.50	15	14.8	7.46	4.3×10^{-4}	0.0289	6.76	24	4.4205	0.0	1.0609	24
30	8.50	30	13.9	7.04	3.1×10^{-4}	0.0417	6.76	34	4.4205	0.0	1.5030	34
45	8.50	45	13.3	6.75	2.5×10^{-4}	0.0504	6.76	40	4.4205	0.0	1.7682	40
60	8.50	60	12.8	6.52	2.1×10^{-4}	0.0565	6.76	44	4.4205	0.0	1.9450	44
90	8.50	90	12.1	6.19	1.69×10^{-4}	0.068	6.76	52	4.4205	0.0	2.2987	52
120	8.50	120	11.5	5.90	1.40×10^{-4}	0.075	6.76	58	4.4205	0.0	2.5639	58
150	8.50	150	11.1	5.71	1.25×10^{-4}	0.084	6.76	63	4.4205	0.0	2.7849	63
180	8.50	180	10.7	5.52	1.11×10^{-4}	0.090	6.76	67	4.4205	0.0	2.9617	67
240	8.50	240	10.1	5.24	9.6×10^{-5}	0.103	6.76	73	4.4205	0.0	3.2270	73
300	8.50	300	9.6	5.00	8.7×10^{-5}	0.117	6.76	79	4.4205	0.0	3.4922	79
420	8.50	420	8.9	4.67	7.8×10^{-5}	0.147	6.76	87	4.4205	0.0	3.8458	87

Table E3

Calculation of Consolidation by Small Strain Theory

for Canaveral Harbor Disposal Area

t days	$\Sigma h_{i,o}$ ft	t' days	$\bar{e}$	$\bar{H}$ ft	c_v ft^2/day	T'	U' %	δ'_∞ ft	δ'' ft	δ' ft	U %
7	8.5	7	16.3	8.17	2.3×10^{-1}	0.0241	6	4.4205	0.0	0.2652	6
15	8.5	15	16.0	8.02	2.0×10^{-1}	0.0466	10	4.4205	0.0	0.4421	10
30	8.5	30	15.5	7.79	1.55×10^{-1}	0.077	16	4.4205	0.0	0.7073	16
45	8.5	45	15.1	7.60	1.27×10^{-1}	0.099	20	4.4205	0.0	0.8841	20
60	8.5	60	14.8	7.46	1.08×10^{-1}	0.116	23	4.4205	0.0	1.0167	23
90	8.5	90	14.3	7.22	8.4×10^{-2}	0.145	28	4.4205	0.0	1.2377	28
120	8.5	120	14.0	7.08	7.2×10^{-2}	0.172	32	4.4205	0.0	1.4146	32
150	8.5	150	13.7	6.94	6.2×10^{-2}	0.193	36	4.4205	0.0	1.5914	36
180	8.5	180	13.4	6.80	5.2×10^{-2}	0.202	38	4.4205	0.0	1.6798	38
240	8.5	240	13.0	6.61	4.35×10^{-2}	0.239	43	4.4205	0.0	1.9008	43
300	8.5	300	12.7	6.47	3.75×10^{-2}	0.269	46	4.4205	0.0	2.0334	46
420	8.5	420	12.2	6.23	2.9×10^{-2}	0.314	52	4.4205	0.0	2.2987	52

APPENDIX F: CALCULATION OF SETTLEMENTS AT MOBILE TEST BASIN

This appendix contains tables of data used for the calculation of settlements in the Mobile test basin. Ultimate settlement and consolidation as a function of time are included.

Table F1

Ultimate Settlement Calculations for Mobile Test Basin

by Primary Void Ratio-Effective Stress Relationship

(e_{oo} = 10.0 ; G_s = 2.70)

i	$h_{i,o}$ ft	$\Sigma h_{i,o}$ ft	ℓ_i ft	$\Sigma \ell_i$ ft	$\sigma'_{i,\infty}$ psf	$e_{i,\infty}$	$h_{i,\infty}$ ft	$\delta_{i,\infty}$ ft	$\Sigma \delta_{i,\infty}$ ft
1	0.958	0.958	0.0871	0.0871	4.62	8.75	0.8493	0.1089	0.1089
2	0.958	1.916	0.0871	0.1742	13.86	6.68	0.6689	0.2893	0.3982
3	0.958	2.875	0.0871	0.2613	23.10	5.65	0.5792	0.3790	0.7772
4	0.958	3.833	0.0871	0.3484	32.34	5.08	0.5296	0.4286	1.2058
5	0.958	4.791	0.0871	0.4355	41.58	4.74	0.5000	0.4582	1.6640
6	0.958	5.749	0.0871	0.5227	50.82	4.47	0.4764	0.4818	2.1458
7	0.958	6.707	0.0871	0.6098	60.06	4.28	0.4599	0.4983	2.6441
8	0.958	7.666	0.0871	0.6969	69.30	4.09	0.4433	0.5149	3.1590
9	0.958	8.624	0.0871	0.7840	78.55	3.95	0.4311	0.5271	3.6861
10	0.958	9.582	0.0871	0.8711	87.79	3.83	0.4207	0.5375	4.2236

Table F2

Ultimate Settlement Calculations for Mobile Test Basin by

Secondary Void Ratio-Effective Stress Relationship

(e_{oo} = 10.0 ; G_s = 2.70)

i	$h_{i,o}$ ft	$\Sigma h_{i,o}$ ft	ℓ_i ft	$\Sigma \ell_i$ ft	$\sigma'_{i,\infty}$ psf	$e_{i,\infty}$	$h_{i,\infty}$ ft	$\delta_{i,\infty}$ ft	$\Sigma \delta_{i,\infty}$ ft
1	0.958	0.958	0.0871	0.0871	4.62	7.61	0.7500	0.2082	0.2082
2	0.958	1.916	0.0871	0.1742	13.86	5.42	0.5592	0.3990	0.6072
3	0.958	2.875	0.0871	0.2613	23.10	4.57	0.4852	0.4730	1.0802
4	0.958	3.833	0.0871	0.3484	32.34	4.13	0.4469	0.5113	1.5915
5	0.958	4.791	0.0871	0.4355	41.58	3.86	0.4234	0.5348	2.1263
6	0.958	5.749	0.0871	0.5227	50.82	3.65	0.4051	0.5531	2.6794
7	0.958	6.707	0.0871	0.6098	60.06	3.51	0.3929	0.5653	3.2447
8	0.958	7.666	0.0871	0.6969	69.30	3.40	0.3833	0.5749	3.8196
9	0.958	8.624	0.0871	0.7840	78.55	3.29	0.3737	0.5845	4.4041
10	0.958	9.582	0.0871	0.8711	87.79	3.22	0.3676	0.5906	4.9947

Table F3

Calculation of Consolidation by Linear Finite Strain Theory

for Mobile Test Basin (Primary Relationships)

t days	$\Sigma h_{i,o}$ ft	t' days	$\bar{e}$	$\bar{H}$ ft	g ft^2/day	T'	N	U' %	δ'_∞ ft	δ'' ft	δ' ft	U %
7	9.58	7	9.8	9.41	7.8×10^{-4}	0.0072	5.08	5	4.2236	0.0	0.2112	5
15	9.58	15	9.6	9.23	6.4×10^{-4}	0.0126	5.08	8	4.2236	0.0	0.3379	8
30	9.58	30	9.4	9.06	5.3×10^{-4}	0.0210	5.08	13	4.2236	0.0	0.5491	13
45	9.58	45	9.2	8.89	4.5×10^{-4}	0.0267	5.08	17	4.2236	0.0	0.7180	17
60	9.58	60	9.1	8.80	4.1×10^{-4}	0.0324	5.08	20	4.2236	0.0	0.8447	20
90	9.58	90	8.8	8.54	3.3×10^{-4}	0.0341	5.08	25	4.2236	0.0	1.0559	25
120	9.58	120	8.6	8.36	2.9×10^{-4}	0.0459	5.08	29	4.2236	0.0	1.2248	29
150	9.58	150	8.4	8.19	2.58×10^{-4}	0.051	5.08	32	4.2236	0.0	1.3516	32
180	9.58	180	8.3	8.10	2.40×10^{-4}	0.057	5.08	35	4.2236	0.0	1.4787	35
240	9.58	240	8.0	7.84	2.10×10^{-5}	0.066	5.08	40	4.2236	0.0	1.6894	40
300	9.58	300	7.8	7.67	1.91×10^{-4}	0.076	5.08	45	4.2236	0.0	1.9006	45
408	9.58	408	7.4	7.32	1.65×10^{-4}	0.089	5.08	53	4.2236	0.0	2.2385	53

Table F4

Calculation of Consolidation by Linear Finite Strain Theory

for Mobile Test Basin (Secondary Relationships)

t days	$\Sigma h_{i,o}$ ft	t' days	$\bar{e}$	$\bar{H}$ ft	g ft^2/day	T'	N	U' %	δ'_∞ ft	δ'' ft	δ' ft	U %
7	9.58	7	9.5	9.15	1.25×10^{-3}	0.0106	7.39	9	4.9947	0.0	0.4495	9
15	9.58	15	9.2	8.89	9.0×10^{-4}	0.0178	7.39	15	4.9947	0.0	0.7491	15
30	9.58	30	8.7	8.45	6.5×10^{-4}	0.0257	7.39	22	4.9947	0.0	1.0988	22
45	9.58	45	8.4	8.19	5.5×10^{-4}	0.0326	7.39	27	4.9947	0.0	1.3486	27
60	9.58	60	8.2	8.01	5.1×10^{-4}	0.0403	7.39	32	4.9947	0.0	1.5983	32
90	9.58	90	7.7	7.58	4.3×10^{-4}	0.051	7.39	41	4.9947	0.0	2.0478	41
120	9.58	120	7.2	7.14	3.8×10^{-4}	0.060	7.39	49	4.9947	0.0	2.4474	49
150	9.58	150	6.7	6.71	3.5×10^{-4}	0.069	7.39	56	4.9947	0.0	2.7970	56
180	9.58	180	6.4	6.45	3.4×10^{-4}	0.081	7.39	63	4.9947	0.0	3.1467	63
240	9.58	240	5.8	5.92	3.2×10^{-4}	0.101	7.39	74	4.9947	0.0	3.6961	74
300	9.58	300	5.3	5.49	3.2×10^{-4}	0.127	7.39	82	4.9947	0.0	4.0957	82
408	9.58	408	4.6	4.88	3.8×10^{-4}	0.204	7.39	95	4.9947	0.0	4.7450	95

Table F5

Calculation of Consolidation by Small Strain Theory

for Mobile Test Basin (Primary Relationships)

t days	$\Sigma h_{i,o}$ ft	t' days	$\bar{e}$	$\bar{H}$ ft	c_v ft^2/day	T'	U' %	δ'_∞ ft	δ'' ft	δ' ft	U %
7	9.58	7	9.9	9.49	1.02×10^{-1}	0.0079	2	4.2236	0.0	0.0845	2
15	9.58	15	9.8	9.41	9.1×10^{-2}	0.0154	3	4.2236	0.0	0.1267	3
30	9.58	30	9.7	9.32	8.0×10^{-2}	0.0276	6	4.2236	0.0	0.2534	6
45	9.58	45	9.6	9.23	7.1×10^{-2}	0.0375	8	4.2236	0.0	0.3379	8
60	9.58	60	9.5	9.15	6.3×10^{-2}	0.0451	10	4.2236	0.0	0.4224	10
90	9.58	90	9.4	9.06	5.6×10^{-2}	0.061	12	4.2236	0.0	0.5068	12
120	9.58	120	9.3	8.97	5.0×10^{-2}	0.075	15	4.2236	0.0	0.6335	15
150	9.58	150	9.2	8.89	4.5×10^{-2}	0.085	17	4.2236	0.0	0.7180	17
180	9.58	180	9.1	8.80	4.1×10^{-2}	0.095	19	4.2236	0.0	0.8025	19
240	9.58	240	9.0	8.71	3.7×10^{-2}	0.110	22	4.2236	0.0	0.9292	22
300	9.58	300	8.8	8.54	3.1×10^{-2}	0.128	25	4.2236	0.0	1.0559	25
408	9.58	408	8.6	8.36	2.6×10^{-2}	0.152	29	4.2236	0.0	1.2248	29

Table F6

Calculation of Consolidation by Small Strain Theory

for Mobile Test Basin (Secondary Relationships)

t days	$\Sigma h_{i,o}$ ft	t' days	$\bar{e}$	$\bar{H}$ ft	c_v ft^2/day	T'	U' %	δ'_∞ ft	δ'' ft	δ' ft	U %
7	9.58	7	9.9	9.49	1.81×10^{-1}	0.0141	3	4.9947	0.0	0.1498	3
15	9.58	15	9.7	9.32	1.50×10^{-1}	0.0259	6	4.9947	0.0	0.2997	6
30	9.58	30	9.4	9.06	1.15×10^{-1}	0.045	9	4.9947	0.0	0.4405	9
45	9.58	45	9.3	8.97	1.05×10^{-1}	0.059	12	4.9947	0.0	0.5994	12
60	9.58	60	9.2	8.89	9.7×10^{-2}	0.074	15	4.9947	0.0	0.7492	15
90	9.58	90	8.9	8.62	7.5×10^{-2}	0.091	18	4.9947	0.0	0.8990	18
120	9.58	120	8.7	8.45	6.4×10^{-2}	0.108	22	4.9947	0.0	1.0988	22
150	9.58	150	8.6	8.36	5.9×10^{-2}	0.127	25	4.9947	0.0	1.2487	25
180	9.58	180	8.5	8.28	5.5×10^{-2}	0.144	28	4.9947	0.0	1.3985	28
240	9.58	240	8.2	8.01	4.4×10^{-2}	0.165	31	4.9947	0.0	1.5484	31
300	9.58	300	8.0	7.84	3.9×10^{-2}	0.190	36	4.9947	0.0	1.7981	36
408	9.58	408	7.7	7.58	3.2×10^{-2}	0.227	41	4.9947	0.0	2.0478	41

Cargill, Kenneth W.
Procedures for prediction of consolidation in soft fine-grained dredged material / by Kenneth W. Cargill (Geotechnical Laboratory, U.S. Army Engineer Waterways Experiment Station). -- Vicksburg, Miss. : The Station ; Springfield, Va. : available from NTIS, 1983.
152 p. in various pagings : ill. ; 27 cm. -- (Technical report ; D-83-1)
Cover title.
"January 1983."
Final report.
"Prepared for Water Resources Support Center and Office, Chief of Engineers, U.S. Army."
"Monitored by Environmental Laboratory, U.S. Army Engineer Waterways Experiment Station."
At head of title: Dredging Operations Technical Support Program.
Bibliography: p. 95-96.

Cargill, Kenneth W.
Procedures for prediction of consolidation in : ... 1983.
(Card 2)

1. Computer programs. 2. Dredging spoil. 3. Soil consolidation. 4. Soils--Testing. I. Water Resources Support Center (U.S.) II. United States. Army. Corps of Engineers. Office of the Chief of Engineers. III. Dredging Operations Technical Support Program. IV. U.S. Army Engineer Waterways Experiment Station. Environmental Laboratory. V. Title VI. Series: Technical report (U.S. Army Engineer Waterways Experiment Station) ; D-83-1.
TA7.W34 no.D-83-1